## Title

Dorsal Horn Errors in Neuronal Positioning Contribute to Nociceptive Abnormalities in Reelin-Signaling Pathway Mutant Mice



## Author

Metta Yvone, Griselda

## Publication Date

2018

Peer reviewed|Thesis/dissertation

UNIVERSITY OF CALIFORNIA

Los Angeles

# Dorsal Horn Errors in Neuronal Positioning Contribute to Nociceptive Abnormalities in Reelin-Signaling Pathway Mutant Mice

A dissertation submitted in partial satisfaction of the requirements for the degree Doctor of Philosophy in Molecular, Cellular, and Integrative Physiology

by

Griselda Metta Yvone

2018

ABSTRACT OF THE DISSERTATION

Dorsal Horn Errors in Neuronal Positioning Contribute to Nociceptive Abnormalities in Reelin-Signaling Pathway Mutant Mice

by

Griselda Metta Yvone

Doctor of Philosophy in Molecular, Cellular, and Integrative Physiology

University of California, Los Angeles, 2018

Professor Patricia Emory Phelps, Chair

Mutant mice with a deletion of Reelin (Reln), or both lipoprotein receptors, or Disabled-1 (Dab1) exhibit neuronal positioning errors, heat hypersensitivity and mechanical insensitivity. Despite the extensive nociceptive abnormalities, anatomical alterations in the lumbar dorsal horn neurons that participate in Reelin signaling were not yet identified. This thesis will identify these Dab1 and Reelin dorsal horn neurons and characterize their positioning errors associated with the nociceptive abnormalities in Reelin-pathway mutants. In the first study, we found that 70% of Dab1-labeled laminae I-II neurons were glutamatergic as they co-expressed the transcription factor Lmx1b. Dab1-Lmx1b neurons were increased within the IB4 layer and reduced within the lateral reticulated area and lateral spinal nucleus (LSN) of *Reln*$^{-/-}$ versus *Reln*$^{+/+}$ mice. Additionally, Dab1-Lmx1b neurons participated in nociceptive circuits as they expressed Fos

following noxious thermal or mechanical stimulation. Importantly, we determined that mispositioned Dab1 neurons that co-expressed Neurokinin-1-receptors contribute specifically to the heat hypersensitivity of *dab1*$^{-/-}$ mice. The second study asked whether the loss of Reelin laminae I-II neurons contributes to the mechanical insensitivity of *dab1*$^{-/-}$ mice. We found that 83% of Reelin laminae I-II neurons co-expressed Lmx1b. Although Reelin-Lmx1b and Dab1-Lmx1b neurons were independent populations, together they comprised 37% of laminae I-II glutamatergic neurons. Reelin-Lmx1b neurons sustained similar positioning errors to the Dab1-Lmx1b neurons, that is, with more of these neurons within the IB4 layer and less in the lateral reticulated area and LSN of *dab1*$^{-/-}$ compared to *dab1*$^{+/+}$ mice. The area of laminae I-II$_{outer}$ was reduced in both *Reln* and *dab1* mutants, but the IB4 layer did not differ between genotypes. We examined the migratory patterns of Reelin and Dab1 neurons and found that they arose from both the early-born (dI5) and late-born (dIL$_B$) Lmx1b-expressing populations during embryonic development. When Dab1 was absent, the migration of Reelin and Reelin-Lmx1b neurons were relatively normal whereas without Reelin, Dab1 and Dab1-Lmx1b neurons exhibited clear migratory errors. In combination, we determined that the neuroanatomical abnormalities in *Reln*$^{-/-}$ and *dab1*$^{-/-}$ dorsal horn are due to the disruption of the Reelin-Dab1-signaling pathway, and these positioning errors contribute to the nociceptive alterations displayed by the mutant mice.

The dissertation of Griselda Metta Yvone is approved.

Gordon L. Fain

Stephanie Ann White

Xianjie Yang

Patricia Emory Phelps, Committee Chair

TABLE OF CONTENTS

LIST OF FIGURES

ACKNOWLEDGEMENTS

I would like to thank all of those who provided guidance, advice, expertise and support throughout my graduate education, which made completion of this dissertation possible. First and foremost, I would like to thank my committee chair and mentor Dr. Patty Phelps for her amazing support and mentorship over the past seven years. I would always be grateful to her for letting me join her lab. In addition, I wish to thank all my PhD committee members Dr. Fain, Dr. White, and Dr. Yang for their critical guidance and evaluation of my dissertation project.

I would like to acknowledge Dr. Brian Howell for providing the Dab1-B3 antibody, Dr. Thomas Müller, and Dr. Carmen Birchmeier for providing the Lmx1b antibody. These resources made it possible for this dissertation to be completed. I would also like to thank Dr. Allan Basbaum, who provided valuable advice and guidance on my first manuscript.

Special thanks to my wonderful undergraduate, mentee, and friend in the lab, Carmine L. Chavez-Martinez, who has helped me tremendously during the past several years to complete this project. Thanks to the other undergraduates and technicians in the lab who have helped me along the way: Deborah Wang and Austin Wang.

I also would like to thank my fellow lab members past or present, especially the ones who took the time to train me in the lab. It was a pleasure to work with each of them as they made my lab experience very enjoyable and eventful.

Chapter 2 of this dissertation is a version of: Yvone GM, Zhao-Fleming HH, Udeochu JC, Chavez-Martinez CL, Wang A, Hirose-Ikeda M, Phelps PE. 2017. Disabled-1 dorsal horn spinal cord neurons co-express Lmx1b and function in nociceptive circuits. Eur J Neurosci. 45:733-47.

I would like to acknowledge the future co-authors who have contributed to the work in chapter 3: Chavez-Martinez CL, Wang D, Phelps PE. Chapter 3 is in preparation to be published.

Finally, a personal acknowledgement is due to my mother and friends in and outside of UCLA with a special thanks to my best friend, Benita Jin. Their continuous support really helped me to persevere and find the strength as I am completing my graduate career and this dissertation.

This study was supported by: the Eureka Scholarship, the Hyde Fellowship, the Dissertation Year Fellowship, National Science Foundation (IOB-0924143 to PEP) and the Microscopy Core of the IDDRC from the NICHD (P30HD004612 and U54HD087101).

VITA

| | |
|---|---|
| 2008 | B.S., Biological Sciences<br>Latin Honor – Cum Laude<br>Cornell University, Ithaca, NY |
| 2008-2011 | Senior Research Technician<br>Principal Investigator: Todd R. Golub, M.D.<br>Broad Institute of MIT Harvard, Cambridge, MA<br>Dana-Farber Cancer Institute, Boston, MA |
| 2011-2018 | Graduate Student Researcher<br>Department of Integrative Biology and Physiology<br>University of California, Los Angeles |
| 2014-2015 | Teaching Assistant (LS23L)<br>Department of Life Sciences<br>University of California, Los Angeles |
| 2014-2015 | Eureka Scholarship<br>University of California, Los Angeles |
| 2015 | Neuroscience Graduate Travel Award<br>Brain Research Institute/Semel Institute<br>University of California, Los Angeles |
| 2016-2017 | Hyde Fellowship<br>University of California, Los Angeles |
| 2017 | Integrative Biology and Physiology Fellowship<br>University of California, Los Angeles |
| 2017-2018 | Dissertation Year Fellowship<br>University of California, Los Angeles |

## PUBLICATIONS

Schmidt JA, **Yvone GM**, Brown WJ. 2010. Membrane topology of human AGPAT3 (LPAAT3). Biochem Biophys Res Commun. 397:661-667.

Abadesco AD, Cilluffo M, **Yvone GM,** Carpenter EM, Howell BW, Phelps PE. 2014. Novel Disabled-1-expressing neurons identified in adult brain and spinal cord. Eur J Neurosci. 39:579-592.

Yu C, Mannan AM, **Yvone GM**, Ross KN, Zhang YL, Marton MA, Taylor BR, Crenshaw A, Gould JZ, Tamayo P, Weir BA, Tsherniak A, Wong B, Garraway LA, Shamji AF, Palmer MA, Foley MA, Winckler W, Schreiber SL, Kung AL, Golub TR. 2016. High-throughput identification of genotype-specific cancer vulnerabilities in mixtures of barcoded tumor cell lines. Nat Biotechnol. 34:419-423.

**Yvone GM**, Zhao-Fleming HH, Udeochu JC, Chavez-Martinez CL, Wang A, Hirose-Ikeda M, Phelps PE. 2017. Disabled-1 dorsal horn spinal cord neurons co-express Lmx1b and function in nociceptive circuits. Eur J Neurosci. 45:733-747.

## PRESENTATIONS

**Yvone GM**, Zhao-Fleming HH, Udeochu JC, Phelps PE. 2015. Disabled-1 expression identifies a subset of Lmx1b superficial dorsal horn neurons involved in nociceptive circuits. Society for Neuroscience, Chicago, IL. 290.22/A38 (October 17-21, 2015).

**Yvone GM**, Zhao-Fleming HH, Udeochu JC, Chavez-Martinez CL, Phelps PE. Disabled-1-expressing neurons share a migratory pathway and positioning errors with Lmx1b-expressing neurons. 2016. Gordon Research Conference, Newport, RI (July 31-August 5, 2016).

**Yvone GM**, Chavez-Martinez CL, Wang D, Phelps PE. 2017. Reelin-expressing superficial dorsal horn neurons co-express Lmx1b and are present in Disabled-1 mutant mice. Society for Neuroscience, Washington, DC. 766.08/Z13 (November 11-15, 2017).

**Yvone GM**, Chavez-Martinez CL, Phelps PE. 2018. Reelin- and Dab1-expressing superficial dorsal horn neurons co-express Lmx1b and migrate together during development. Society for Neuroscience, San Diego, CA. 637.04/A32 (November 3-7, 2018).

*Chapter 1*

## Introduction: Review of the Literature

### Mouse mutants and the Reelin-signaling pathway

The naturally occurring mouse mutant called *reeler* (*Reln*$^{-/-}$) was first described over 60 years ago by Falconer (1951) and reported to have a reeling gait, tremors, ataxia, and lamination defects in the cerebral and cerebellar cortices. D'Arcangelo and colleagues (1995) were the first to clone the mouse *reelin* gene and characterize its structure and components. The mouse *reelin* gene is located on chromosome 5. It encodes the Reelin protein, which has 3461 amino acids, a relative molecular mass of 388kDa, and contains eight consecutive Reelin repeats. These Reelin repeats contain Epidermal Growth Factor (EGF)-like domains, which are most closely related to those of the tenascin and integrin families (D'Arcangelo *et al*., 1995). Based on its structural components and secretion into the extracellular space, Reelin is considered an extracellular matrix protein and is now known to mediate neuronal adhesion and migration during development.

D'Arcangelo *et al*. (1995) also determined that *reelin* mRNA is highly expressed in multiple areas in the developing CNS, and that its expression persists at lower levels in postnatal and adult ages. In the telencephalon and diencephalon, *reelin* transcripts are first detected at embryonic day 10 (E10), and transcript expression continues at high levels between E14 to postnatal day 5 (P5; D'Arcangelo *et al*., 1995; Ikeda and Terashima, 1997; Alcántara *et al*., 1998). During neocortical development, *reelin* mRNA is expressed initially by the Cajal-Retzius cells in the marginal zone. It is also found in areas containing migrating neurons in the developing hippocampus, olfactory bulb, and the cerebellum (D'Arcangelo *et al*., 1995). Using immunohistochemistry, Alcántara *et al*. (1998) showed that many of these Reelin-expressing

neurons in the cerebral cortex and hippocampal formation are also immunoreactive for glutamic acid decarboxylase (GAD65/67) and thus are inhibitory neurons. During development, *reelin* transcripts are detected throughout the spinal cord – in both the superficial dorsal horn and the ventral horn (Ikeda and Terashima, 1997).

Howell *et al*. (1997a) identified the mouse homolog of the *Drosophila* Disabled gene, *mDab1*. This gene codes for the protein Dab1, which functions as an intracellular adaptor molecule in neural development. Howell *et al*. (1997a) mapped the mouse *dab1* gene to chromosome 4 and reported high Dab1 protein expression in the developing brain. Additionally, these authors showed that tyrosine phosphorylation of Dab1 is the highest during nervous system development and decreases in adulthood. Several studies (Howell *et al*., 1997b; Sheldon *et al*., 1997; Rice *et al*., 1998) reported that Dab1-expressing cells respond to Reelin signaling and that Reelin and Dab1 are expressed in adjacent cell populations during neural development. For example, Reelin is in Cajal-Retzius cells of the cerebral cortex, while Dab1 is expressed by cortical plate neurons. In the hippocampus, Reelin is in the molecular layer and marginal zone, while the pyramidal neurons and dentate granule cells both express Dab1. In the cerebellum, granule cells express Reelin, and Dab1 is expressed by Purkinje cells (Howell *et al*., 1997b; Sheldon *et al*., 1997; Rice *et al*., 1998). Rice *et al*. (1998) and others (Howell *et al*., 1997b; Sheldon *et al*., 1997) found that the *dab1* mRNA levels are similar in wild-type and *Reln*$^{-/-}$ mice, yet the Dab1-expressing neurons in *Reln*$^{-/-}$ mice contain 10-fold more Dab1 protein than wild-type mice. These findings suggest that Reelin signaling results in increased Dab1 degradation.

Mice lacking Reelin, or Dab1, or both Apolipoprotein E receptor 2 (Apoer2) and the Very-low-density lipoprotein receptor (Vldlr) exhibit the same characteristic motor and neuroanatomical defects in the CNS, suggesting that these proteins are all part of the same

signaling pathway (Howell *et al*., 1997b; Hiesberger *et al*., 1999; Trommsdorff *et al*., 1999). D'Arcangelo *et al*. (1999) and Hiesberger *et al*. (1999) further showed that Reelin binds to the extracellular domains of Apoer2 and Vldlr, and then induces Dab1 tyrosine phosphorylation by Src-family kinases. Both *Apoer2* and *Vldlr* mRNA are expressed by Dab1-labeled cells that respond to Reelin signaling in the CNS and may function cooperatively (Trommsdorff *et al*., 1999). Thus, although Dab1 protein levels increased 2- to 3-fold in immunoblots of brain extracts from single-receptor knockout mice, the increase was 13-fold in double-receptor knockout mice (Trommsdorff *et al*., 1999). Consequently, neuroanatomical defects in mice lacking only one lipoprotein receptor are mild, but those found in double-receptor knockout mice are indistinguishable from $Reln^{-/-}$ and $dab1^{-/-}$ mice (Trommsdorff *et al*., 1999).

All these and further studies have elucidated the Reelin-signaling pathway and the interactions between these four proteins are now well-established (see Fig. 1). Reelin binding to Apoer2 and Vldlr leads to receptor clustering and the recruitment of Dab1 to the NPxY motifs on the intracellular domain of the receptors (Howell *et al*., 1999; Trommsdorff *et al*., 1999; Strasser *et al*., 2004). At that point, Src-family kinases (SFKs) are recruited and phosphorylate Dab1 on its tyrosine residues. Phosphorylated Dab1 then activates downstream pathways that regulate cell adhesion and neuronal migration, such as the phosphatidyl-inositol-3-kinase (PI3K) or the Crk/Crk-like pathways (Hiesberger *et al*., 1999; Beffert *et al*., 2002; Ballif *et al*., 2004; Herz and Chen, 2006). Reelin signaling is terminated when phosphorylated Dab1 is polyubiquitinated and degraded (Arnaud *et al*., 2003). When Reelin is absent, Dab1 will accumulate in mispositioned neurons (Arnaud *et al*., 2003; Herz and Chen, 2006). The similarities in the mouse mutants for Reelin, Apoer2 and Vldlr, and Dab1 played a critical role in establishing the canonical Reelin-signaling pathway.

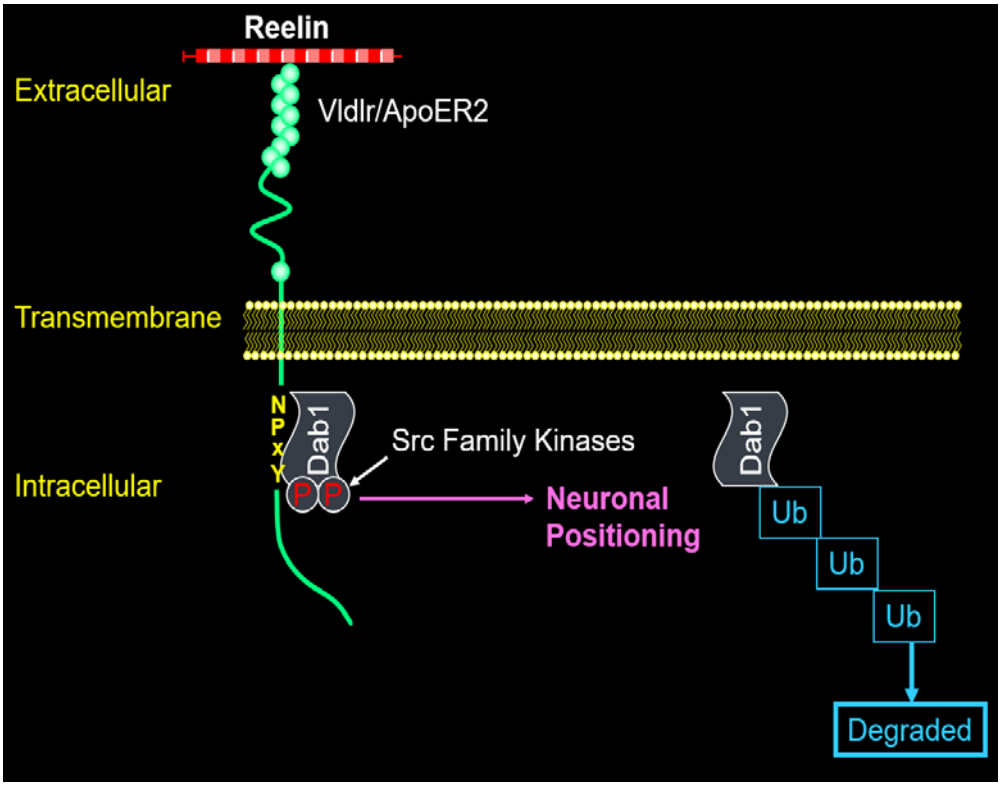


Figure 1: Schematic of the Reelin-signaling pathway. The binding of Reelin to the two lipoprotein receptors, Apoer2 and Vldlr, results in the recruitment and tyrosine phosphorylation of Dab1 by Src-family kinases. Eventually phosphorylated Dab1 gets polyubiquitinated and degraded, but in the absence of Reelin or both Apoer2 and Vldlr, Dab1 does not get degraded and will accumulate in mispositioned neurons.

**The role of the Reelin-signaling pathway in cortical development**

The abnormal neuronal migration found in *Reln*$^{-/-}$ cerebral cortex was characterized many years before the signaling pathway was discovered. The first cells detected in the cerebral cortex are the Reelin-secreting Cajal-Retzius cells, a transient neuronal population found in the marginal zone (König *et al*. 1977; D'Arcangelo *et al*., 1995; Meyer and Goffinet, 1998). Next the subplate neurons migrate along radial glia fibers, and together with the Cajal-Retzius cells they form the preplate (Caviness and Rakic, 1978). The later-born cortical neurons, many of which are Dab1-positive, migrate past the subplate neurons and settle beneath the Cajal-Retzius cells and thus "split the preplate". The remaining neocortical layers form between the Cajal-Retzius cells and

the subplate in an “inside-out” manner; that is, the later-born neurons are positioned in the superficial layers while the earlier-born neurons are located in the deeper layers (Caviness and Rakic, 1978). In *Reln*$^{-/-}$mice, the preplate forms normally, but subsequent neurons fail to split the preplate (Caviness and Rakic, 1978). Furthermore, newly generated neurons are unable to migrate past their predecessors and accumulate in the cortical plate. Thus, in *Reln*$^{-/-}$ mice, the newly born neurons form inverted cortical layers (Caviness and Rakic, 1978; Caviness, 1982; Rice and Curran, 1999).

The specific role of Reelin in neuronal migration and cortical development, however, is still controversial. Ogawa *et al*. (1995) proposed that Reelin produced by Cajal-Retzius cells regulates alignment of cortical plate neurons through cell-cell interactions. Reelin was proposed to inhibit neuronal migration by binding with α3β1 integrins and by stimulating the detachment of neurons from radial glia, but no single integrin defect simulates the *reeler*-like phenotype (Dulabon *et al*., 2000). Magdaleno *et al*. (2002) ectopically expressed Reelin in the ventricular zone under the *nestin* promoter and partially rescued the *reeler* mutant phenotype in the cerebral cortex. Reelin expressed only in the ventricular zone restored tyrosine phosphorylation of Dab1 in premigratory neurons, partially induced preplate splitting during cortical development, and rescued ataxia; but other defects remained (Magdaleno *et al*., 2002). Neither the ectopic expression of Reelin in the ventricular zone nor endogenous Reelin attracted cortical plate neurons or prematurely terminated neuronal migration, suggesting that Reelin did not function as a simple attractant or a stop signal (Magdaleno *et al*., 2002). Based on their findings, Magdaleno *et al*. (2002) instead proposed that Reelin contributed to proper cortical neuron alignment together with other positional cues.

Nadarajah *et al*. (2001) profiled two modes of migration of cortical neurons. One is called locomotion, which involves movement of the whole cell and which is radial glia-dependent. The other, termed *somal* translocation, is radial glia-independent and involves the cell extending a leading process directed toward the pia mater, within which the nucleus moves toward its destination (Nadarajah *et al*., 2001). Sekine *et al*. (2011; 2012) showed that during cerebral cortical development, Reelin switches the migration mode from locomotion to terminal *somal* translocation. This transition promotes adhesion to the extracellular matrix for proper positioning of neocortical neurons through the interaction of Reelin with integrin α5β1 and the intracellular Dab1-Crk/Crk-like-C3G-Rap1 pathway (Sekine *et al*., 2012).

**Role of the Reelin-signaling pathway in cerebellum development**

The major cell populations of the cerebellum are the Purkinje neurons and the granule cells, which both participate in the Reelin-signaling pathway (Tissir and Goffinet, 2003). During normal cerebellar development, the Purkinje neurons are generated in the ventricular zone and migrate radially along Bergmann glia to form the Purkinje cell layer (Goffinet, 1992). In contrast, the granule cell precursors are generated from a proliferative zone called the rhombic lip, and numerous granule cells migrate into the cerebellum (Hatten, 1985; Alder *et al*., 1996). As the granule cells differentiate, their axons branch to form the parallel fibers that fill the molecular layer of the cerebellum. The granule cell bodies migrate along Bergmann glia as they descend past the Purkinje cells to form the granule cell layer of the cerebellum (Hatten, 1985).

In the *Reln*$^{-/-}$ cerebellum, the Dab1-labeled Purkinje cells form ectopic aggregates rather than a cell layer, and only a small number of the Reelin-expressing granule cells migrate to the cerebellum from the rhombic lip (Mariani *et al*., 1977; Tissir and Goffinet, 2003). The defects in the granule cells are attributed to aberrant Sonic hedgehog signaling (Dahmane and Ruiz I

Altaba, 1999). *Reln*$^{-/-}$ mice lack cerebellar foliation and lamination, and the mutant cerebellum is about one-fifth the size of normal cerebellum (Mariani *et al*., 1977; Goffinet, 1992; Tissir and Goffinet, 2003). When exogenous Reelin from normal cerebellar granule cells was co-cultured with explants from *Reln*$^{-/-}$ cerebellum, Purkinje cell misalignment was rescued (Miyata *et al*., 1997). Purkinje cell alignment, however, was inhibited by CR-50, an antibody that blocks Reelin function (Miyata *et al*., 1997). Thus, Reelin synthesized by cerebellar granule cells controls the proper positioning of the Dab1-expressing Purkinje cells (Miyata *et al*., 1997).

**Postnatal and adult functions of the Reelin-signaling pathway in the brain**

Although the Reelin-signaling pathway components have their highest expression during embryonic development and decrease their levels postnatally (Alcántara *et al*., 1998), this pathway has important functions throughout life. Some studies have reported that Reelin promotes postnatal dendritic development in hippocampal pyramidal and cortical pyramidal neurons through the Apoer2-Vldlr-Dab1 and Crk/Crk-like pathways (Niu *et al*., 2004; Olson *et al*., 2006; Matsuki *et al*., 2008). Teixeira and colleagues (2012) found that Reelin signaling is also required for adult neurogenesis in the hippocampal dentate gyrus. Additionally, the Apoer2-Vldlr-Dab1 pathway is highly expressed in neuroblasts within the rostral migratory chain migration from the subventricular zone to the olfactory bulb. In this region, however, the ligand Thrombospondin-1 binds to the lipoprotein receptors rather than Reelin (Andrade *et al*., 2007; Blake *et al*., 2008).

In adult mice, Reelin signaling is implicated in learning and memory as it enhances hippocampal long-term potentiation and synaptic plasticity. In addition, Reelin modulates N-methyl-d-aspartate (NMDA)-type and α-amino-3-hydroxy-5-methyl-4-isoxazolepropionic acid (AMPA)-type glutamate receptors during synaptic transmission (Weeber *et al*., 2002; Chen *et*

*al*., 2005; Qiu *et al*., 2006; Pujadas *et al*., 2010). Beffert *et al*. (2005) showed that Reelin modulates NMDA receptor function and hippocampal synaptic activity through the Apoer2 splice variant of exon 19, and that mice lacking Apoer2-exon 19 perform poorly in learning and memory tasks. In summary, despite the comparatively low levels of Reelin and Dab1 in adult mice, this pathway continues to be critical for adult brain functions.

**Influence of Reelin signaling on the migration of autonomic and somatic motor neurons in the spinal cord**

The first abnormalities detected in the *Reln*$^{-/-}$ spinal cord were the abnormal migration of sympathetic preganglionic neurons (SPNs) and parasympathetic preganglionic neurons (PPNs; see Yip *et al*., 2000; Phelps *et al*., 2002). During normal development, postmitotic SPNs migrate together with the somatic motor neurons from the ventricular zone to the primitive motor column in the ventrolateral spinal cord (Phelps *et al*., 1991). The somatic motor neurons then settle in the ventral spinal cord, whereas the SPNs continue their migration dorsally until they reach the intermediolateral gray matter (Phelps *et al*., 1991; Barber *et al*., 1993; Phelps *et al*., 1993). In *Reln*$^{-/-}$ spinal cord, most SPNs migrate past the intermediolateral gray matter along radial glial fibers and settle near the central canal (Yip *et al*., 2000; Phelps *et al*., 2002). In addition, the PPNs in *Reln*$^{-/-}$ mice are scattered along the mediolateral axis of the intermediate sacral spinal cord instead of forming the intermediolateral sacral nucleus (Phelps *et al*., 2002). The SPNs and PPNs both express Dab1, whereas cells that border them express Reelin (Phelps *et al*., 2002). When other groups of cholinergic spinal cord neurons were analyzed, such as the dorsal horn interneurons, they appeared to be normally positioned (Phelps *et al*., 2002).

The role of Reelin signaling in regulating the migration of SPNs and PPNs may be to interfere with the ability of these neurons to detach from the radial glia fibers (Phelps *et al*.,

2002). Krüger *et al*. (2010) reported that Reelin located in the area between the intermediolateral column and the central canal induced the phosphorylation of Cofilin in the SPNs and prevented their aberrant medial migration toward the central canal. When Apoer2, Dab1, or Reelin was absent, however, Krüger *et al*. (2010) showed that SPNs do not express phosphorylated Cofilin and they were mispositioned in the spinal cord. Thus, the interaction of Reelin and Cofilin may function to terminate migration of the autonomic motor neurons (Krüger *et al*., 2010).

Unlike the SPNs and PPNs, the somatic motor neurons in *Reln*$^{-/-}$ mice were initially thought to be correctly positioned. When these motor neurons were mapped and analyzed carefully, however, the developing (Palmesino *et al*., 2010) and adult (Abadesco *et al*., 2014) lateral motor column neurons expressed Dab1 and were located in more medial and ventral positions in *Reln*$^{-/-}$ versus *Reln*$^{+/+}$ spinal cords. The positioning errors of the somatic motor neurons, therefore, are more subtle than those of the autonomic motor neurons (Yip *et al*., 2000; Phelps *et al*., 2002; Abadesco *et al*., 2014). Taken together, these findings suggest that Reelin acts in a context-dependent manner together with additional positional cues to regulate neuronal migration in different parts of the CNS, and that the disruption of the Reelin-signaling pathway may lead to a variety of neuroanatomical defects.

**Contribution of neuronal identity during development to the functioning of sensory circuits in the dorsal horn**

Reelin-labeled cells are first detected during mouse development extending from the ventricular zone to the ventrolateral side of the dorsal horn. By E14.5, they had migrated into their final locations in the laminae I-II (superficial dorsal horn). A few large Reelin-labeled cells have been observed that resemble Waldeyer projection neurons and were found in lamina I, whereas the majority of Reelin laminae I-II cells were smaller. At E17.5, high levels of diffuse Reelin

expression and occasional large cells were detected in the lateral spinal nucleus (LSN), a small region in the dorsolateral funiculus which contains about 10 neurons per 40 µm hemisections (Burstein *et al*., 1990; Villeda *et al*., 2006; Akopians *et al*., 2008). The pattern of Dab1 protein expression during development closely resembled that of Reelin expression (Villeda *et al*., 2006), and this overlap suggests the importance of this pathway in the dorsal horn.

During spinal cord development, six early-born (E10-12.5) dorsal interneuron groups (dI1-6) and two late-born (E11-13; $dIL_{A-B}$) dorsal interneuron populations are defined as they differentiate into postmitotic neurons by the combinatorial expression of transcription factors (Gross *et al*., 2002; Müller *et al*., 2002; Helms and Johnson, 2003). The specification of dI1-3 neuronal populations depends upon Bone Morphogenetic Protein (BMP) levels, whereas the dI4-6 populations are generated independent of BMP signaling (Müller *et al*., 2002). The dI4-6 populations are derived from the *Lbx1* lineage and can be further divided into inhibitory $dI4/dIL_A$ and dI6 populations that express *Pax2,* and excitatory $dI5/dIL_B$ populations that express *Tlx3* and *Lmx1b* (Gross *et al*., 2002; Müller *et al*., 2002; Helms and Johnson, 2003). These different neuronal populations migrate and settle in specific regions in the spinal cord.

The dorsal interneuron progenitor cells important to the Reelin-signaling pathway are likely born from dorso-intermediate regions of the ventricular zone ($dI4/dIL_A$-$dI5/dIL_B$). These interneurons migrate laterally and dorsally and are localized throughout the dorsal horn with their highest concentration in laminae I-II (Gross *et al*., 2002; Müller *et al*., 2002; Helms and Johnson, 2003). In addition, a portion of the $dI4/dIL_A$ and $dI5/dIL_B$ populations reportedly form circuits and pathways involved in pain, thermosensation, itch, and touch (Gross *et al*., 2002; Lai *et al*., 2016).

**Dorsal-horn positioning errors and nociceptive abnormalities are found in Reelin signaling-pathway mutant mice**

Reelin and Dab1 are both expressed in adult neurons in the nociceptive areas of the dorsal horn, that is: in laminae I-II, in the lateral reticulated area of lamina V, and in the LSN (Kubasak *et al*., 2004; Villeda *et al*, 2006; Akopians *et al*., 2008). The neurons in laminae I-II are 20-30% inhibitory (GABA and/or glycine-containing) and the remainder are excitatory interneurons (glutamatergic; Todd, 2010). Laminae I-II neurons mostly receive noxious input from Aδ and C-fibers, whereas the deep dorsal horn (in laminae III-V) neurons respond to innocuous input from Aβ fibers (Basbaum *et al*., 2009; Todd, 2010).

Importantly, projection neurons that transmit pain information to the brainstem and thalamic nuclei, such as the caudal ventrolateral medulla and the lateral parabrachial area, are located in lamina I (Todd, 2010) and the LSN (Burstein *et al*., 1990). Most lamina I projection neurons that respond to noxious heat stimuli express the Neurokinin-1 receptor (NK1R), and additional NK1R-expressing projection neurons are also located in laminae III-IV (Todd, 2010). There are also a few large lamina I neurons that do not express NK1R, termed “giant cells”. The giant cells comprise about 2-3% of the lamina-I projection neurons and express Fos, an immediate early gene indicating neuronal activation after noxious stimulation. Additionally, they project to thalamic nuclei, and are considered part of the Waldeyer cell population (Todd, 2010). Many neurons in the lateral reticulated area of lamina V are called “wide-dynamic range” projection neurons, because they receive both innocuous and noxious input directly via Aβ and Aδ fibers and indirectly from C-fibers (Basbaum *et al*., 2009; Todd, 2010).

Mice with mutations in the Reelin-signaling pathway have profound changes in sensory perception (Villeda *et al*., 2006; Akopians *et al*., 2008; Wang *et al*., 2012). *Reln*$^{-/-}$ and *dab1*$^{-/-}$

mice have increased thermal heat sensitivity compared to wild-type mice as analyzed with the Hargreaves paw withdrawal test (Hargreaves *et al*., 1988; Villeda *et al*., 2006; Akopians *et al*., 2008). Confirming these sensory test results, Wang *et al*. (2012) found that noxious heat stimulation resulted in a greater number of Fos-expressing neurons within laminae I-II in *Reln*$^{-/-}$ and *dab1*$^{-/-}$ as compared to wild-type mice. Interestingly, they also observed a reduction in the number of Fos-positive neurons in the lateral reticulated area and LSN of *Reln*$^{-/-}$ and *dab1*$^{-/-}$ mice versus the wild-type mice (Wang *et al*., 2012).

When tested for mechanical sensitivity with the von Frey test (up-down test of Chaplan; see Chaplan *et al*., 1994), *Reln*$^{-/-}$ and *dab1*$^{-/-}$ mice have profoundly reduced responses to mechanical pain compared to their respective wild-type controls (Villeda *et al*., 2006; Akopians *et al*., 2008). The single *Apoer2* and *Vldlr* knockout mice did not exhibit either thermal hypersensitivity or mechanical insensitivity, and the *Apoer2/Vldlr* double-receptor knockout mice could not be tested as they rarely survived beyond 2-3 weeks after birth (Akopians *et al*., 2008). Following noxious mechanical stimulation, the number of neurons that expressed Fos in the superficial dorsal horn, the lateral reticulated area, and the LSN was reduced in *Reln*$^{-/-}$ and *dab1*$^{-/-}$ mice as compared to wild-type mice (Wang *et al*, 2012).

Results from the formalin test showed that responses to chemical pain also were reduced in *Reln*$^{-/-}$ and *dab1*$^{-/-}$ mice, but neither the acetic-acid test of visceral pain nor cold-pain responsiveness differed from wild-type mice (Wang *et al*., 2012). Because both *Reln*$^{-/-}$ and *dab1*$^{-/-}$ mice exhibited the same unusual combination of sensory deficits, this observation confirms that these abnormalities are linked to the Reelin-signaling pathway. Furthermore, these results suggest that the specific pain abnormalities in the mutant mice are associated with pain modality-specific lines.

Despite the dramatic nociceptive abnormalities displayed by Reelin-signaling pathway mutants, our laboratory had previously found relatively few positioning errors in the dorsal horn. Together, Villeda *et al*. (2006) and Akopians *et al*. (2008) reported neuronal compaction in lamina I, as well as a neuron-sparse region within laminae I-$II_{outer}$, and large Neurokinin-1 receptor (NK1R)-expressing neurons aberrantly located in deep within lamina II. Some of these NK1R-expressing neurons co-expressed Dab1. In addition, the number of neurons in the LSN was consistently reduced in *Reln*$^{-/-}$ and *dab1*$^{-/-}$ mice (Villeda *et al*., 2006; Akopians *et al*., 2008; Wang *et al*., 2012). When the termination patterns of the peptidergic and non-peptidergic primary afferents were examined in lumbar spinal cord, they appeared relatively normal in the absence of Reelin or Dab1 (Villeda *et al*., 2006; Akopians *et al*., 2008). A major goal of this thesis is to elucidate the contribution of the positioning errors of Reelin and Dab1 neurons in the dorsal horn to the nociceptive abnormalities exhibited by Reelin-pathway mutant mice.

**Proposed Research Project**

Given the importance of the dorsal horn in pain transmission and the extensive changes in nociceptive behavior detected in Reelin-signaling pathway mutants, the anatomical errors detected in the dorsal horn to date are very limited. The proposed studies will characterize the expression pattern, positioning and identity of Dab1- and Reelin-positive neurons in the developing and adult dorsal horn. Additionally, we hope to determine how the loss of Reelin signaling leads to the dorsal-horn positioning errors that contribute to the heat hypersensitivity versus positioning errors that cause mechanical insensitivity in these mutant mice.

**Specific Aim 1: Identify the Dab1-expressing dorsal horn neurons that respond to Reelin signaling and participate in nociceptive circuits. Characterize their neuronal positioning errors in *Reln*$^{-/-}$ mice.** The results of this aim are published (Yvone *et al*., 2017) and reprinted in Chapter 2.

*Hypothesis 1a: Dab1 dorsal horn neurons are comprised of multiple neuronal populations that are both inhibitory and excitatory.* Results suggest that a subset of Dab1-positive neurons in laminae I-II co-express Lmx1b, a transcription factor that marks many glutamatergic dorsal horn neurons (Cheng *et al*., 2004). We will analyze the percentage of Dab1 neurons that co-express Lmx1b in the nociceptive areas of the dorsal horn and determine whether there are inhibitory neurons expressing Dab1.

*Hypothesis 1b: Dab1-expressing neurons exhibit positioning errors in the nociceptive regions of the Reln*$^{-/-}$ *dorsal horn, i.e., laminae I-II, lateral lamina V and the LSN.* After determining the identity of the Dab1 dorsal horn neurons, we will compare the number of neurons that express Dab1 in each of the nociceptive areas of adult *Reln*$^{+/+}$ and *Reln*$^{-/-}$ dorsal horn.

*Hypothesis 1c: Dab1-positive dorsal horn neurons participate in thermal and mechanical nociceptive circuits.* We will examine whether Dab1 and Dab1-Lmx1b neurons co-express Fos after noxious thermal and mechanical stimulation.

**Specific Aim 2: Determine the identity of Reelin-positive dorsal horn neurons and ask whether these cells sustain positioning errors. Examine the migration patterns of Reelin- and Dab1-expressing dorsal horn neurons relative to those of Lmx1b-labeled neurons.**

*Hypothesis 2a: Reelin-labeled dorsal horn neurons are mostly glutamatergic neurons and co-express the transcription factor Lmx1b.* We will determine the percentage of adult Reelin dorsal

horn neurons that co-express Lmx1b and then test whether the Reelin-Lmx1b and Dab1-Lmx1b neurons represent the same or a separate population of Lmx1b-labeled cells.

*Hypothesis 2b: Reelin-expressing neurons exhibit positioning errors in multiple dorsal horn areas, and these errors should match those found in the Dab1-labeled cells (Chapter 2).* We will compare the number of neurons that express Reelin in laminae I-II, in the lateral reticulated area of lamina V, and in the LSN in *dab1*$^{+/+}$ versus *dab1*$^{-/-}$ mice.

*Hypothesis 2c: Reelin and Dab1 dorsal horn neurons share a common migratory pathway with one or more subsets of Lmx1b dorsal horn neuronal populations.* We will characterize the expression pattern and migration of Reelin and Reelin-Lmx1b dorsal horn neurons in pairs of *dab1* embryonic lumbar spinal cord between E11.5-E15.5. Additionally, the migratory patterns of Dab1 and Dab1-Lmx1b neurons will be compared in *Reln*$^{+/+}$ and *Reln*$^{-/-}$ E11.5-E15.5 sections.

**References**

Abadesco AD, Cilluffo M, Yvone GM, Carpenter EM, Howell BW, Phelps PE. 2013. Novel Disabled-1-expressing neurons identified in adult brain and spinal cord. Eur J Neurosci. 39:579-92.

Akopians AL, Babayan AH, Beffert U, Herz J, Basbaum AI, Phelps PE. 2008. Contribution of the Reelin signaling pathways to nociceptive processing. Eur J Neurosci. 27:523-37.

Alcántara S, Ruiz M, D'Arcangelo G, Ezan F, de Lecea L, Curran T, Sotelo C, Soriano E. 1998. Regional and cellular patterns of reelin mRNA expression in the forebrain of the developing and adult mouse. J Neurosci. 18:7779-99.

Alder J, Cho NK, Hatten ME. 1996. Embryonic precursor cells from the rhombic lip are specified to a cerebellar granule neuron identity. Neuron. 17:389-99.

Andrade N, Komnenovic V, Blake SM, Jossin Y, Howell B, Goffinet A, Schneider WJ, Nimpf J. 2007. ApoER2/VLDL receptor and Dab1 in the rostral migratory stream function in postnatal neuronal migration independently of Reelin. Proc Natl Acad Sci U S A. 104:8508-13.

Arnaud L, Ballif BA, Cooper JA. 2003. Regulation of protein tyrosine kinase signaling by substrate degradation during brain development. Mol Cell Biol. 23:9293-302.

Ballif BA, Arnaud L, Arthur WT, Guris D, Imamoto A, Cooper JA. 2004. Activation of Dab1/CrkL/C3G/ Rap1 pathway in Reelin-stimulated neurons. Curr Biol. 14:606-10.

Barber RP, Phelps PE, Vaughn JE. 1993. Preganglionic autonomic motor neurons display normal translocation patterns in slice cultures of embryonic rat spinal cord. J Neurosci. 13:4898-907.

Basbaum AI, Bautista DM, Scherrer G, Julius D. 2009. Cellular and molecular mechanisms of pain. Cell. 139:267-84.

Beffert U, Morfini G, Bock HH, Reyna H, Brady ST, Herz J. 2002. Reelin-mediated signaling locally regulates protein kinase B/Akt and glycogen synthase kinase 3beta. J Biol Chem. 277:49958-64.

Beffert U, Weeber EJ, Durudas A, Qiu S, Masiulis I, Sweatt JD, Li WP, Adelmann G, Frotscher M, Hammer RE, Herz J. 2005. Modulation of synaptic plasticity and memory by Reelin involves differential splicing of the lipoprotein receptor Apoer2. Neuron. 47:567-79.

Blake SM, Strasser V, Andrade N, Duit S, Hofbauer R, Schneider WJ, Nimpf J. 2008. Thrombospondin-1 binds to ApoER2 and VLDL receptor and functions in postnatal neuronal migration. EMBO J. 27:3069-80.

Burstein R, Dado RJ, Giesler GJ Jr. 1990. The cells of origin of the spinothalamic tract of the rat: a quantitative reexamination. Brain Res. 511:329-37.

Caviness VS Jr. 1982. Neocortical histogenesis in normal and reeler mice: a developmental study based upon [3H] thymidine autoradiography. Brain Res. 256:293-302.

Caviness VS Jr, Rakic P. 1978. Mechanisms of cortical development: a view from mutations in mice. Annu Rev Neurosci. 1:297-326.

Chaplan SR, Bach FW, Pogrel JW, Chung JM, Yaksh TL. 1994. Quantitative assessment of tactile allodynia in the rat paw. J Neurosci Methods. 53:55-63.

Chen Y, Beffert U, Ertunc M, Tang TS, Kavalali ET, Bezprozvanny I, Herz J. 2005. Reelin modulates NMDA receptor activity in cortical neurons. J Neurosci. 25:8209-16.

Cheng L, Arata A, Mizuguchi R, Qian Y, Karunaratne A, Gray PA, Arata S, Shirasawa S, Bouchard M, Luo P, Chen CL, Busslinger M, Goulding M, Onimaru H, Ma Q. 2004. Tlx3 and Tlx1 are post-mitotic selector genes determining glutamatergic over GABAergic cell fates. Nat Neurosci. 7:510-7.

D'Arcangelo G, Homayouni R, Keshvara L, Rice DS, Sheldon M, Curran T. 1999. Reelin is a ligand for lipoprotein receptors. Neuron. 24:471-9.

D'Arcangelo G, Miao GG, Chen SC, Soares HD, Morgan JI, Curran T. 1995. A protein related to extracellular matrix proteins deleted in the mouse mutant reeler. Nature. 374:719-23.

Dahmane N, Ruiz i Altaba A. 1999. Sonic hedgehog regulates the growth and patterning of the cerebellum. Development. 126:3089-100.

Dulabon L, Olson EC, Taglienti MG, Eisenhuth S, McGrath B, Walsh CA, Kreidberg JA, Anton ES. 2000. Reelin binds alpha3beta1 integrin and inhibits neuronal migration. Neuron. 27:33-44.

Falconer DS. 1951. Two new mutants, *trembler* and *reeler*, with neurological actions in the house mouse. J Genet. 50:192-201.

Goffinet AM. 1992. The reeler gene: a clue to brain development and evolution. Int J Dev Biol. 36:101-7.

Gross MK, Dottori M, Goulding M. 2002. Lbx1 specifies somatosensory association interneurons in the dorsal spinal cord. Neuron. 34:535-49.

Hargreaves K, Dubner R, Brown F, Flores C, Joris J. 1988. A new and sensitive method for measuring thermal nociception in cutaneous hyperalgesia. Pain. 32:77-88.

Hatten ME. 1985. Neuronal regulation of astroglial morphology and proliferation in vitro. J Cell Biol. 100:384-96.

Helms AW, Johnson JE. 2003. Specification of dorsal spinal cord interneurons. Curr Opin Neurobiol. 13:42-9.

Herz J, Chen Y. 2006. Reelin, lipoprotein receptors and synaptic plasticity. Nat Rev Neurosci. 7:850-9.

Hiesberger T, Trommsdorff M, Howell BW, Goffinet A, Mumby MC, Cooper JA, Herz J. 1999. Direct binding of Reelin to VLDL receptor and ApoE receptor 2 induces tyrosine phosphorylation of disabled-1 and modulates tau phosphorylation. Neuron. 24:481-9.

Howell BW, Gertler FB, Cooper JA. 1997a. Mouse disabled (mDab1): a Src binding protein implicated in neuronal development. EMBO J. 16:121-32.

Howell BW, Hawkes R, Soriano P, Cooper JA. 1997b. Neuronal position in the developing brain is regulated by mouse disabled-1. Nature. 389:733-7.

Howell BW, Lanier LM, Frank R, Gertler FB, Cooper JA. 1999. The disabled 1 phosphotyrosine-binding domain binds to the internalization signals of transmembrane glycoproteins and to phospholipids. Mol Cell Biol. 19:5179-88.

Ikeda Y, Terashima T. 1997. Expression of reelin, the gene responsible for the reeler mutation, in embryonic development and adulthood in the mouse. Dev Dyn. 210:157-72.

König N, Valat J, Fulcrand J, Marty R. 1977. The time of origin of Cajal-Retzius cells in the rat temporal cortex. An autoradiographic study. Neurosci Lett. 4:21-6.

Krüger MT, Zhao S, Chai X, Brunne B, Bouché E, Bock HH, Frotscher M. 2010. Role for Reelin-induced cofilin phosphorylation in the assembly of sympathetic preganglionic neurons in the murine intermediolateral column. Eur J Neurosci. 32:1611-7.

Kubasak MD, Brooks R, Chen S, Villeda SA, Phelps PE. 2004. Developmental distribution of reelin-positive cells and their secreted product in the rodent spinal cord. J Comp Neurol. 468:165-78.

Lai HC, Seal RP, Johnson JE. 2016. Making sense out of spinal cord somatosensory development. Development. 143:3434-48.

Magdaleno S, Keshvara L, Curran T. 2002. Rescue of ataxia and preplate splitting by ectopic expression of Reelin in reeler mice. Neuron. 33:573-86.

Mariani J, Crepel F, Mikoshiba K, Changeux JP, Sotelo C. 1977. Anatomical, physiological and biochemical studies of the cerebellum from Reeler mutant mouse. Philos Trans R Soc Lond B Biol Sci. 281:1-28.

Matsuki T, Pramatarova A, Howell BW. 2008. Reduction of Crk and CrkL expression blocks reelin-induced dendritogenesis. J Cell Sci. 121:1869-75.

Meyer G, Goffinet AM. 1998. Prenatal development of reelin-immunoreactive neurons in the human neocortex. J Comp Neurol. 397:29-40.

Miyata T, Nakajima K, Mikoshiba K, Ogawa M. 1997. Regulation of Purkinje cell alignment by reelin as revealed with CR-50 antibody. J Neurosci. 17:3599-609.

Müller T, Brohmann H, Pierani A, Heppenstall PA, Lewin GR, Jessell TM, Birchmeier C. 2002. The homeodomain factor Lbx1 distinguishes two major programs of neuronal differentiation in the dorsal spinal cord. Neuron. 34:551-62.

Nadarajah B, Brunstrom JE, Grutzendler J, Wong RO, Pearlman AL. 2001. Two modes of radial migration in early development of the cerebral cortex. Nat Neurosci. 4:143-50.

Niu S, Renfro A, Quattrocchi CC, Sheldon M, D'Arcangelo G. 2004. Reelin promotes hippocampal dendrite development through the VLDLR/ApoER2-Dab1 pathway. Neuron. 41:71-84.

Ogawa M, Miyata T, Nakajima K, Yagyu K, Seike M, Ikenaka K, Yamamoto H, Mikoshiba K. 1995. The reeler gene-associated antigen on Cajal-Retzius neurons is a crucial molecule for laminar organization of cortical neurons. Neuron. 14:899-912.

Olson EC, Kim S, Walsh CA. 2006. Impaired neuronal positioning and dendritogenesis in the neocortex after cell-autonomous Dab1 suppression. J Neurosci. 26:1767-75.

Palmesino E, Rousso DL, Kao TJ, Klar A, Laufer E, Uemura O, Okamoto H, Novitch BG, Kania A. 2010. Foxp1 and lhx1 coordinate motor neuron migration with axon trajectory choice by gating Reelin signaling. PLoS Biol. 8:e1000446.

Phelps PE, Barber RP, Vaughn JE. 1991. Embryonic development of choline acetyltransferase in thoracic spinal motor neurons: somatic and autonomic neurons may be derived from a common cellular group. J Comp Neurol. 307:77-86.

Phelps PE, Barber RP, Vaughn JE. 1993. Embryonic development of rat sympathetic preganglionic neurons: possible migratory substrates. J Comp Neurol. 330:1-14.

Phelps PE, Rich R, Dupuy-Davies S, Ríos Y, Wong T. 2002. Evidence for a cell-specific action of Reelin in the spinal cord. Dev Biol. 244:180-98.

Pujadas L, Gruart A, Bosch C, Delgado L, Teixeira CM, Rossi D, de Lecea L, Martínez A, Delgado-García JM, Soriano E. 2010. Reelin regulates postnatal neurogenesis and enhances spine hypertrophy and long-term potentiation. J Neurosci. 30:4636-49.

Qiu S, Zhao LF, Korwek KM, Weeber EJ. 2006. Differential reelin-induced enhancement of NMDA and AMPA receptor activity in the adult hippocampus. J Neurosci. 26:12943-55.

Rice DS, Curran T. 1999. Mutant mice with scrambled brains: understanding the signaling pathways that control cell positioning in the CNS. Genes Dev. 13:2758-73.

Rice DS, Sheldon M, D'Arcangelo G, Nakajima K, Goldowitz D, Curran T. 1998. Disabled-1 acts downstream of Reelin in a signaling pathway that controls laminar organization in the mammalian brain. Development. 125:3719-29.

Sekine K, Honda T, Kawauchi T, Kubo K, Nakajima K. 2011. The outermost region of the developing cortical plate is crucial for both the switch of the radial migration mode and the Dab1-dependent "inside-out" lamination in the neocortex. J Neurosci. 31:9426-39.

Sekine K, Kawauchi T, Kubo K, Honda T, Herz J, Hattori M, Kinashi T, Nakajima K. 2012. Reelin controls neuronal positioning by promoting cell-matrix adhesion via inside-out activation of integrin α5β1. Neuron. 76:353-69.

Sheldon M, Rice DS, D'Arcangelo G, Yoneshima H, Nakajima K, Mikoshiba K, Howell BW, Cooper JA, Goldowitz D, Curran T. 1997. Scrambler and yotari disrupt the disabled gene and produce a reeler-like phenotype in mice. Nature. 389:730-3.

Strasser V, Fasching D, Hauser C, Mayer H, Bock HH, Hiesberger T, Herz J, Weeber EJ, Sweatt JD, Pramatarova A, Howell B, Schneider WJ, Nimpf J. 2004. Receptor clustering is involved in Reelin signaling. Mol Cell Biol. 24:1378-86.

Teixeira CM, Kron MM, Masachs N, Zhang H, Lagace DC, Martinez A, Reillo I, Duan X, Bosch C, Pujadas L, Brunso L, Song H, Eisch AJ, Borrell V, Howell BW, Parent JM, Soriano E. 2012. Cell-autonomous inactivation of the reelin pathway impairs adult neurogenesis in the hippocampus. J Neurosci. 32:12051-65.

Tissir F, Goffinet AM. 2003. Reelin and brain development. Nat Rev Neurosci. 4:496-505.

Todd AJ. 2010. Neuronal circuitry for pain processing in the dorsal horn. Nat Rev Neurosci. 11:823-36.

Trommsdorff M, Gotthardt M, Hiesberger T, Shelton J, Stockinger W, Nimpf J, Hammer RE, Richardson JA, Herz J.1999. Reeler/Disabled-like disruption of neuronal migration in knockout mice lacking the VLDL receptor and ApoE receptor 2. Cell. 97:689-701.

Villeda SA, Akopians AL, Babayan AH, Basbaum AI, Phelps PE. 2006. Absence of Reelin results in altered nociception and aberrant neuronal positioning in the dorsal spinal cord. Neuroscience. 139:1385-96.

Wang X, Babayan AH, Basbaum AI, Phelps PE. 2012. Loss of the Reelin-signaling pathway differentially disrupts heat, mechanical and chemical nociceptive processing. Neuroscience. 226:441-50.

Weeber EJ, Beffert U, Jones C, Christian JM, Forster E, Sweatt JD, Herz J. 2002. Reelin and ApoE receptors cooperate to enhance hippocampal synaptic plasticity and learning. J Biol Chem. 277:39944-52.

Yip JW, Yip YP, Nakajima K, Capriotti C. 2000. Reelin controls position of autonomic neurons in the spinal cord. Proc Natl Acad Sci U S A. 97:8612-6.

Yvone GM, Zhao-Fleming HH, Udeochu JC, Chavez-Martinez CL, Wang A, Hirose-Ikeda M, Phelps PE. 2017. Disabled-1 dorsal horn spinal cord neurons co-express Lmx1b and function in nociceptive circuits. Eur J Neurosci. 45:733-747.

*Chapter 2*

## Disabled-1 dorsal horn spinal cord neurons co-express Lmx1b and function in nociceptive circuits

Yvone GM, Zhao-Fleming HH, Udeochu JC, Chavez-Martinez CL, Wang A, Hirose-Ikeda M, Phelps PE. 2017. Disabled-1 dorsal horn spinal cord neurons co-express Lmx1b and function in nociceptive circuits. Eur J Neurosci. 45:733-747.

### Abstract

The Reelin-signaling pathway is essential for correct neuronal positioning within the central nervous system. Mutant mice with a deletion of Reelin, its lipoprotein receptors, or its intracellular adaptor protein Disabled-1 (Dab1), exhibit nociceptive abnormalities: thermal (heat) hyperalgesia and reduced mechanical sensitivity. To determine dorsal horn alterations associated with these nociceptive abnormalities, we first characterized the correctly positioned Dab1 neurons in wild-type and mispositioned neurons in Reelin-signaling pathway mutant lumbar spinal cord. Using immunofluorescence, we found that 70% of the numerous Dab1 neurons in *Reln*$^{+/+}$ laminae I–II and 67% of those in the lateral reticulated area and lateral spinal nucleus (LSN) co-express the LIM homeobox transcription factor 1 beta (Lmx1b), an excitatory glutamatergic neuron marker. Evidence of Dab1- and Dab1-Lmx1b neuronal positioning errors was found within the isolectin B4 terminal region of *Reln*$^{-/-}$ lamina IIinner and in the lateral reticulated area and LSN, where about 50% of the Dab1-Lmx1b neurons are missing. Importantly, Dab1-Lmx1b neurons in laminae I–II and the lateral reticulated area express Fos after noxious thermal or mechanical stimulation and thus participate in these circuits. In another pain relevant locus – the lateral cervical nucleus (LCN), we also found about a 50% loss of Dab1-Lmx1b neurons in *Reln*$^{-/-}$ mice. We suggest that extensively mispositioned Dab1 projection neurons in the lateral reticulated area, LSN, and LCN and the more subtle positioning

errors of Dab1 interneurons in laminae I–II contribute to the abnormalities in pain responses found in Reelin-signaling pathway mutants.

## Introduction

During development, the canonical Reelin pathway contributes to the correct positioning of specific neuronal populations, particularly in highly laminated areas including cerebral and cerebellar cortices (Rice *et al*., 1998; Rice and Curran, 2001; Honda *et al.*, 2011). Reelin is secreted by neurons and binds to two lipoprotein receptors, Apolipoprotein E receptor 2 (Apoer2) and the Very-low-density lipoprotein receptor (Vldlr), which are expressed on nearby neurons. Reelin binding recruits the adaptor protein Dab1 to the intracellular domains of the lipoprotein receptors and stimulates Dab1 phosphorylation by Src-family kinases. This phosphorylation event initiates the downstream signaling necessary for correct neuronal positioning after which migration ceases (Howell *et al*., 1997; Arnaud *et al*., 2003; Bock and Herz, 2003). Mice with mutations in various components of the Reelin-signaling pathway produce similar positioning errors in the central nervous system (CNS; Howell *et al*., 1997; Trommsdorff *et al*., 1999).

The role of Reelin signaling is extensively studied in higher brain structures, but much less is understood in the spinal cord. Sympathetic and parasympathetic preganglionic neurons in *Reln*$^{-/-}$, *Apoer2*$^{-/-}$*/Vldlr*$^{-/-}$, and *dab1*$^{-/-}$ mice have extensive alterations in their migratory pathways as they fail to stop in their normal lateral locations and instead are found medially (Yip *et al*., 2000; Phelps *et al*., 2002; Yip *et al*., 2004). In comparison, the somatic motor neurons in *Reln*$^{-/-}$ and *dab1*$^{-/-}$ mice have more subtle positioning errors in the ventral spinal cord (Palmesino *et al*., 2010; Abadesco *et al*., 2014).

Previously we reported that *Reln*$^{-/-}$ and *dab1*$^{-/-}$ mice have pronounced dysfunction in pain processing, including increased noxious heat and reduced noxious mechanical sensitivity (Villeda *et al*., 2006; Akopians *et al*., 2008; Wang *et al*., 2012). Despite the extensive functional

nociceptive alterations in mutants, the anatomical changes in *Reln*$^{-/-}$ and *dab1*$^{-/-}$ dorsal horns that lead to these abnormalities remain unclear. Information about noxious stimuli is relayed by nociceptors in the dorsal root ganglion to discrete laminae of the superficial dorsal horn (i.e., laminae I-II; Basbaum *et al*., 2009; Todd, 2010). Some injury messages are transmitted directly via spinal cord projection neurons, whereas most information first engages interneuronal circuits in the dorsal horn; these interneurons, in turn, transmit the information to the projection neurons in the deep dorsal horn and from there to the brainstem and brain (Basbaum *et al*., 2009; Todd, 2010). Notably, Reelin- and Dab1-expressing neurons are distributed in dorsal horn areas associated with nociception, including the superficial dorsal horn, and two regions containing projection neurons, the lateral reticulated area of lamina V and the LSN (Menétrey *et al*., 1982; Burstein *et al*., 1987; Kayalioglu *et al*., 1999; Kubasak *et al*., 2004; Villeda *et al*., 2006; Akopians *et al*., 2008; Wang *et al*., 2012). In previous studies, however, we did not identify differences in nociceptor termination patterns in Reelin-signaling pathway mutants (Villeda *et al*., 2006; Akopians *et al*., 2008) which suggests that the defects in mutants lie within the dorsal horn circuitry.

To better understand how the disruption of Reelin signaling alters thermal and mechanical nociceptive circuits, we aim to identify the phenotype of Dab1-labeled dorsal horn neurons. Mispositioned Reelin-responsive neurons can be identified in *Reln*$^{-/-}$ by their high levels of Dab1 expression compared to wild-type neurons that continually ubiquitinate and degrade Dab1 (Howell *et al*., 1997; Rice *et al*., 1998). Additionally, we will examine a less well-known nociceptive area in cervical levels C1-3, the lateral cervical nucleus (LCN), a region that contains ascending projection neurons involved in thermal and mechanical pain processing (Giesler *et al*., 1979; Kajander and Giesler, 1987; Burstein *et al*., 1990). We suspect that the mispositioning of

multiple populations of Dab1-positive dorsal horn neurons contributes to the extensive nociceptive abnormalities observed in mutant mice of the Reelin pathway.

## Materials and Methods

### Animals

The *dab1*$^{lacZ}$ mice: The generation and characterization of *dab1*$^{lacZ}$ mice were described in Pramatarova *et al*. (2008) and Abadesco *et al*. (2014), and mice were obtained from Dr. Brian Howell (SUNY Upstate Medical University, Syracuse, NY). The *dab1*$^{lacZ/+}$ mice have one normal allele that expresses *dab1*, whereas in *dab1*$^{lacZ/lacZ}$ mice, *dab1* expression is eliminated.

*Reln* mice: We used adult *Reln* mice to investigate Dab1 expression in mutants. The *Reln* (B6C3Fe-ala-*Reln*$^{rl}$) mice were originally obtained from Jackson Laboratory.

*Reln*$^{rl\text{-}Orl}$; *GAD67*$^{GFP}$ mice: The *Reln*$^{rl\text{-}Orl}$ strain was previously described by Takahara *et al.* (1996) and the *GAD67*$^{GFP}$ line was generated by Tamamaki *et al*. (2003). These mice were interbred as described in Abadesco *et al*. (2014) to determine if Dab1 neurons were GABAergic. Genotyping of *dab1*$^{lacZ}$, *Reln*, and *Reln*$^{rl\text{-}Orl}$*; GAD67*$^{GFP}$ mice was adapted from Pramatarova *et al.* (2008), D'Arcangelo *et al.* (1996), and Hammond *et al*. (2006), respectively.

### Behavioral tests

All experiments were approved by the Chancellor's Animal Research Committee at UCLA and conducted according to the National Institute of Health guidelines. Earlier studies of *Reln* or *dab1* mice found that their responses did not differ by sex (Villeda *et al*., 2006; Akopians *et al*., 2008).

*1. Thermal (heat) Hargreaves test*: Thermal nociception was examined with the Hargreaves' paw withdrawal test (model 336G stimulator, IITC; Hargreaves *et al*., 1988). Prior to testing, the optimal intensity of the heat source was determined to be 12% to elicit a 10 sec response from wild-type mice. Six males of all three genotypes (*dab1*$^{+/+}$, *dab1*$^{lacZ/+}$, and *dab1*$^{lacZ/lacZ}$) were acclimated in clear plastic tubes for 45 min before the heat source was focused onto the plantar

surface of the hind paws for 3 trials each and withdrawal responses were recorded. This model turns off at 20 secs to prevent injury.

*2. Thermal (heat) Fos stimulation*: Five to seven age-matched sets of female mice, lightly anesthetized with Sodium Pentobarbital (50-60 mg/kg), were used and 15 mins after anesthesia induction, the left hindpaw was dipped into 50ºC water for 3 sec/min for 10 min. Due to the inconsistent responses of *dab1*$^{lacZ/+}$ and *dab1*$^{lacZ/lacZ}$ mice to the anesthetic, we set criteria for inclusion into the study. Mice were judged to be over-sedated if they responded to less than 8 of the 10 stimulations or under-sedated if their response to the heat involved exaggerated full body movements. We let such mice recover and re-tested them 1-2 weeks later.

*3. Mechanical von Frey test*: Five to six male mice of each genotype were placed in plastic chambers on an elevated wire mesh for 1 hr before testing with the up-down paradigm of Chaplan (Chaplan *et al*., 1994). Calibrated von Frey monofilaments (0.008 - 4.0 g) were applied to the center of the plantar surface of the left hindpaw in series, starting with the 0.4 filament. Responses were tabulated and the 50% response for the withdrawal threshold was determined.

*4. Mechanical Fos stimulation*: Six to seven age-matched male mice from all three genotypes were used and set up as described above for thermal Fos stimulation. The left hindpaw was stimulated with a padded alligator clip for 20 sec every 3 min for 15 min. The same criteria as reported for thermal Fos experiments were used to decide whether to continue with the experiment or re-test later.

**Tissue preparation and immunohistochemistry**

One hour after noxious stimulation, *dab1*$^{lacZ}$ mice were re-anesthetized (Sodium Pentobarbital, 100 mg/kg) and perfused transcardially with 4% paraformaldehyde, and post-fixed for 1 hour (4ºC) in the same fixative. *Reln* and *Reln*$^{rl\text{-}Orl}$*;GAD67*$^{GFP}$ mice received the same fixative but

with a 1-3-hour post-fix. Following an overnight wash with 0.12M phosphate buffer (PB), spinal cords were dissected and cryoprotected in 30% sucrose/PB for 2-3 days. Upper cervical (C1-3) and lumbar (L4-5) segments were blocked and frozen in Optimum Cutting Temperature (Sakura) and stored at -80ºC.

To evaluate Fos expression, we immunostained 5-6 40 µm coronal cryostat sections per mouse lumbar levels 4-5. We used rabbit anti-Fos (1:10,000; Calbiochem, PC38) with 0.1M Tris buffer with 1.4% NaCl and 0.1% bovine serum albumin (TBS). Standard avidin-biotin techniques combined with Nickle-intensified diaminobenzidine were used to visualize Fos expression. Sections were mounted, dried, dehydrated, cleared and coverslipped. Coronal or sagittal sections (25-30 µm) were used for double immunofluorescent experiments.

*β-galactosidase histochemistry:* Free-floating sections were washed with PB, preincubated for 2-7 h in an X-gal reaction buffer [5 mM $K_3Fe(CN)_6$, 5 mM $K_4Fe(CN)_6$-$3H_2O$, 1 mM $MgCl_2$, 0.01% deoxycholic acid and 0.02% Igepal; Sigma] and reacted in the same buffer plus 1 mg/mL X-gal (Gold Biotechnology) for 1–12 h. After staining, sections were washed with PB and processed for diaminobenzidine immunohistochemistry (Abadesco *et al*., 2014).

*Immunohistochemical procedures:* Following β-gal localization, a rabbit antiserum to Dab1 (B3; 1:5,000-1:10,000; generous gift of Dr. Brian Howell; Howell *et al*., 1997) was used to detect Dab1 protein in free-floating spinal cord sections as in Abadesco *et al*. (2014). Other primary antibodies used include: guinea pig anti-Lmx1b (1:20,000; generous gift of Drs. Müller and Birchmeier; Müller *et al*., 2002), chick anti-Green Fluorescent Protein (GFP; 1:1,000; Aves Labs, GFP-1020), goat anti-Choline acetyltransferase (ChAT; 1:750; Chemicon, AB144P), mouse anti-Neuronal nuclei (NeuN; 1:900; Millipore, MAB377), and rabbit anti-Neurokinin-1

receptor (NK1R; 1:8,000; Sigma, S8305). Isolectin B4 (IB4) was visualized using a biotinylated IB4 conjugate (1:200; Vector, B-1205).

Most double or triple-labeling immunofluorescence experiments used the Tyramide Signal Amplification Plus kit (PerkinElmer) as reported (Shields *et al*., 2010; Abadesco *et al*., 2014), together with the appropriate biotinylated secondary antibodies. All secondary antibodies were purchased from Jackson Immunoresearch. Those used at a 1:500 dilution were donkey anti-chick Alexa Fluor 488, and biotinylated donkey anti-mouse or rabbit for diaminobenzidine reactions. Streptavidin Alexa Fluor 488 (1:1,000) was used for the IB4 conjugate. For Dab1-Fos-Lmx1b triple labeling, citric acid treatment was performed as described in Abadesco *et al*. (2014) to co-localize two rabbit antisera, i.e. Dab1 and Fos.

A Zeiss Laser Scanning Microscope (LSM510) was used to obtain thin confocal images of the immunofluorescent co-localization as stated in the figure legends. Low magnification confocal images were obtained with 10x, and high magnification images, with a 40x objective. Each confocal image represents a 3 µm thick slice except for those of the lateral reticulated area and LSN. Due to the small number of neurons present in these two areas, their 3 µm slices were collapsed into a single image. Fluorescent and brightfield images were collected with a Zeiss AxioCam HRc camera on an Olympus AX70 microscope. Images were analyzed with LSM Image browser, and then transferred to Photoshop for assembly, cropping, and adjustment of brightness and contrast.

**Statistical Analyses**

*Fos stimulation studies*: Five to six hemisections per mouse with the highest number of Fos-localized cells were photographed and analyzed. Laminae I-II, III-IV, V-VI, and the LSN were delineated and Fos-positive cells/area counted as in Wang *et al.* (2012). The means of Fos-

positive cells were compared by genotype and spinal area using a 3 x 4 repeated measures two-way analysis of variance (ANOVA) model where the spinal area is the repeated within-group factor and genotype is the between-group factor. Under this ANOVA model, *post hoc* mean comparisons were judged significant using the Fisher least significant difference criterion unless specified. For the Hargreaves test, mean values were evaluated with ANOVA. For the von Frey test, significance of the mean threshold values was evaluated with the Kruskal-Wallis test. Calculations were carried out with JMP 10 (SAS Inc.) or Sigma Plot 12.0 (Systat Software Inc.), respectively.

*Mispositioning and Dab1-Lmx1b co-localization analyses:* Coronal sections at lumbar 4-5 levels were imaged with confocal microscopy. Between 5-7 hemisections per mouse from 4-5 *Reln* pairs were analyzed. Cell counting in the superficial dorsal horn was carried out in a single 3 µm confocal slice. The superficial dorsal horn and LSN were determined as in Wang *et al*. (2012). The delineation of the LCN/LSN in cervical levels C1-3 is shown in the LCN figure. Cells in the lateral reticulated area of lamina V were counted in a box (17000 $\mu m^2$) drawn on the 40x confocal image with the LSN as the lateral border. The means of Dab1- and Dab1-Lmx1b-labeled cells were compared by genotype and/or area for each cell type with a 1 x 2 or 2 x 2 repeated measures two-way ANOVA and *post-hoc* t-tests. Significance of other analyses including IB4 area measurements, NeuN and NK1R width for the LCN/LSN were determined using ANOVA and *post-hoc* t-tests. Calculations were done using Microsoft Excel or with JMP 10 (SAS Inc.).

## Results

### The *dab1*$^{lacZ/lacZ}$ mice have increased thermal sensitivity and enhanced Fos expression

Before characterizing the dorsal horn in *dab1*$^{lacZ}$ mice, we asked if the nociceptive behavior of *dab1*$^{lacZ/+}$ mice was comparable to *dab1*$^{+/+}$ and if *dab1*$^{lacZ/lacZ}$ mice displayed nociceptive abnormalities typical of other Reelin-signaling pathway mutants. Results from the Hargreaves test of thermal sensitivity found no differences in the withdrawal latencies between *dab1*$^{+/+}$ and *dab1*$^{lacZ/+}$ mice, whereas *dab1*$^{lacZ/lacZ}$ mice had a significantly shorter latency (Fig. 2A).

We used Fos expression following noxious heat stimulation as a marker of neuronal activity and found no differences between the number of Fos-labeled cells in the *dab1*$^{+/+}$ and *dab1*$^{lacZ/+}$ dorsal horns (Fig. 2B). The *dab1*$^{+/+}$ and *dab1*$^{lacZ/+}$ laminae I-II had fewer Fos-labeled cells than in *dab1*$^{lacZ/lacZ}$ mice (Fig. 2B-E). However, in the *dab1*$^{+/+}$ and *dab1*$^{lacZ/+}$ LSN (Fig. 2C-E, short arrows), there were more Fos-labeled nuclei than in *dab1*$^{lacZ/lacZ}$ mice (Fig. 2B-E). These somewhat contradictory findings can be explained by the 50% reduction in the number of neurons in the LSN of Reelin-signaling pathway mutants (Villeda *et al*., 2006; Akopians *et al*., 2008). Individual observations of the *dab1*$^{+/+}$ and *dab1*$^{lacZ/+}$ lateral reticulated area (Fig. 2C-E, long arrows) frequently had more Fos-expressing cells than those of *dab1*$^{lacZ/lacZ}$ mice, but the total cell numbers did not differ when evaluated in combination with laminae V-VI (Fig. 2B-E). Overall, our results confirm that *dab1*$^{lacZ/lacZ}$ mice display thermal hyperalgesia, as found in other Reelin-signaling pathway mutants (Villeda *et al*., 2006; Akopians *et al*., 2008).

### Reduced mechanical sensitivity and Fos expression characterize *dab1*$^{lacZ/lacZ}$ mice

Results from the Chaplan up-down test of mechanical sensitivity found no differences in the 50% withdrawal latencies between *dab1*$^{+/+}$ and *dab1*$^{lacZ/+}$ mice (Fig. 2F). The *dab1*$^{lacZ/lacZ}$ mice, however, had much higher mechanical thresholds (Fig. 2F). After noxious mechanical

stimulation the number of Fos-labeled cells did not differ between the *dab1*$^{+/+}$ and *dab1*$^{lacZ/+}$ dorsal horns (Fig. 2G), whereas the *dab1*$^{lacZ/lacZ}$ mice had fewer Fos-expressing cells in laminae I-II and LSN (Fig. 2G-J, short arrows). Again, Fos-labeled neurons in *dab1*$^{+/+}$ and *dab1*$^{lacZ/+}$ lateral reticulated area were greatly reduced in *dab1*$^{lacZ/lacZ}$ mice (Fig. 2H-J, long arrows). These results support our previous findings on reduced mechanical pain sensitivity in *Reln* and *dab1* mutants (Villeda *et al*., 2006; Akopians *et al*., 2008; Wang *et al*., 2012).

**Dab1 expression in the adult dorsal horn**

As mutations in the Reelin pathway cause abnormalities in neuronal positioning, we then characterized Dab1 expression in adult dorsal horn using a combination of β-gal histochemistry and Dab1 immunohistochemistry. In the superficial dorsal horn, it is difficult to distinguish Dab1-expressing neurons due to extensive terminal staining. Dab1 expression in *dab1*$^{+/+}$ appeared as diffuse reaction product and a few discernible neurons (small arrowheads in Fig. 3A). Several Dab1 cells are detected in laminae III-IV, while the lateral reticulated area of lamina V has a number of medium and a few large Dab1-labeled neurons (large arrowheads in Fig. 3A). The LSN contained strong Dab1 reaction product and a few labeled cells.

In the *dab1*$^{lacZ/+}$ dorsal horn, the β-gal reaction product and Dab1 immunoreactivity are found within the same areas and co-localize within cells of the lateral reticulated area (Fig. 3B and inset), confirming that both methods identify the same neurons. As expected, the *dab1*$^{lacZ/lacZ}$ dorsal horn contained only β-gal deposits which were concentrated in laminae I-II and the lateral reticulated area (Fig. 3C), similar to the protein expression pattern in *dab1*$^{+/+}$ dorsal horn (Fig. 3A). Because β-gal deposits are not found in axons of Dab1 neurons (Abadesco *et al*., 2014), the heavy β-gal product in the superficial dorsal horn suggests that there are many more Dab1-labeled neurons than we previously reported (Villeda *et al*., 2006; Akopians *et al*., 2008). The

heterogeneity in size and regional distribution suggests that Dab1 is widely expressed in several distinct dorsal horn populations.

**Superficial dorsal horn: most Dab1 cells co-express the transcription factor *Lmx1b***

Next, we sought to identify the phenotype of the small Dab1 neurons in laminae I-II that resemble the classically defined nociceptive-specific dorsal horn neurons. Because the majority of interneurons in this area are excitatory (Todd, 2010), we asked whether they were glutamatergic neurons. There are two homeobox proteins, Lmx1b and Tlx3 (T-Cell Leukemia Homeobox 3), that mark a late-generated dorsal neuron population ($dIL^B$) that migrates to the superficial laminae of the dorsal horn and differentiates into an excitatory glutamatergic phenotype (Gross *et al*., 2002; Müller *et al*., 2002; Cheng *et al*., 2004; Cheng *et al*., 2005; Dai *et al*., 2008; Rebelo *et al*., 2010). Because Lmx1b expression is maintained in adults (Dunston *et al*., 2005; Dai *et al*., 2008), we asked if Dab1 dorsal horn neurons express Lmx1b. The β-gal product was detected in the same $dab1^{lacZ/+}$ and $dab1^{lacZ/lacZ}$ dorsal horn areas as Lmx1b (data not shown). To better identify the Dab1-expressing neurons, we conducted double immunolabeling experiments, confocal imaging and extensive analyses on $Reln^{+/+}$ and $Reln^{-/-}$ dorsal horns and confirmed Dab1 and Lmx1b co-localization (Fig. 4A-F). Analyses of 3 µm confocal images revealed that 70% of the small to medium Dab1-expressing superficial dorsal horn neurons co-express Lmx1b (yellow arrowheads in Fig. 4B, B1-2, E, E1-2; $Reln^{+/+}$ 71±2%; $Reln^{-/-}$ 70±2%). Compared to $Reln^{+/+}$, there are a few medium and large-sized Dab1-Lmx1b neurons in $Reln^{-/-}$ laminae I-II (Fig. 4F; compare Fig. 4A to D and Fig. 4G to H) and dorsal funiculus (data not shown). Based on previous studies (Cheng *et al*., 2004; Cheng *et al*., 2005; Dai *et al*., 2008), the Dab1-Lmx1b neurons are likely to be glutamatergic.

We also tested other common markers of excitatory superficial dorsal horn neurons (Antal *et al*., 1991; Todd, 2010; Gutierrez-Mecinas *et al*., 2016). Although many Protein Kinase C gamma (PKCγ)-positive interneurons express Lmx1b, none of the Dab1-labeled neurons co-expressed PKCγ (data not shown). The Dab1 neurons also did not express Calretinin, but a few Dab1-Lmx1b neurons did contain Calbindin and Somatostatin (data not shown). Additionally, our previous studies showed that a few Dab1 dorsal horn neurons expressed the Neurokinin-1 receptor that binds substance P and were mispositioned in Reelin-signaling pathway mutant dorsal horns (Villeda *et al*., 2006; Akopians *et al*., 2008). We conclude that most of the Dab1 neurons in the superficial dorsal horn are excitatory glutamatergic neurons.

**Superficial dorsal horn: Dab1-Lmx1b-expressing neurons are mispositioned in *Reln*$^{-/-}$ mice**

As mispositioned neurons in *Reln*$^{-/-}$ mice tend to express high levels of Dab1, we compared the distribution of Dab1 and Dab1-Lmx1b neurons in *Reln*$^{+/+}$ and *Reln*$^{-/-}$ superficial dorsal horn. Initial analyses divided laminae I-II into equal-sized bins in both the mediolateral and dorsoventral divisions, but the number of Dab1 neurons per bin did not differ between genotypes.

Because the superficial dorsal horn lamination pattern is precisely defined by primary afferent terminations, we next focused our analysis on lamina II inner, which is marked by isolectin B4 (IB4) and receives nonpeptidergic nociceptive afferents (Basbaum *et al*., 2009; Todd, 2010). Although the area identified by IB4-positive afferents did not vary by genotype, we found fewer Dab1-only (*Reln*$^{+/+}$ 4±0.4; *Reln*$^{-/-}$ 8±1; $p$=0.002, Fig. 4I) and Dab1-Lmx1b neurons (*Reln*$^{+/+}$ 13±2; *Reln*$^{-/-}$ 18±2; $p$=0.043, Fig. 4I) in the *Reln*$^{+/+}$ than *Reln*$^{-/-}$ IB4 region. Additionally, the IB4 band in *Reln*$^{-/-}$ lamina II inner appeared shifted dorsally and perhaps laterally (Fig. 4G-H). Consistent with the more dorsal location of IB4-positive terminals, the area of laminae I-II

outer was larger in *Reln*$^{+/+}$ than in *Reln*$^{-/-}$ mice (*Reln*$^{+/+}$ 17,444± 1,357 μm$^2$; *Reln*$^{-/-}$ 11,264± 978 μm$^2$; $p$=0.002, Fig. 4G-H). Despite the reduced area in *Reln*$^{-/-}$ laminae I-II outer, the number of Dab1 cells in this area did not vary by genotype (Fig. 4I). To verify that the Dab1 cells did not die selectively in *Reln*$^{-/-}$, we compared total Dab1 neurons per 3 μm hemisections of *Reln*$^{+/+}$ (65±14 neurons) and *Reln*$^{-/-}$ (77±11 neurons) mice and found no significant difference ($p$=0.15). Thus, the Dab1- and Dab1-Lmx1b-labeled laminae I-II neurons, and the IB4-positive terminals all appear to be mispositioned in *Reln*$^{-/-}$ superficial dorsal horn.

**Superficial dorsal horn: several Dab1 neurons are GABAergic**

After finding that 70% of the Dab1 superficial dorsal horn neurons are excitatory, we asked if the other Dab1 neurons in laminae I-II might be inhibitory and express glutamic acid decarboxylase (GAD67). To best answer this question, we used *Reln*$^{rl\text{-}Orl}$ mice interbred with a well-characterized *GAD67*$^{GFP}$ line that expresses GFP under the GAD67 promoter (Tamamaki *et al.*, 2003; Abadesco *et al*., 2014). The majority of GAD67$^{GFP}$-labeled neurons did not co-localize with Dab1 in *Reln*$^{rl\text{-}Orl/+}$ or *Reln*$^{rl/Orl/rl\text{-}Orl}$ superficial dorsal horn (Fig. 5A-D). A few double-labeled neurons were present, however, in laminae I-II (yellow arrowheads in Fig. 5B, B1-2, D, D1-2). We also observed Dab1 and Dab1-GAD67$^{GFP}$ neurons in the white matter dorsal to lamina I in *Reln-Orl*$^{+/+}$ (Fig. 5E1-3) and *Reln*$^{rl/Orl/rl\text{-}Orl}$ (Fig. 5F1-3) sagittal sections. More large Dab1-immunoreactive neurons appeared to be located in *Reln*$^{rl/Orl/rl\text{-}Orl}$ than in *Reln-Orl*$^{+/+}$ superficial dorsal horn (Fig. 5F1, 3 vs. 5E1, 3). Markers of subsets of GABAergic dorsal horn interneurons, such as those that express neuronal nitric acid synthase, Parvalbumin, and ChAT also were tested and did not co-localize with Dab1 cells (Fig. 5G-H; data not shown; Laing *et al*., 1994). We conclude that relatively few Dab1 neurons are inhibitory.

**Lateral reticulated area and LSN: Dab1-Lmx1b neurons are mispositioned in *Reln*$^{-/-}$ mice**

Previously we found Dab1 neurons in the lateral reticulated area of lamina V, an important nociceptive area containing projection neurons for which few markers have been identified. Here we asked if the Dab1 neurons in the lateral reticulated area also express Lmx1b and found that 67% of Dab1 neurons co-express Lmx1b in both genotypes (Fig. 6A, yellow arrowheads in Fig. 6C, C1-2, E, E1-2). We then analyzed both Dab1- and Dab1-Lmx1b-labeled neurons to look for evidence of neuronal positioning errors in *Reln*$^{-/-}$ mice. Greater numbers of Dab1-Lmx1b neurons are found in the *Reln*$^{+/+}$ (4±0.4) than in *Reln*$^{-/-}$ lateral reticulated area (2±0.3; $p$=0.0004, Fig. 6G), whereas fewer single-labeled Dab1 neurons are present in *Reln*$^{+/+}$ (2±0.3) than *Reln*$^{-/-}$ mice (4±0.6; $p$=0.002, Fig. 6G). Several cholinergic neurons in the lateral reticulated area (Phelps *et al*., 1984) also expressed Dab1 in *Reln*$^{+/+}$ and *Reln*$^{-/-}$ mice (yellow arrowheads in Fig. 5G1-3 and 5H1-3), but due to the small number of double-labeled cells, positioning errors were not evaluated.

As with other Reelin pathway mutants, we recorded about 50% more NeuN-labeled neurons in the LSN of *dab1*$^{+/+}$ and *dab1*$^{lacZ/+}$ than found in *dab1*$^{lacZ/lacZ}$ mice (*dab1*$^{+/+}$ 11±1; *dab1*$^{lacZ/+}$ 11±1; *dab1*$^{lacZ/lacZ}$ 5±1; *dab1*$^{+/+}$ vs. *dab1*$^{lacZ/lacZ}$ $p$=0.003; *dab1*$^{lacZ/+}$ vs. *dab1*$^{lacZ/lacZ}$ $p$=0.004; Villeda *et al*., 2006; Akopians *et al*., 2008). Here we report that almost 70% of the Dab1 neurons in the LSN co-express Lmx1b (Fig. 6B, yellow arrowheads in Fig. 6D, D1-2, F, F1-2), with almost twice as many Dab1-Lmx1b neurons in *Reln*$^{+/+}$ (3.2±0.5) than *Reln*$^{-/-}$ LSN (1.7±0.2; $p$=0.008, Fig. 6H). The total Dab1-positive neurons in *Reln*$^{+/+}$ (5±1) is also greater than in *Reln*$^{-/-}$ LSN (3±0.3; $p$=0.02, Fig. 6H). Thus, Dab1 cells from the lateral reticulated area and the LSN are incorrectly positioned in *Reln*$^{-/-}$ mice, including those that co-localize with Lmx1b.

**Dab1-Lmx1b-positive neurons participate in nociceptive circuits**

Having determined that the majority of the Dab1-expressing neurons in the superficial dorsal horn, lateral reticulated area, and LSN co-express Lmx1b, we next asked if the Dab1-Lmx1b neurons are activated by noxious thermal or mechanical stimulation. We found clear examples of Fos protein expression in Dab1-Lmx1b-positive neurons in *dab1*$^{+/+}$ and *Reln*$^{+/+}$ superficial dorsal horn (Fig. 7A, A1-4, C, C1-4). Triple-labeled cells (white arrowheads) in the wild-type lateral reticulated area (Fig. 7B, B1-4, D, D1-4) also were detected after thermal or mechanical stimulation. Dab1-Fos- (magenta arrows) and Lmx1b-Fos- (cyan arrows) expressing neurons also were evident (colored arrows in Fig. 7A, A1-3, B, B1-3, C, C1-3, D, D1-3). Thus Dab1-, Lmx1b-, and Dab1-Lmx1b neurons participate in both noxious heat and mechanical circuits.

**Lateral cervical nucleus: Dab1 neurons sustain positioning errors in Reelin-signaling pathway mutants**

The neurons of the lateral cervical nucleus (LCN; Fig. 8A) are surrounded by axons of the dorsolateral funiculus, but only in cervical levels 1-3 (Kajander and Giesler, 1987). The areas of LCN and LSN cannot be differentiated in these upper cervical levels and thus are analyzed together (Burstein *et al*., 1990). The LCN neurons receive nociceptive information from neurons throughout the spinal cord and convey it rostrally as part of the spinocervicothalamic pathway (Giesler *et al*., 1979; Kajander and Giesler, 1987; Burstein *et al*., 1990). Most LCN neurons project to contralateral thalamus and respond to a wide-range of innocuous and noxious thermal and mechanical stimuli (Giesler *et al*., 1979; Kajander and Giesler, 1987).

Due to the importance of this area in relaying nociceptive information, we first examined the LCN to determine if neuronal mispositioning in this region might contribute to the sensory abnormalities in Reelin pathway mutants. The Dab1 expression in the C1-3 segments had strong

immunoreactivity in neurons of laminae I-II and in the combined LCN/LSN (Fig. 8B-D). The *dab1*$^{lacZ/+}$ LCN/LSN contains neurons that are double-labeled with β-gal and Dab1 (brown, Fig. 8E), whereas the *dab1*$^{lacZ/lacZ}$ has only β-gal concentrated in laminae I-II, the lateral reticulated area, and in the LCN/LSN area (Fig. 8F). This demonstrates that the pattern of Dab1 expression at high cervical levels resembles that in lumbar spinal cord (Fig. 3).

We next asked if LCN neurons are mispositioned in *dab1*$^{lacZ/lacZ}$ mice. The *dab1*$^{+/+}$ LCN/LSN contained an average of 90±6 neurons/dorsal horn and did not differ from *dab1*$^{lacZ/+}$ LCN/LSN with 87±5 neurons. The *dab1*$^{lacZ/lacZ}$ LCN/LSN contained 46±2 NeuN-labeled neurons, 49% and 47% fewer neurons than in *dab1*$^{+/+}$ and *dab1*$^{lacZ/+}$ mice, respectively (*dab1*$^{+/+}$ vs. *dab1*$^{lacZ/lacZ}$ $p$=0.00002; *dab1*$^{lacZ/+}$ vs. *dab1*$^{lacZ/lacZ}$ $p$=0.00004; Fig. 8G-I). We also analyzed *Reln*$^{+/+}$ and *Reln*$^{-/-}$ LCN/LSN neurons and found that on average, *Reln*$^{+/+}$ LCN/LSN contained 78±7 neurons/dorsal horn while *Reln*$^{-/-}$ mice had 41±5 neurons, a 48% reduction in LCN/LSN neurons ($p$=0.007). Interestingly, nearly 50% of both *dab1*$^{lacZ/lacZ}$ and *Reln*$^{-/-}$ LCN/LSN neurons are displaced, findings which support our contention that this disruption is due to the loss of the canonical Reelin-Dab1 signaling pathway.

**The LCN/LSN contains fewer Dab1-Lmx1b neurons and is compressed in Reelin-signaling pathway mutants**

Previously we reported that the LSN contained many NK1R-labeled processes (Akopians *et al.*, 2008). Therefore, to further analyze the LCN/LSN, we estimated the width of this region by measuring the distribution of NK1R expression in *dab1*$^{lacZ}$ and *Reln* C1-3 segments. NK-1R expression in the LCN/LSN area was measured from the base of the dorsal horn to the most ventral processes that express NK-1R. This distance was greater in the *dab1*$^{+/+}$ (146±6 μm) and *dab1*$^{lacZ/+}$ (140±5 μm) than in *dab1*$^{lacZ/lacZ}$ LCN/LSN (107±0.4 μm; *dab1*$^{+/+}$ vs. *dab1*$^{lacZ/lacZ}$

$p$=0.0005; *dab1*$^{lacZ/+}$vs. *dab1*$^{lacZ/lacZ}$ $p$=0.001; Fig. 8J-L). A similar result was found when comparing the *Reln*$^{+/+}$ and *Reln*$^{-/-}$ LCN/LSN (*Reln*$^{+/+}$ 141±0.7 µm; *Reln*$^{-/-}$ 103±3 µm; $p$=0.0002). Thus, the LCN/LSN in mutants is compacted, consistent with the loss of ~50% of their neurons.

We then analyzed the distribution of Dab1 and Dab1-Lmx1b in the *Reln* LCN/LSN neurons. On average, both *Reln*$^{+/+}$ and *Reln*$^{-/-}$ LCN/LSN contained 11±1 single-labeled Dab1 neurons, but *Reln*$^{+/+}$ had about twice as many Dab1-Lmx1b neurons as *Reln*$^{-/-}$ LCN/LSN (*Reln*$^{+/+}$ 12±1; *Reln*$^{-/-}$ 6±1; $p$=0.004; yellow arrowheads in Fig. 9A1-3, B1-3). These results showed that although 52% of Dab1 cells in *Reln*$^{+/+}$ LCN/LSN co-express Lmx1b, only 36% of Dab1 cells in *Reln*$^{-/-}$ LCN/LSN are double-labeled. Because the LCN/LSN region contains many projection neurons that convey nociceptive signals rostrally, changes in both neuronal density and distribution in Reelin-signaling pathway mutants likely impact the fidelity with which pain messages are transmitted rostrally.

## Discussion

To identify anatomical defects in mutants of the Reelin-Dab1 signaling pathway, we first characterized the Dab1-expressing dorsal horn neurons. We found many small Dab1-labeled dorsal horn neurons in laminae I-II and discovered that 70% of these Dab1 interneurons co-expressed the transcription factor Lmx1b. Additionally, areas that contain projection neurons for pain processing, such as the lateral reticulated area, LSN, and the LCN, also contained Dab1 neurons and 50-70% of them co-expressed Lmx1b. Based on previous reports, these neuronal populations are likely to be excitatory glutamatergic neurons (Cheng *et al*., 2004; Cheng *et al*., 2005; Dai *et al*., 2008). Importantly, we found evidence of mispositioned Dab1 neurons in multiple areas of the *Reln*$^{-/-}$ dorsal horn when compared to *Reln*$^{+/+}$: 1) More Dab1 and Dab1-Lmx1b cells are found within the IB4-terminal zone and the IB4 band itself was shifted dorsally, 2) The lateral reticulated area and LSN were missing about 50% of their Dab1-Lmx1b neurons, and 3) The combined LCN/LSN was compressed and missing nearly 50% of its neurons, including many that co-express Dab1-Lmx1b. Additionally, Dab1-Lmx1b neurons in the superficial dorsal horn and lateral reticulated area expressed Fos after thermal and mechanical stimulation and thus actively participated in these nociceptive circuits. Together, we have identified populations of Dab1-expressing dorsal horn interneurons and projection neurons that sustain positioning errors in Reelin-signaling pathway mutants, including a number of glutamatergic neurons. Thus, the thermal hyperalgesia and reduced mechanical sensitivity in *Reln*$^{-/-}$ suggests multiple disruptions in the dorsal horn pain circuits that involve mispositioned Dab1-Lmx1b neurons. These findings highlight the importance of the canonical Reelin-Dab1 signaling pathway in regulating neuronal positioning in dorsal horn nociceptive areas and now correlate anatomical defects with the pain abnormalities observed in mutant mice.

**The loss of Reelin in the spinal cord affects Dab1 neurons differently**

Both somatic and preganglionic motor neurons in the spinal cord express Dab1 and respond to Reelin signaling, yet in *Reln*$^{-/-}$ and *dab1*$^{-/-}$ mice, somatic motor neurons have rather subtle positioning errors compared to the extensively mispositioned sympathetic and parasympathetic preganglionic neurons (Yip *et al*., 2000; Phelps *et al*., 2002; Palmesino *et al*., 2010; Abadesco *et al*., 2014). Dab1-labeled dorsal horn neurons also show differences in the extent of their positioning errors. Disruptions in the cellular organization of the smaller Dab1 interneurons in *Reln*$^{-/-}$ laminae I-II were difficult to identify, whereas the larger Dab1 projection neurons in *Reln*$^{-/-}$ lateral reticulated area, LSN, and LCN/LSN were clearly missing from their respective areas. The final locations of these mispositioned Dab1 projection neurons remain unclear but likely include the extra Dab1 and Dab1-Lmx1b neurons in the IB4 area of laminae II inner and large ectopic cells detected along the outer edge of lamina I.

Based on previous studies, the migratory pathway of Dab1 and the late-born Lmx1b (dIL$^{B}$) neurons overlap extensively, both temporally and spatially (Müller *et al*., 2002; Dunston *et al*., 2005; Villeda *et al*., 2006; Rebelo *et al*., 2010). If Reelin functions to terminate the migration of the laterally located Dab1 neurons in the lateral reticulated area, LSN and LCN as reported with the sympathetic preganglionic neurons, then the absence of Reelin would cause these dorsal horn projection neurons to fail to stop laterally and instead migrate past their normal locations or return to the midline (Yip *et al*., 2000; Phelps *et al*., 2002; Krüger *et al*., 2010). On the other hand, the Dab1 neurons in the *Reln*$^{-/-}$ superficial dorsal horn seem to remain near their correct laminae but are somewhat out of place compared to *Reln*$^{+/+}$ mice. Because the number of Dab1 neurons and the percentage of Dab1 neurons co-expressing Lmx1b do not differ between *Reln*$^{+/+}$ and *Reln*$^{-/-}$ superficial dorsal horns, there is no evidence of selective cell death in our

model. Furthermore, based on previous studies (Caviness and Rakic, 1978; Rice and Curran, 2001), neuronal generation is usually normal in Reelin-signaling pathway mutants, but their migration pathways are altered.

Dab1 and Lmx1b both identify large neurons in the lateral reticulated area which express Fos following mechanical or thermal stimulation. Based on their size, location, and response to stimulation, these Dab1- and Dab1-Lmx1b cells likely correspond to the so-called wide-dynamic-range neurons that relay nociceptive information to rostral targets (Menetrey *et al*., 1980). Similarly, Dab1 and Lmx1b also identify large neurons in the LCN/LSN, many of which are likely to be projection neurons that relay nociceptive information to the thalamus (Giesler *et al*., 1979; Kajander and Geisler, 1987). The significant positioning errors sustained by these neurons imply that Reelin regulates their migration during development. Although generally the correct afferents still contact mispositioned neurons, it is unclear whether or not normal functional connections are formed (Yip *et al*., 2003; Pascual *et al*., 2004), especially since Reelin signaling was found to play a role in regulating hippocampal synaptic function (Qiu *et al*., 2006; Pujadas *et al*., 2010). In addition, Reelin-Dab1 signaling has been implicated in dendrite development in the hippocampus and the cerebral cortex (Niu *et al*., 2004; Olson *et al*., 2006; Matsuki *et al*., 2008). *Reln*$^{-/-}$ and *dab1*$^{-/-}$ somatic motor neurons also have stunted dendrites compared to wild-type mice (Phelps *et al*., 2002; Abadesco *et al*., 2014). Thus, without Reelin, the Dab1 dorsal horn neurons also may have abnormal dendrites, in addition to being mispositioned, which would further impair their neuronal connections.

**The contributions of Reelin and Lmx1b to nociception**

Three recent mutant mouse studies (Wang *et al*., 2013; Xu *et al*., 2013; Szabo *et al*., 2015) that characterized excitatory interneurons in the superficial dorsal horn found elevated withdrawal

thresholds in response to mechanical stimulation and morphological alterations that resemble the phenotypic changes reported in our study. Furthermore, the brain-sparing deletion of *Lmx1b* (Szabo *et al*., 2015), the removal of *Tlx3* from the excitatory dI5 and $dIL^B$ neurons (Xu *et al*., 2013), and the CNS-specific deletion of *TR4*, a testicular orphan nuclear receptor (Wang *et al*., 2013), all reported changes in the lamination pattern of the superficial dorsal horn and a loss in the number of laminae I-II neurons. Of particular interest to our study was the loss of about 70% of Reelin-labeled superficial dorsal horn cells in both *TR4* and *Lmx1b* mutant mice (Wang *et al*., 2013; Szabo *et al*., 2015). The absence of Reelin-expressing cells in the superficial dorsal horn would likely impact Dab1-expressing cells severely.

Although Reelin-signaling pathway mutants are relatively insensitive to mechanical stimulation as are the *TR4* and *Lmx1b* conditional knockout mice, it is interesting that $Reln^{-/-}$ and $dab1^{-/-}$ mice have the opposite response to heat, i.e., thermal hyperalgesia (Villeda *et al*., 2006; Akopians *et al*., 2008; Wang *et al*., 2012). Thus, there must be a different neural circuit involving the Reelin-signaling pathway by which heat sensitivity is increased. These findings imply that the canonical Reelin pathway differentially affects circuits that process noxious thermal heat and mechanical signals and adds further support to the concept of modality-specific circuits that process painful heat and mechanical messages.

**References**


Abadesco AD, Cilluffo M, Yvone GM, Carpenter EM, Howell BW, Phelps PE. 2013. Novel Disabled-1-expressing neurons identified in adult brain and spinal cord. Eur J Neurosci. 39:579-92.

Akopians AL, Babayan AH, Beffert U, Herz J, Basbaum AI, Phelps PE. 2008. Contribution of the Reelin signaling pathways to nociceptive processing. Eur J Neurosci. 27:523-37.

Antal M, Polgár E, Chalmers J, Minson JB, Llewellyn-Smith I, Heizmann CW, Somogyi P. 1991. Different populations of parvalbumin- and calbindin-D28k-immunoreactive neurons contain GABA and accumulate $^{3}$H-D-aspartate in the dorsal horn of the rat spinal cord. J Comp Neurol. 314:114-24.

Arnaud L, Ballif BA, Cooper JA. 2003. Regulation of protein tyrosine kinase signaling by substrate degradation during brain development. Mol Cell Biol. 23:9293-302.

Basbaum AI, Bautista DM, Scherrer G, Julius D. 2009. Cellular and molecular mechanisms of pain. Cell. 139:267-84.

Bock HH, Herz J. 2003. Reelin activates SRC family tyrosine kinases in neurons. Curr Biol. 13: 18-26.

Burstein R, Cliffer KD, Giesler GJ Jr. 1987. Direct somatosensory projections from the spinal cord to the hypothalamus and telencephelon. J Neurosci. **7**:4159-64.

Burstein R, Dado RJ, Giesler GJ Jr. 1990. The cells of origin of the spinothalamic tract of the rat: a quantitative reexamination. Brain Res. 511:329-37.

Caviness VS Jr, Rakic P. 1978. Mechanisms of cortical development: a view from mutations in mice. Annu Rev Neurosci. 1:297-326.

Chaplan SR, Bach FW, Pogrel JW, Chung JM, Yaksh TL. 1994. Quantitative assessment of tactile allodynia in the rat paw. J Neurosci Methods. 53:55-63.

Cheng L, Arata A, Mizuguchi R, Qian Y, Karunaratne A, Gray PA, Arata S, Shirasawa S, Bouchard M, Luo P, Chen CL, Busslinger M, Goulding M, Onimaru H, Ma Q. 2004. Tlx3 and Tlx1 are post-mitotic selector genes determining glutamatergic over GABAergic cell fates. Nat Neurosci. 7:510-7.

Cheng L, Samad OA, Xu Y, Mizuguchi R, Luo P, Shirasawa S, Goulding M, Ma Q. 2005. Lbx1 and Tlx3 are opposing switches in determining GABAergic versus glutamatergic transmitter phenotypes. Nat Neurosci. 8:1510-15.

D'Arcangelo G, Miao GG, Curran T. 1996. Detection of the reelin breakpoint in reeler mice. Brain Res Mol Brain Res. 39:234-36.

Dai JX, Hu ZL, Shi M, Guo C, Ding YQ. 2008. Postnatal ontogeny of the transcription factor Lmx1b in the mouse central nervous system. J Comp Neurol. 509:341-55.

Dunston JA, Reimschisel T, Ding YQ, Sweeney E, Johnson RL, Chen ZF, McIntosh I. 2005. A neurological phenotype in nail patella syndrome (NPS) patients illuminated by studies of murine Lmx1b expression. Eur J Hum Genet. 13:330-35.

Giesler GJ Jr, Urca G, Cannon JT, Liebeskind JC. 1979. Response properties of neurons of the lateral cervical nucleus in the rat. J Comp Neurol. 186:65-77.

Gross MK, Dottori M, Goulding M. 2002. Lbx1 specifies somatosensory association interneurons in the dorsal spinal cord. Neuron. 34:535-49.

Gutierrez-Mecinas M, Furuta T, Watanabe M, Todd AJ. 2016. A quantitative study of neurochemically defined excitatory interneuron populations in laminae I-III of the mouse spinal cord. Mol Pain. 12: pii:1744806916629065.

Hammond V, So E, Gunnersen J, Valcanis H, Kalloniatis M, Tan SS. 2006. Layer positioning of late-born cortical interneurons is dependent on Reelin but not p35 signaling. J Neurosci. 26: 1646-55.

Hargreaves K, Dubner R, Brown F, Flores C, Joris J. 1988. A new and sensitive method for measuring thermal nociception in cutaneous hyperalgesia. Pain. 32:77-88.

Honda T, Kobayashi K, Mikoshiba K, Nakajima K. 2011. Regulation of cortical neuron migration by the Reelin signaling pathway. Neurochem Res. 36:1270-79.

Howell BW, Hawkes R, Soriano P, Cooper JA. 1997. Neuronal position in the developing brain is regulated by mouse disabled-1. Nature. 389:733-7.

Kajander KC, Giesler GJ Jr. 1987. Responses of neurons in the lateral cervical nucleus of the cat to noxious cutaneous stimulation. J Neurophysiol. 57:1686-704.

Kayalioglu G, Robertson B, Kristensson K, Grant G. 1999. Nitric oxide synthase and interferon-gamma receptor immunoreactivities in relation to ascending spinal pathways to thalamus, hypothalamus, and the periaqueductal grey in the rat. Somatosens Mot Res. 16:280-90.

Krüger MT, Zhao S, Chai X, Brunne B, Bouché E, Bock HH, Frotscher M. 2010. Role for Reelin-induced cofilin phosphorylation in the assembly of sympathetic preganglionic neurons in the murine intermediolateral column. Eur J Neurosci. 32:1611-7.

Kubasak MD, Brooks R, Chen S, Villeda SA, Phelps PE. 2004. Developmental distribution of reelin-positive cells and their secreted product in the rodent spinal cord. J Comp Neurol. 468:165-78.

Laing I, Todd AJ, Heizmann CW, Schmidt HH. 1994. Subpopulations of GABAergic neurons in laminae I-III of rat spinal dorsal horn defined by coexistence with classical transmitters, peptides, nitric oxide synthase or parvalbumin. Neuroscience. 61:123-32.

Matsuki T, Pramatarova A, Howell BW. 2008. Reduction of Crk and CrkL expression blocks reelin-induced dendritogenesis. J Cell Sci. 121:1869-75.

Menétrey D, Chaouch A, Besson JM. 1980. Location and properties of dorsal horn neurons at origin of spinoreticular tract in lumbar enlargement of the rat. J Neurophysiol. 44:862-77.

Menétrey D, Chaouch A, Binder D, Besson JM. 1982. The origin of the spinomesencephalic tract in the rat: an anatomical study using the retrograde transport of horseradish peroxidase. J Comp Neurol. 206:193-207.

Müller T, Brohmann H, Pierani A, Heppenstall PA, Lewin GR, Jessell TM, Birchmeier C. 2002. The homeodomain factor Lbx1 distinguishes two major programs of neuronal differentiation in the dorsal spinal cord. Neuron. 34:551-62.

Niu S, Renfro A, Quattrocchi CC, Sheldon M, D'Arcangelo G. 2004. Reelin promotes hippocampal dendrite development through the VLDLR/ApoER2-Dab1 pathway. Neuron. 41:71-84.

Olson EC, Kim S, Walsh CA. 2006. Impaired neuronal positioning and dendritogenesis in the neocortex after cell-autonomous Dab1 suppression. J Neurosci. 26:1767-75.

Palmesino E, Rousso DL, Kao TJ, Klar A, Laufer E, Uemura O, Okamoto H, Novitch BG, Kania A. 2010. Foxp1 and lhx1 coordinate motor neuron migration with axon trajectory choice by gating Reelin signalling. PLoS Biol. 8:e1000446.

Pascual M, Pérez-Sust P, Soriano E. 2004. The GABAergic septohippocampal pathway in control and reeler mice: target specificity and termination onto Reelin-expressing interneurons. Mol Cell Neurosci. 25:679-91.

Phelps PE, Barber RP, Houser CR, Crawford GD, Salvaterra PM, Vaughn JE. 1984. Postnatal development of neurons containing choline acetyltransferase in rat spinal cord: an immunocytochemical study. J Comp Neurol. 229:347-61.

Phelps PE, Rich R, Dupuy-Davies S, Ríos Y, Wong T. 2002. Evidence for a cell-specific action of Reelin in the spinal cord. Dev Biol. 244:180-98.

Pramatarova A, Chen K, Howell BW. 2008. A genetic interaction between the APP and Dab1 genes influences brain development. Mol Cell Neurosci. 37:178-86.

Pujadas L, Gruart A, Bosch C, Delgado L, Teixeira CM, Rossi D, de Lecea L, Martínez A, Delgado-García JM, Soriano E. 2010. Reelin regulates postnatal neurogenesis and enhances spine hypertrophy and long-term potentiation. J Neurosci. 30:4636-49.

Qiu S, Korwek KM, Pratt-Davis AR, Peters M, Bergman MY, Weeber EJ. 2006. Cognitive disruption and altered hippocampus synaptic function in Reelin haploinsufficient mice. Neurobiol Learn Mem. 85:228-42.

Rebelo S, Reguenga C, Lopes C, Lima D. 2010. Prrxl1 is required for the generation of a subset of nociceptive glutamatergic superficial spinal dorsal horn neurons. Dev Dyn. 239:1684-94.

Rice DS, Sheldon M, D'Arcangelo G, Nakajima K, Goldowitz D, Curran T. 1998. Disabled-1 acts downstream of Reelin in a signaling pathway that controls laminar organization in the mammalian brain. Development. 125:3719-29.

Rice DS, Curran T. 2001. Role of the reelin signaling pathway in central nervous system development. Annu Rev Neurosci. 24:1005-39.

Shields SD, Moore KD, Phelps PE, Basbaum AI. 2010. Olfactory ensheathing glia express Aquaporin 1. J Comp Neurol. 518:4329-41.

Szabo NE, da Silva RV, Sotocinal SG, Zeilhofer HU, Mogil JS, Kania A. 2015. Hoxb8 intersection defines a role for Lmx1b in excitatory dorsal horn neuron development, spinofugal connectivity, and nociception. J Neurosci. 35:5233-46.

Takahara T, Ohsumi T, Kuromitsu J, Shibata K, Sasaki N, Okazaki Y, Shibata H, Sato S, Yoshiki A, Kusakabe M, Muramatsu M, Ueki M, Okuda K, Hayashizaki Y. 1996. Dysfunction of the Orleans reeler gene arising from exon skipping due to transposition of a full-length copy of an active L1 sequence into the skipped exon. Hum Mol Genet. 5:989-93.

Tamamaki N, Yanagawa Y, Tomioka R, Miyazaki J, Obata K, Kaneko T. 2003. Green fluorescent protein expression and colocalization with calretinin, parvalbumin, and somatostatin in the GAD67-GFP knock-in mouse. J Comp Neurol. 467:60-79.

Todd AJ. 2010. Neuronal circuitry for pain processing in the dorsal horn. Nat Rev Neurosci. 11:823-36.

Trommsdorff M, Gotthardt M, Hiesberger T, Shelton J, Stockinger W, Nimpf J, Hammer RE, Richardson JA, Herz J.1999. Reeler/Disabled-like disruption of neuronal migration in knockout mice lacking the VLDL receptor and ApoE receptor 2. Cell. 97:689-701.

Villeda SA, Akopians AL, Babayan AH, Basbaum AI, Phelps PE. 2006. Absence of Reelin results in altered nociception and aberrant neuronal positioning in the dorsal spinal cord. Neuroscience. 139:1385-96.

Wang X, Babayan AH, Basbaum AI, Phelps PE. 2012. Loss of the Reelin-signaling pathway differentially disrupts heat, mechanical and chemical nociceptive processing. Neuroscience. 226:441-50.

Wang X, Zhang J, Eberhart D, Urban R, Meda K, Solorzano C, Yamanaka H, Rice D, Basbaum AI. 2013. Excitatory superficial dorsal horn interneurons are functionally heterogeneous and required for the full behavioral expression of pain and itch. Neuron. 78:312-24.

Xu Y, Lopes C, Wende H, Guo Z, Cheng L, Birchmeier C, Ma Q. 2013. Ontogeny of excitatory spinal neurons processing distinct somatic sensory modalities. J Neurosci. 33:14738-48.

Yip JW, Yip YP, Nakajima K, Capriotti C. 2000. Reelin controls position of autonomic neurons in the spinal cord. Proc Natl Acad Sci U S A. 97:8612-6.

Yip YP, Rinaman L, Capriotti C, Yip JW. 2003. Ectopic sympathetic preganglionic neurons maintain proper connectivity in the reeler mutant mouse. Neuroscience. 118:439-50.

**Figure 2. The *dab1*$^{lacZ/lacZ}$ mice are hypersensitive to thermal and have reduced sensitivity to mechanical stimulation.**

***A***, Thermal sensitivity measured by the Hargreaves test. The mean latency±SEM for *dab1*$^{+/+}$ is 9.9±0.5s, for *dab1*$^{lacZ/+}$ is 10.8±0.3s, and for *dab1*$^{lacZ/lacZ}$ is 8.2±0.4s. There are significant differences between *dab1*$^{+/+}$ vs *dab1*$^{lacZ/lacZ}$ ($p$=0.01) and for *dab1*$^{lacZ/+}$ vs *dab1*$^{lacZ/lacZ}$ ($p$=0.0005). ***B***, After heat stimulation, there are on average fewer Fos-positive neurons in *dab1*$^{+/+}$ (60.5±2.9 neurons) and *dab1*$^{lacZ/+}$(55.6±6) than in *dab1*$^{lacZ/lacZ}$ (75.9±3.9) laminae I-II (*dab1*$^{+/+}$ vs *dab1*$^{lacZ/lacZ}$ $p$=0.047; *dab1*$^{lacZ/+}$ vs *dab1*$^{lacZ/lacZ}$ $p$=0.01). More Fos-positive neurons were present in the lateral spinal nucleus (LSN) of *dab1*$^{+/+}$ (2.6±0.4) and *dab1*$^{lacZ/+}$ (2.1±0.5) than in *dab1*$^{lacZ/lacZ}$ mice (0.6±0.1; *dab1*$^{+/+}$ vs *dab1*$^{lacZ/lacZ}$ $p$=0.004; *dab1*$^{lacZ/+}$ vs *dab1*$^{lacZ/lacZ}$ $p$=0.02). ***C-E***, After heat stimulation, there are fewer Fos-labeled neurons in laminae I-II but more in the lateral reticulated area (long arrows) and LSN (short arrows) of *dab1*$^{+/+}$ and *dab1*$^{lacZ/+}$ than in *dab1*$^{lacZ/lacZ}$ mice (medial to the right in coronal sections of all figures). ***F***, The von Frey test of mechanical sensitivity found that the withdrawal thresholds from *dab1*$^{+/+}$ (0.07±0.02g) and *dab1*$^{lacZ/+}$ (0.07±0.01g) mice do not differ, whereas *dab1*$^{lacZ/lacZ}$ responses are profoundly slower (1.37±0.3g; *dab1*$^{+/+}$ vs *dab1*$^{lacZ/lacZ}$ $p$=0.004; *dab1*$^{lacZ/+}$ vs *dab1*$^{lacZ/lacZ}$ $p$=0.004). ***G***, After mechanical stimulation, more Fos-positive neurons are in *dab1*$^{+/+}$ (43.8±5) and *dab1*$^{lacZ/+}$ (39.2±1.8) compared with *dab1*$^{lacZ/lacZ}$ laminae I-II (24.5±5; *dab1*$^{+/+}$ vs *dab1*$^{lacZ/lacZ}$ $p$=0.005; *dab1*$^{lacZ/+}$ vs *dab1*$^{lacZ/lacZ}$ $p$=0.03) and in *dab1*$^{+/+}$ (1.8±0.4) and *dab1*$^{lacZ/+}$ (1.3±0.1) than *dab1*$^{lacZ/lacZ}$ LSN (0.4±0.2; *dab1*$^{+/+}$ vs *dab1*$^{lacZ/lacZ}$ $p$=0.004; *dab1*$^{lacZ/+}$ vs *dab1*$^{lacZ/lacZ}$ $p$=0.047). ***H-J***, More Fos-expressing cells appear in *dab1*$^{+/+}$ and *dab1*$^{lacZ/+}$ laminae I–II, lateral reticulated area (long arrows), and LSN (short arrows) than in *dab1*$^{lacZ/lacZ}$ mice. Scale bars: ***C-E***; ***H-J***, 200 μm.

**Figure 2**

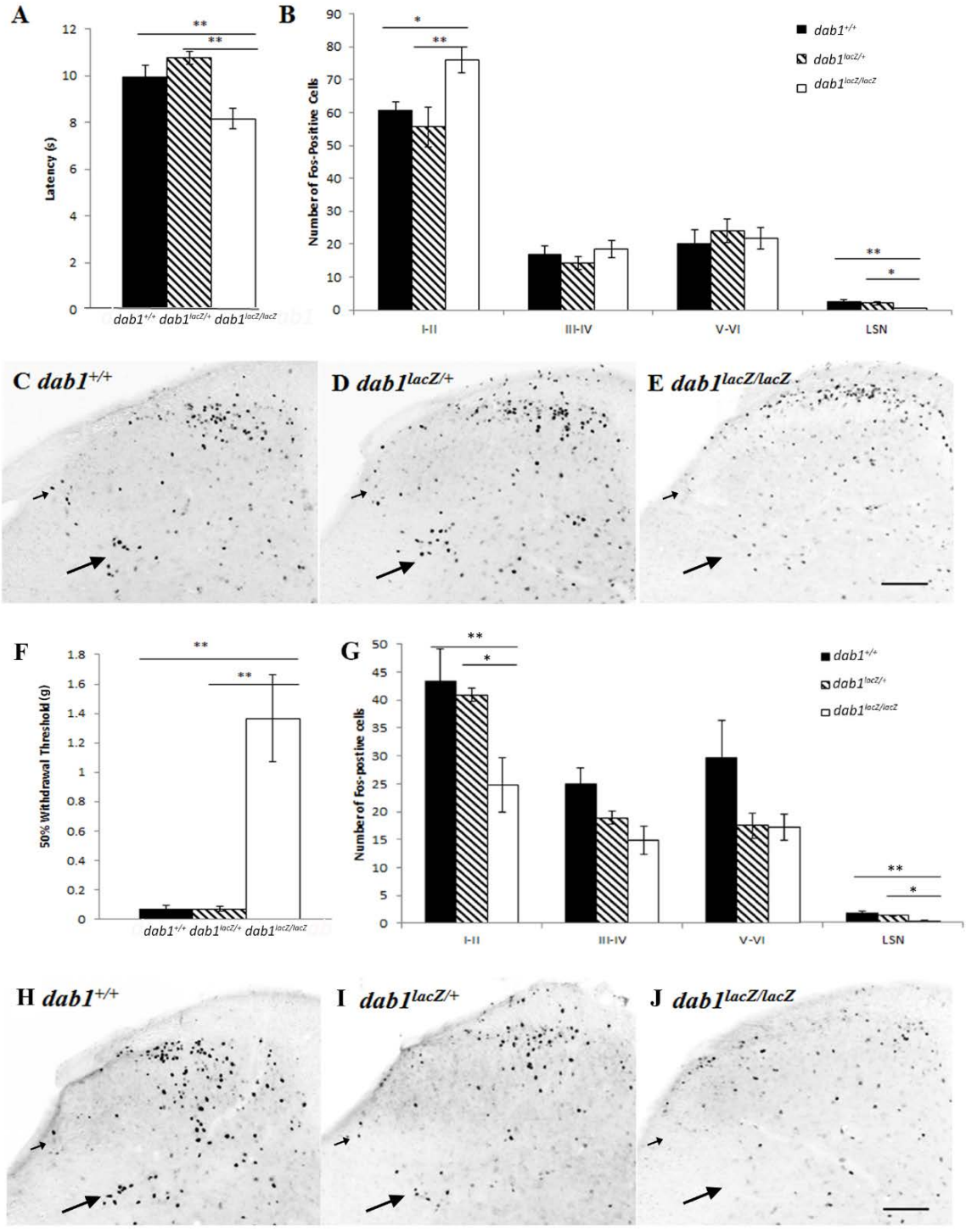
A
B
Latency (s)
Number of Fos-Positive Cells
dab1+/+
dab1lacZ/+
dab1lacZ/lacZ
I-II
III-IV
V-VI
LSN
C dab1+/+
D dab1lacZ/+
E dab1lacZ/lacZ
F
50% Withdrawal Threshold (g)
G
Number of Fos-positive cells
H dab1+/+
I dab1lacZ/+
J dab1lacZ/lacZ

**Figure 3. Dab1 and β-galactosidase are co-expressed in the dorsal horn.**

***A***, Dab1 immunoreactivity (brown) concentrated in *dab1*$^{+/+}$ laminae I-II, lateral reticulated area of lamina V, and the lateral spinal nucleus (LSN). Relatively small Dab1 neurons (small arrowheads) are in laminae I-II whereas medium and large Dab1 neurons (large arrowheads) are found in the lateral reticulated area. ***B***, The *dab1*$^{lacZ/+}$ dorsal horn contains both brown Dab1 and blue β-gal precipitate. The colocalization seen in the boxed lateral reticulated area that is enlarged in the inset. ***C***, The *dab1*$^{lacZ/lacZ}$ dorsal horn contains a pattern of blue β-gal reaction product similar to Dab1 immunoreactivity shown in A and B. Scale bar: ***A***-***C***, 200 µm. Inset in ***B***, 50 µm.

**Figure 3**

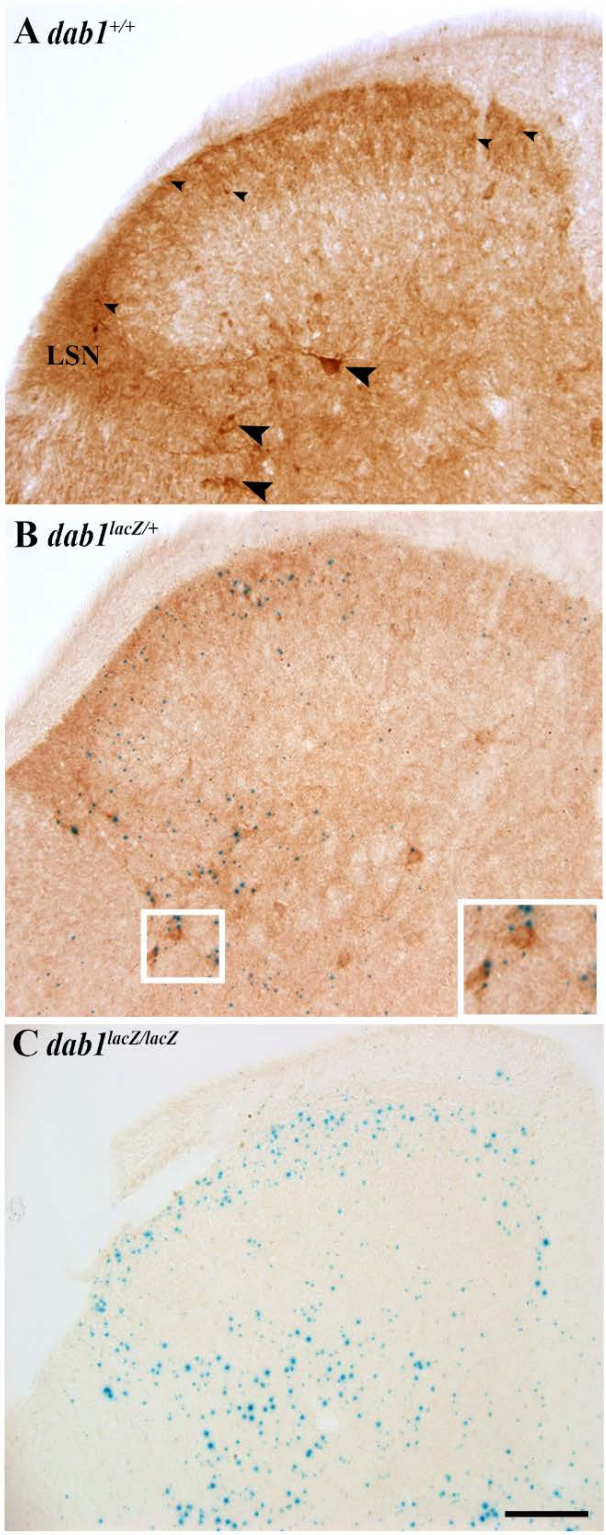

**Figure 4. Superficial dorsal horn: 70% of Dab1 cells co-express Lmx1b and are mispositioned within the *Reln*$^{-/-}$ IB4 terminal zone.**

***A-F***, Confocal 3 µm thick images of *Reln*$^{+/+}$ (***A-C***) and *Reln*$^{-/-}$ (***D-F***) lumbar dorsal horns show that many cells express both Dab1 (red cytoplasm) and Lmx1b (green nucleus), including small interneurons in laminae I-II (small yellow arrowheads) and large neurons in laminae I-III (large yellow arrowheads). Examples of single-labeled Dab1 cells are marked by white arrows. Boxes in ***A*** and ***D*** are enlarged in ***B***, ***C***, ***E***, and ***F***. Individual channels of ***B*** and ***E*** are labeled ***B1-2*** and ***E1-2***. ***G-H***, Lumbar confocal images show the distribution of Dab1 (red) and Lmx1b (cyan) within and above the IB4 (green) band of terminals. Although the area of lamina II marked by IB4 afferents does not vary by genotype, the area of laminae I-IIouter, located dorsal to the IB4 terminals, is larger in *Reln*$^{+/+}$ than in *Reln*$^{-/-}$ mice. An arrowhead marks a large ectopic Dab1-Lmx1b neuron in *Reln*$^{-/-}$ lamina I. ***I***, The number of Dab1 cells in laminae I-IIouter, i.e., above the IB4 area, do not vary by genotype, but more Dab1, Dab1-Lmx1b, and total Dab1 neurons are found within the *Reln*$^{-/-}$ compared to the *Reln*$^{+/+}$ IB4 band (n=4 mice/genotype). Scale bars: ***A***, ***D***; ***G-H***, 100 µm; ***B***, ***E***; ***C***, ***F***; ***B1-2***, ***E1-2***, 50 µm.

**Figure 4**

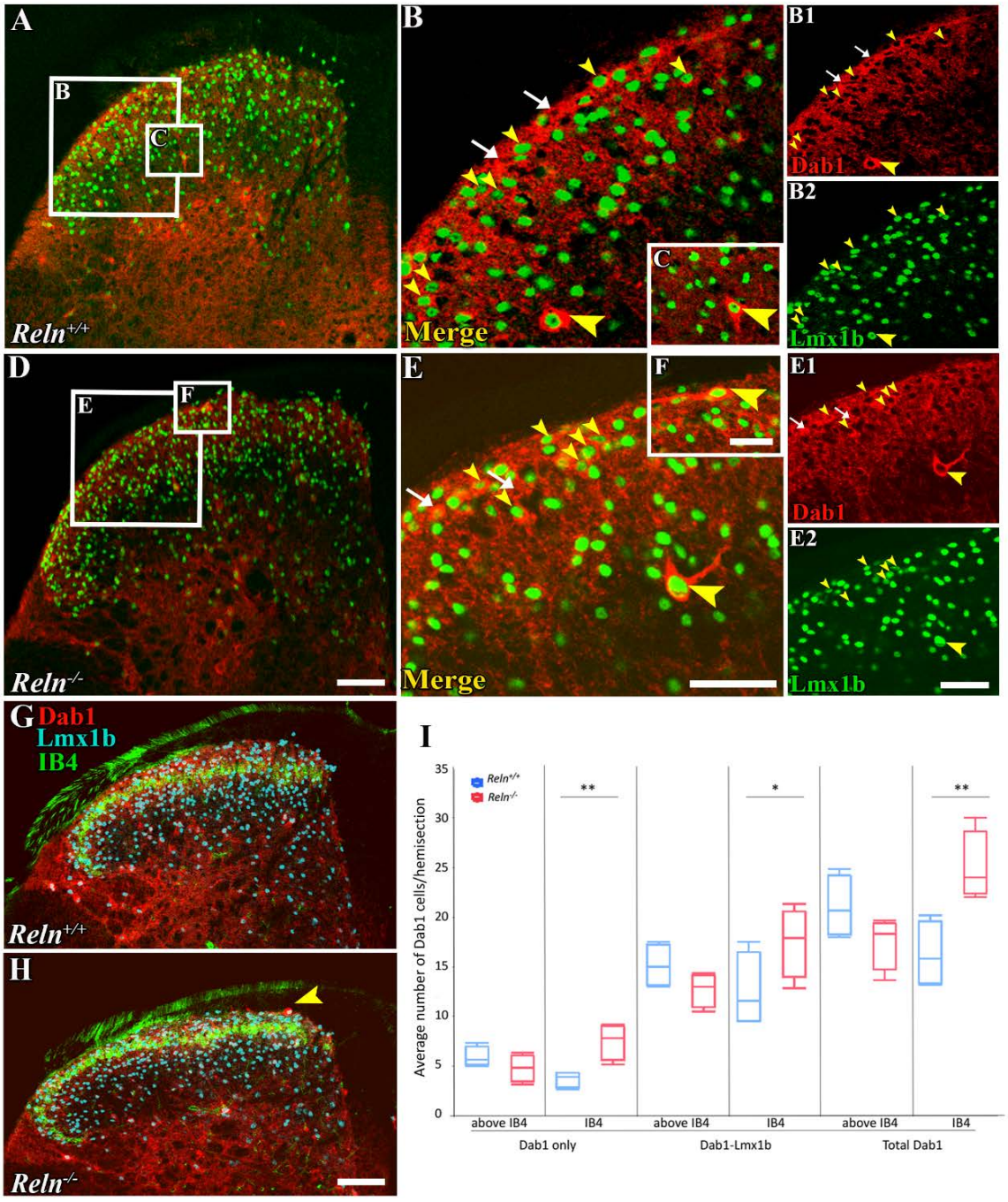
A
B
C
Reln+/+
B
Merge
C
B1
Dab1
B2
Lmx1b
D
E
F
Reln-/-
E
Merge
F
E1
Dab1
E2
Lmx1b
G Dab1
Lmx1b
IB4
Reln+/+
H
Reln-/-
I
Reln+/+
Reln-/-
Average number of Dab1 cells/hemisection
35
30
25
20
15
10
5
0
**
*
**
above IB4
IB4
above IB4
IB4
above IB4
IB4
Dab1 only
Dab1-Lmx1b
Total Dab1

**Figure 5. A small number of Dab1 neurons in laminae I-II are GABAergic and in the lateral reticulated area are cholinergic.**

***A-D***, Confocal images of *Reln*$^{rl\text{-}Orl/+}$*; GAD67*$^{GFP/+}$ (***A-B***) and *Reln*$^{rl\text{-}Orl/rl\text{-}Orl}$*; GAD67*$^{GFP/+}$ (***C-D***) lumbar dorsal horns. Boxes in ***A*** and ***C*** are enlarged in ***B*** and ***D***, with individual channels in ***B1-2*** and ***D1-2***. A few Dab1 (red) and GAD67$^{GFP}$ neurons appear co-localized (yellow arrowheads in ***B*** and ***D***). ***E-F***, Sagittal lumbar dorsal horn sections from *Reln-Orl*$^{+/+}$*;GAD67*$^{GFP/+}$ (***E1-3***) and *Reln*$^{rl\text{-}Orl/rl\text{-}Orl}$*; GAD67*$^{GFP/+}$ (***F1-3***) mice illustrate ectopic cells in the white matter dorsal to lamina I. Dab1 (white arrows in ***E1***, ***3***) and Dab1-GAD67$^{GFP}$-labeled (yellow arrowheads in ***E1-3***, ***F1-3***) neurons are frequently found dorsal to lamina I (top of image). ***G-H***, *Reln*$^{+/+}$ and *Reln*$^{-/-}$ dorsal horns show that Dab1 (red) and ChAT-positive neurons (green) do not co-localize in laminae I-IV, but double-labeled cells boxed in ***G*** and ***H*** (yellow arrowheads in ***G1-3***, ***H1-3***) are found in the lateral reticulated area of lamina V. Single-labeled Dab1 and ChAT neurons are marked with white arrows. Scale bars: ***A***, ***C***; ***G-H***, 100 μm; ***B***, ***D***; ***B1-2***, ***D1-2***; ***E1-3***, ***F1-3***; ***G1-3***, ***H1-3***, 50 μm.

**Figure 5**

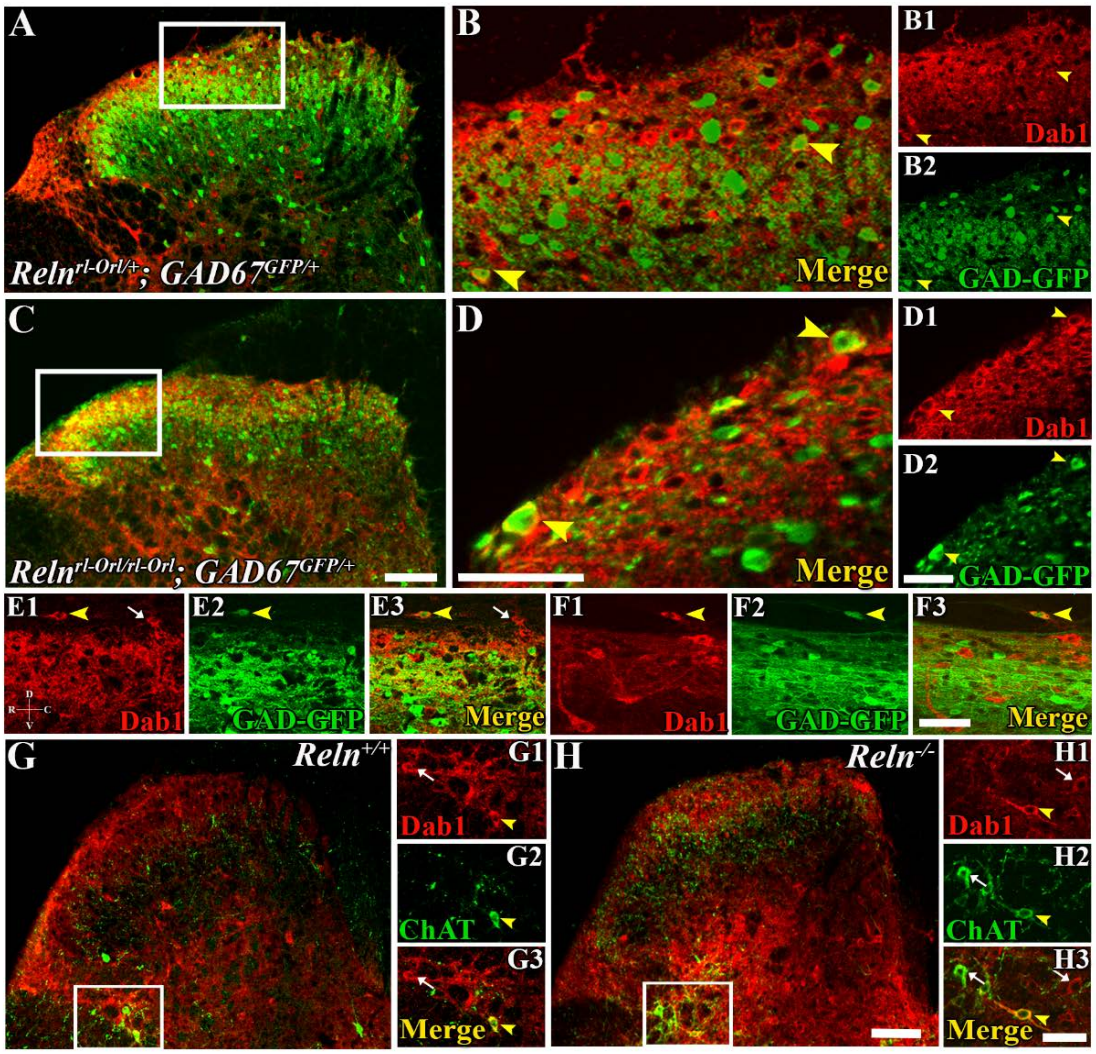
A
Reln^rl-Orl/+; GAD67^GFP/+
B
Merge
B1
Dab1
B2
GAD-GFP
C
Reln^rl-Orl/rl-Orl; GAD67^GFP/+
D
Merge
D1
Dab1
D2
GAD-GFP
E1
Dab1
E2
GAD-GFP
E3
Merge
F1
Dab1
F2
GAD-GFP
F3
Merge
G
Reln+/+
G1
Dab1
G2
ChAT
G3
Merge
H
Reln-/-
H1
Dab1
H2
ChAT
H3
Merge

**Figure 6. Lateral reticulated area and LSN: Dab1-Lmx1b-labeled cells are mispositioned in *Reln* mutants.**

***A-F***, Lumbar confocal images show that Dab1 (red) and Lmx1b (green) are co-expressed in $Reln^{+/+}$ (***A-D***) and $Reln^{-/-}$ (***E-F***) lateral reticulated area of lamina V (***A***, ***C***, ***E***, yellow arrowheads) and LSN (***B***, ***D***, ***F***, yellow arrowheads). Close to 70% of Dab1 neurons in both areas co-express Lmx1b. Single-labeled Dab1 cells are marked with white arrows. ***A***, ***C***, ***E***, Boxed area in ***A*** is enlarged in ***C*** and shows a more organized array of Dab1-Lmx1b neurons in $Reln^{+/+}$ than $Reln^{-/-}$ lateral reticulated area (***E***). ***B***, ***D***, ***F***, Boxed area of $Reln^{+/+}$ LSN is enlarged in ***D*** and contains more Dab1-Lmx1b-labeled cells than in $Reln^{-/-}$ LSN (***F***). ***G***, Fewer Dab1 only and more Dab1-Lmx1b-labeled cells are in $Reln^{+/+}$ than in $Reln^{-/-}$ lateral reticulated area. ***H***, More Dab1-Lmx1b-labeled and total Dab1 cells are seen in $Reln^{+/+}$ than $Reln^{-/-}$ LSN (n=5 mice per genotype). Scale bars: ***A***, ***B***, 100 µm; ***C-F***; ***C1-2***, ***D1-2***, ***E1-2***, ***F1-2***, 50 µm.

**Figure 6**

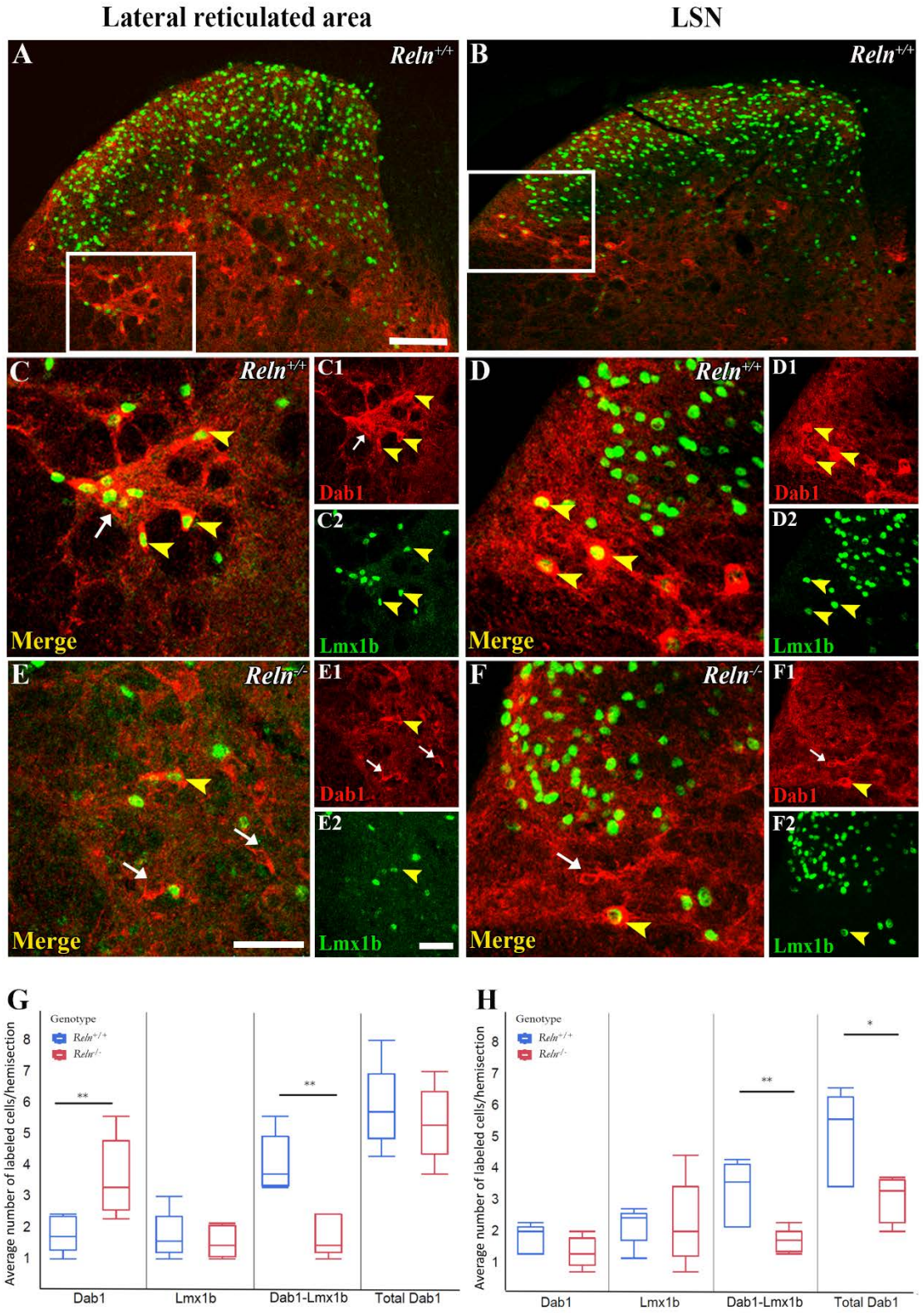
Lateral reticulated area
LSN
A
Reln+/+
B
Reln+/+
C
Reln+/+
C1
Dab1
C2
Lmx1b
Merge
D
Reln+/+
D1
Dab1
D2
Lmx1b
Merge
E
Reln-/-
E1
Dab1
E2
Lmx1b
Merge
F
Reln-/-
F1
Dab1
F2
Lmx1b
Merge
G
Genotype
Reln+/+
Reln-/-
Average number of labeled cells/hemisection
Dab1
Lmx1b
Dab1-Lmx1b
Total Dab1
H
Genotype
Reln+/+
Reln-/-
Average number of labeled cells/hemisection
Dab1
Lmx1b
Dab1-Lmx1b
Total Dab1

**Figure 7. Noxious stimulation induced Fos expression in Dab1-Lmx1b neurons.**

Triple TSA immunofluorescence labeling showed that after both thermal (***A***-***B***) and mechanical stimulation (***C-D***), some Dab1 (red) and Lmx1b (green)-positive neurons express Fos (cyan) in *dab1*$^{+/+}$ (***A***-***B***) and *Reln*$^{+/+}$ (***C-D***) superficial dorsal horns (***A***, ***A1-4***, ***C***, ***C1-4***) and in the lateral reticulated area (***B***, ***B1-4***, ***D***, ***D1-4***). Boxed areas in ***A4-D4*** are enlarged in ***A***-***D***, respectively. Triple-labeled cells are marked with white arrowheads. Double-labeled Dab1-Fos (magenta), Lmx1b-Fos (cyan), and Dab1-Lmx1b (yellow) cells are marked with color-matched arrows. Heat and mechanical stimulation induced Fos in medium to large-sized Dab1-Lmx1b neurons in the superficial dorsal horn and the lateral reticulated area. More Lmx1b neurons appeared to express Fos after mechanical stimulation especially in the superficial dorsal horn. Dab1-Lmx1b neurons in the lateral reticulated area appear as an organized array in wild-type mice (***B, D***). Scale bars: ***A4***; ***B4***; ***C4***; ***D4***, 100 μm; ***A***, ***A1-3***; ***B***, ***B1-3***; ***C***, ***C1-3***; ***D***, ***D1-3***, 50 μm.

**Figure 7**

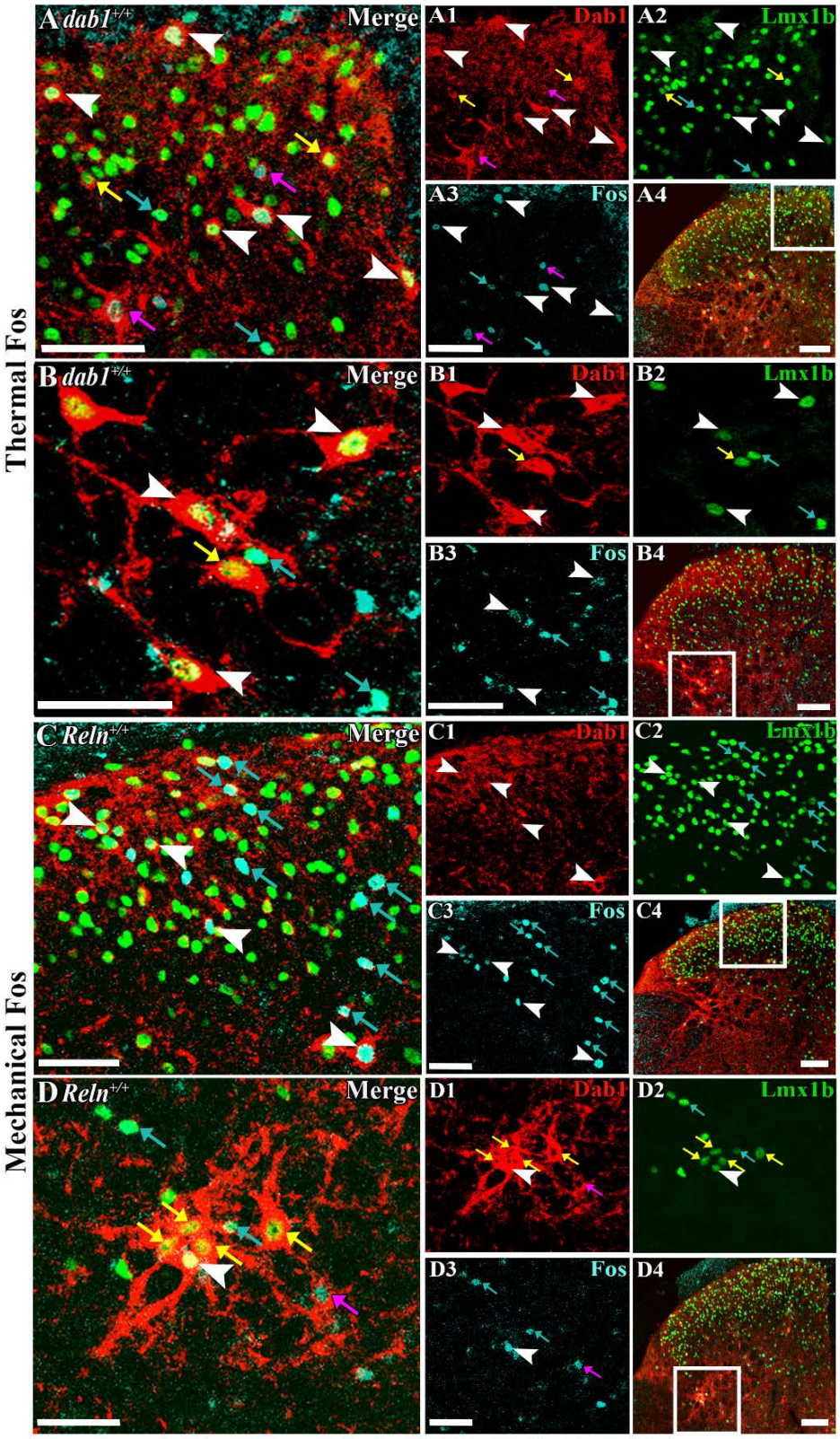
Thermal Fos
Mechanical Fos
A dab1+/+
Merge
A1
Dab1
A2
Lmx1b
A3
Fos
A4
B dab1+/+
Merge
B1
Dab1
B2
Lmx1b
B3
Fos
B4
C Reln+/+
Merge
C1
Dab1
C2
Lmx1b
C3
Fos
C4
D Reln+/+
Merge
D1
Dab1
D2
Lmx1b
D3
Fos
D4

**Figure 8. Lateral cervical nucleus: Neurons are mispositioned in Reelin pathway mutants.** ***A***, Schematic of the lateral cervical nucleus (LCN) found at levels C1-3. As there is no delineation between the LCN and LSN, they were analyzed together. ***B-C***, Dab1 expression in *Reln*$^{+/+}$ (***B***) and *Reln*$^{-/-}$ (***C***) cervical dorsal horn is concentrated in the superficial dorsal horn and LCN/LSN. ***D-F***, β-gal histochemistry followed by Dab1 immunoreaction reveals brown Dab1 protein (*dab1*$^{+/+}$, *dab1*$^{lacZ/+}$) and blue β-gal (*dab1*$^{lacZ/+}$, *dab1*$^{lacZ/lacZ}$) in the superficial dorsal horn and LCN/LSN. ***G-I***, The *dab1*$^{+/+}$ and *dab1*$^{lacZ/+}$ LCN/LSN contain about twice as many NeuN-labeled cells as *dab1*$^{lacZ/lacZ}$ mice (n=5 mice/genotype). ***J-L***, Neurons and their processes that express the Neurokinin-1 receptor show a compression in the *dab1*$^{lacZ/lacZ}$ (***L***) compared to *dab1*$^{+/+}$ (***J***) and *dab1*$^{lacZ/+}$ (***K***) LCN/LSN (n=3 mice/genotype). Scale bars: ***B-F***, 200 µm; ***G-L***, 100 µm.

**Figure 8**

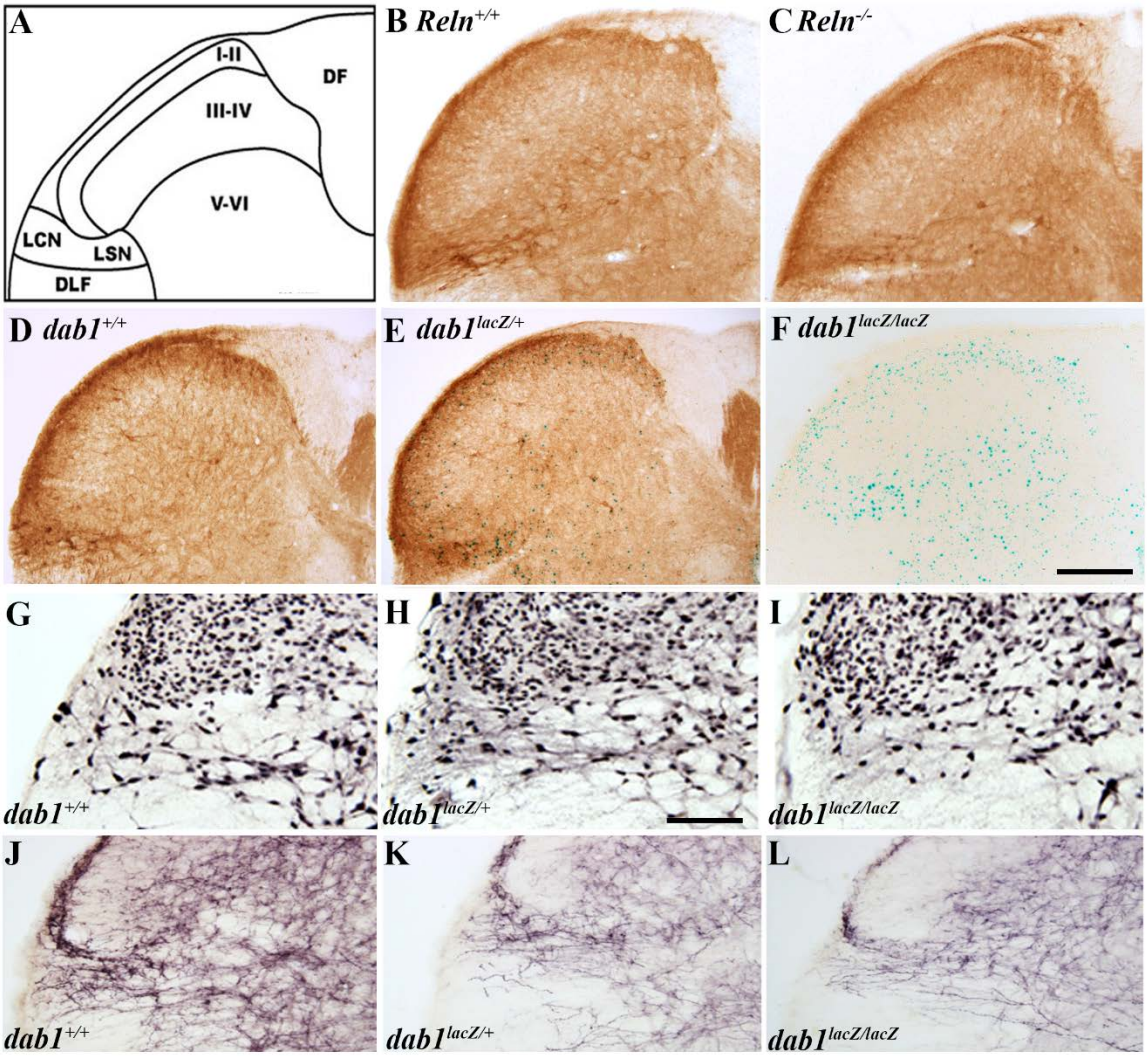
A
I-II
DF
III-IV
V-VI
LCN
LSN
DLF
B Reln+/+
C Reln-/-
D dab1+/+
E dab1lacZ/+
F dab1lacZ/lacZ
G
H
I
dab1+/+
dab1lacZ/+
dab1lacZ/lacZ
J
K
L
dab1+/+
dab1lacZ/+
dab1lacZ/lacZ

**Figure 9. Lateral cervical nucleus: Dab1-Lmx1b neurons are mispositioned in *Reln* mutants.**

***A-B***, Confocal images of cervical level C2 sections of $Reln^{+/+}$ (***A***) and $Reln^{-/-}$ (***B***) dorsal horn. LCN/LSN is designated by a dashed line and boxed areas in ***A*** and ***B*** are enlarged in ***A1-3*** and ***B1-3***. White arrows mark single-labeled red Dab1 or green Lmx1b cells and yellow arrowheads indicate co-localization. About 50% of the Dab1-Lmx1b neurons are missing from $Reln^{-/-}$ LCN/LSN (n=5 mice/genotype). Scale bars: ***A***; ***B***, 100 µm; ***A1-3***; ***B1-3***, 50 µm.

**Figure 9**

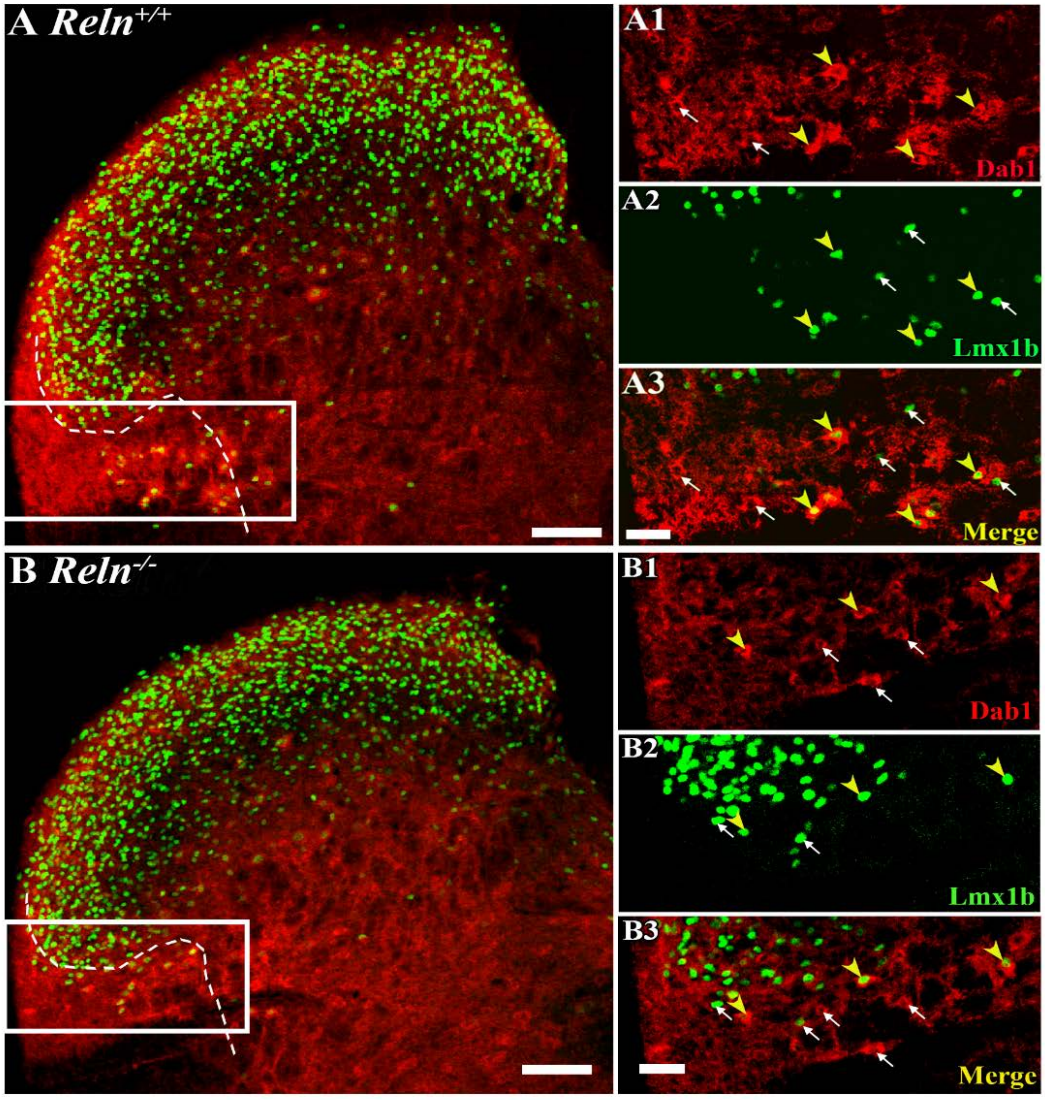
A Reln+/+
A1
Dab1
A2
Lmx1b
A3
Merge
B Reln-/-
B1
Dab1
B2
Lmx1b
B3
Merge

*Chapter 3*

**Reelin dorsal horn neurons are glutamatergic and migrate with Dab1 cells and subsets of Lmx1b-expressing neurons**


**Abstract**

Adult Reelin-signaling pathway mutant mice exhibit dorsal horn positioning errors in nociceptive areas, heat hypersensitivity, and mechanical insensitivity. The extracellular matrix glycoprotein Reelin binds its lipoprotein receptors, leading to the recruitment and phosphorylation of the adaptor protein Disabled-1 (Dab1). This event, in turn, activates downstream pathways that regulate neuronal migration. We reported that 70% of Dab1 laminae I-II neurons co-expressed Lmx1b and now show that about 90% of Reelin-labeled neurons in laminae I-II also express Lmx1b. Next, we determined that Reelin-Lmx1b and Dab1-Lmx1b neurons are separate populations and when combined, comprise 37% of Lmx1b-positive cells within and above the IB4 layer of wild-type mice. The *dab1* mutants have increased number of Reelin-Lmx1b neurons within the IB4 layer and reduced number of Reelin-Lmx1b neurons within the lateral reticulated area and lateral spinal nucleus. These findings are similar to those reported for the Dab1-Lmx1b neurons in *Reln* mutants. Importantly, we examined the migratory patterns of Reelin- and Dab1-Lmx1b dorsal horn neurons and show that most Reelin and Dab1 neurons contribute to the Lmx1b-positive dI5 and $dIL_B$ dorsal interneuron populations. In *dab1* mutants, the migration of Reelin cells is relatively normal, whereas in $Reln^{-/-}$ embryos, aberrantly positioned Dab1 neurons are apparent. Together, our results suggest that the similar neuroanatomical abnormalities in nociceptive areas of *Reln* and *dab1* mutants are caused primarily by migratory errors of Dab1 and Dab1-Lmx1b neurons. These migratory errors likely contribute to the nociceptive abnormalities displayed by the Reelin-signaling mutant mice.

## Introduction

The canonical Reelin-signaling pathway begins when secreted Reelin (Reln) binds to its receptors, Apolipoprotein E receptor 2 (Apoer2) and Very-low-density-lipoprotein receptor (Vldlr). Reln binding leads to receptor clustering and the recruitment and phosphorylation of the intracellular adaptor protein Disabled-1 (Dab1). Phosphorylated Dab1 then activates downstream pathways that regulate neuronal positioning during embryonic development (Howell *et al*., 1997; Arnaud *et al*., 2003; Bock & Herz, 2003). Reelin-signaling is terminated with the polyubiquitination and degradation of phosphorylated Dab1 (Arnaud *et al*., 2003). Mice with mutations in Reelin (*Reln*$^{-/-}$), or both lipoprotein receptors or Dab1 (*dab1*$^{-/-}$) demonstrate similar neuronal positioning errors (Howell *et al*., 1997; Trommsdorff *et al*., 1999). In *Reln*$^{-/-}$ mice, Dab1 does not get degraded and accumulates in mispositioned neurons. Although the expression of Reelin-signaling pathway components decreases after embryonic development, this pathway has crucial functions throughout life. Reelin signaling plays a role in postnatal dendritic outgrowth, branching and orientation (Niu *et al*., 2004; Matsuki *et al*., 2008), and Reelin deficiency in adults results in reduced levels of postsynaptic proteins, including postsynaptic density-95 (PSD-95) and N-methyl D-aspartate (NMDA)-receptor subunits NR2A and B (Weeber *et al*., 2002; Ventruti *et al*., 2011).

Previously, we reported that *Reln*$^{-/-}$, *dab1*$^{-/-}$, and *dab1*$^{lacZ/lacZ}$ mice demonstrate hypersensitivity in response to noxious heat stimulation and reduced sensitivity to mechanical stimulation (Villeda *et al*., 2006; Akopians *et al*., 2008; Yvone *et al*., 2017). Moreover, Reelin and Dab1 are concentrated in lumbar dorsal horn areas known to participate in pain transmission: laminae I-II (the superficial dorsal horn), the lateral reticulated area of lamina V, and the lateral spinal nucleus (LSN; Villeda *et al*., 2006). Nociceptive primary afferents terminate in

characteristic laminar patterns in laminae I-II, and then interneurons relay messages to projection neurons in laminae I, V, and the LSN which in turn transmit noxious signals to supraspinal areas (Basbaum *et al*., 2009; Todd, 2010). Recently, we reported that 70% of Dab1 laminae I-II neurons co-express the LIM-homeobox transcription factor 1-beta (Lmx1b), a marker of glutamatergic neurons derived from the dI5/dIL$_B$ cell groups during embryonic development (Gross *et al*., 2002; Müller *et al*., 2002; Cheng *et al*., 2004; Yvone *et al*., 2017). We also detected mispositioned Dab1 and Dab1-Lmx1b neurons in *Reln*$^{-/-}$ within the Isolectin B4 (IB4) layer, lateral lamina V, and the LSN, plus a compaction of the area dorsal to the IB4 layer (i.e., laminae I-II$_{outer}$; Yvone *et al*., 2017). Such anatomical abnormalities likely contribute to the changes in nociceptive functions seen in *Reln*$^{-/-}$ mice.

With the majority of Dab1 dorsal horn neurons identified, we turned to the Reelin-expressing neurons in this region. Recent studies that used either the brain-sparing Lmx1b conditional knockout mice (Szabo *et al*., 2015) or the CNS-specific deletion of the testicular orphan nuclear receptor (*TR4;* Wang *et al*., 2013) reported a large reduction of Reelin-positive cells in laminae I-II together with excitatory neurons marked by Calbindin (Wang *et al*., 2013; Szabo *et al*., 2015) or the Neurokinin-1-receptor (NK1R; Szabo *et al*., 2015). In addition, both mutant mouse lines exhibited a reduction of response to mechanical pain (Wang *et al*., 2013; Szabo *et al*., 2015). Results from these studies suggest that the loss of excitatory neurons in the superficial dorsal horn correlates with reduced mechanical sensitivity.

Initially, we asked whether Reelin-expressing dorsal horn neurons also express Lmx1b, and if so, whether Reelin and Dab1 neurons represent the same or separate populations of excitatory neurons. Next, we evaluated neuroanatomical abnormalities of Reelin-expressing neurons in the adult lumbar dorsal horns of *dab1* mouse pairs. Finally, we examined Reelin and

Dab1 neurons during embryonic development to correlate their migratory pathways with those of the two established subsets of Lmx1b-positive cell populations, i.e., dI5 and $dIL_B$ (Gross *et al*., 2002; Müller *et al*., 2002).

## Materials and Methods

### Animals

*Reln* mice: The *Reln* (B6C3Fe-ala-*Reln*$^{rl}$) mice were obtained from Jackson Laboratory, and a breeding colony was established at UCLA. Mice were genotyped according to D'Arcangelo *et al*. (1996) and will be referred to as *Reln*$^{+/+}$ and *Reln*$^{-/-}$ mice based on Jackson Laboratory annotations.

*Apoer2/Vldlr* mice: *Apoer2* (B6; 129S6-$^{Lrp8tm1Her}$, generous gift from Dr. T. Curran) and *Vldlr* (B6; 129S7-*Vldlr*$^{tm1Her}$, Jackson Laboratory) mice were generated from breeding colonies maintained at UCLA. *Apoer2*$^{-/-}$ and *Vldlr*$^{-/-}$ mutant mice were described and genotyped following protocols adapted from Frykman *et al*. (1995) and Trommsdorff *et al*. (1999).

The *dab1* mice: Mice were obtained from Dr. Brian Howell (SUNY Upstate Medical University, Syracuse, NY). These mice have a *lacZ* reporter fused with the first 22 amino acids of the *dab1* locus, replacing Dab1 expression with β-gal reaction product. The generation and characterization of the *dab1*$^{lacZ}$ mice were described and genotyped according to Pramatarova *et al*. (2008) and Abadesco *et al*. (2014). In *dab1*$^{lacZ/+}$ mice, there is one normal *dab1* allele present, whereas in *dab1*$^{lacZ/lacZ}$ mice, *dab1* expression is eliminated. These mice will be referred to as *dab1*$^{+/+}$ and *dab1*$^{-/-}$ mice (Pramatarova et al., 2008).

*Reln*$^{rl-Orl}$*; GAD67*$^{GFP}$ mice: Mice were generated as described in Abadesco *et al*. (2014). The *Reeler Orleans* (*Reln*$^{rl-Orl}$) mutation causes defective Reelin secretion (de Bergeyck *et al*., 1997). Genotyping was adapted from Hammond *et al*. (2006). The *GAD67*$^{GFP}$ line was generated by Tamamaki *et al*. (2003). *GAD67*$^{GFP/+}$ mice were intercrossed with *Reln*$^{rl-Orl}$ mice to introduce the GFP reporter into Reelin-signaling pathway mutants.

**Tissue preparation and immunohistochemistry**

Adult mice were anesthetized (sodium pentobarbital, 100 mg/kg), perfused transcardially with 4% paraformaldehyde, and post-fixed for 1-3 h at 4°C in the same fixative. Following an overnight wash with 0.12 M phosphate buffer (PB), spinal cords were dissected and cryoprotected in 30% sucrose in PB for 2 days. Lumbar (L4–5) segments were blocked and frozen in Optimum Cutting Temperature embedding medium (Fisher Scientific #4585) and stored at -80°C. For embryonic studies, the day of plug detection is considered embryonic day 0.5 (E0.5). Pregnant mice were deeply anesthetized, and embryos (E11.5–E15.5) were delivered by Cesarean section and immersed in 2% PLP (2% Paraformaldehyde; 0.075M Lysine-HCL-monohydride; 0.010M Sodium periodate; 0.1M sodium phosphate) overnight at 4°C. After multiple washes with 0.12 M PB, the lumbar region was blocked and cryoprotected in 30% sucrose/PB for 1-2 days before being frozen in M-1 embedding matrix (Thermo-Scientific, Shandon #1310) and stored at -80°C.

*Immunohistochemical procedures*: For Reelin immunofluorescence on adult mouse sections, mouse anti-Reelin was used with a Tyramide Signal Amplification (TSA) kit. 25 µm thick, free-floating sections were incubated with 3% hydrogen peroxide and 10% methanol in 0.1M phosphate buffered saline (PBS) followed by a blocking solution of 1% nonfat milk, 0.2% gelatin, 10% normal donkey serum (NDS), and 0.5% Triton X-100 in PBS for 1 h. Sections were then incubated overnight with mouse anti-Reelin (G10; see Table 1 for primary antibody information) at 4°C, followed by repeated washes in PBS and a 1 h incubation with biotinylated donkey anti-mouse IgG (1:800; Jackson Immunoresearch #715-065-150) in PBS. Multiple washes with TNT (0.1M Tris-HCl; 0.15M NaCl; 0.05% Tween) preceded a 1 h incubation with streptavidin-conjugated horseradish peroxidase (1:1,000; PerkinElmer #NEL750001EA) in TSA-

specific blocking solution (TNB), and a 5-min incubation with TSA Plus Fluorescein (1:150; PerkinElmer #NEL741001KT) or Cy5 (1:100; PerkinElmer #NEL745001KT). Sections were washed with the appropriate buffers before subsequent immunofluorescence protocols.

For Reelin immunolabeling on embryos, goat anti-Reelin was used together with a TSA kit. 30 µm thick, slide-mounted sections were first incubated in 1% hydrogen peroxide and 0.1% sodium azide in PBS. Then, 10% NDS and 0.1% Triton X-100 in PBS was used as the blocking solution. Sections were incubated with Avidin-Biotin blocking kit (Vector laboratories; #SP-2001) before overnight incubation with goat anti-Reelin at RT. Sections were washed in PBS followed by TNT buffer, and then a 1 h incubation with biotinylated horse anti-goat IgG (1:1,000; Vector laboratories #BA-9500) in TNB. Then, multiple washes with TNT preceded a 1 h incubation with streptavidin-conjugated horseradish peroxidase as above (1:1,000) in TNB, and a 5-min incubation with TSA Plus Fluorescein (1:200).

For Dab1 labeling, the TSA protocol used was similar to that reported for goat anti-Reelin, except that 5% NDS in 0.1M PBS and 0.3% Triton X-100 was used as the blocking solution followed by Avidin-Biotin and a 48-hour incubation with rabbit anti-Dab1. For Lmx1b and Pax2 labeling, 5% NDS and 0.1% Triton X-100 in PBS was used as the blocking solution followed by an overnight incubation with the primary antibodies. The standard TSA immunofluorescence protocol described above was then used. IB4 was visualized using a biotinylated IB4 conjugate as published (Yvone *et al*., 2017). Routine immunofluorescence techniques were used to localize GAD67 with chick anti-green fluorescent protein as reported (GFP; Abadesco *et al*., 2014). Most secondary antibodies were purchased from Jackson Immunoresearch including: biotinylated donkey anti-guinea pig (#706-065-148) and donkey anti-rabbit IgG (#711-065-152) for TSA experiments. Streptavidin-Alexa Fluor 488 (Invitrogen,

Molecular Probes #S32354) was used to visualize IB4 conjugate, and donkey anti-chick Alexa Fluor 488 (#703-545-155) was used to detect GFP. Some sections were counterstained with Hoechst nucleic acid stain (1:500; Molecular Probes #H1398), mounted, dried, and cover-slipped.

We used a Zeiss LSM800 confocal microscope to obtain the dorsal horn images for all statistical analyses. Hemisections were imaged with a 10x objective, while images for the superficial dorsal horn analyses were taken with a 40x objective. ZEN (Zeiss Efficient Navigation) lite imaging software was used for all analyses. Images were transferred to Photoshop for figure assembly.

**Statistical analyses**

To compare the absolute mean numbers of Reelin and Reelin-Lmx1b neurons and percent colocalization of Reelin-Lmx1b neurons between genotypes, we counted labeled neurons within the superficial dorsal horn (~120 μm from the dorsal-most grey matter) in 3 μm-thick confocal slices. 5 hemisections per animal were analyzed in 3 pairs of *dab1*$^{+/+}$ and *dab1*$^{-/-}$ mice. The mean numbers of Reelin and Reelin-Lmx1b neurons were compared by genotype and cell type with 2x2 repeated measures ANOVA. The total numbers of Reelin cells and the percentages of Reelin-Lmx1b out of total Reelin neurons were compared by genotype in a separate analysis with ANOVA. The corresponding post hoc p-values for all mean comparisons are reported. All calculations were done with JMP 10 (SAS Inc.).

To identify positioning errors and the percentage of total Lmx1b neurons that were Reelin-positive in laminae I-II, Reelin-, Lmx1b-, and double-labeled cells were counted within the IB4 layer (lamina $II_{inner\ dorsal}$) and above the IB4 layer (laminae I-$II_{outer}$). Analyses were done in 3 μm-thick confocal slices of 3 hemisections per animal in 4 pairs of *dab1*$^{+/+}$ and *dab1*$^{-/-}$ mice.

The means of Reelin-, Lmx1b-, and Reelin-Lmx1b-labeled cells were compared by genotype and area stratified by each cell type with 2x2 repeated measures ANOVA and post hoc t-tests. The mean numbers of total Reelin and Lmx1b neurons were compared using ANOVA similar as above. Significance of the IB4 areal measurements was determined using 2x2 repeated measures ANOVA and post hoc t-tests. Percentages of Reelin-Lmx1b neurons out of total Reelin or total Lmx1b neurons were obtained by combining the numbers of cells within and above the IB4 layer (laminae I-$II_{inner\ dorsal}$) and compared between genotypes using repeated measures ANOVA and post hoc t-tests.

For the current study, we used a previously analyzed dataset of Dab1 and Dab1-Lmx1b neurons the laminae I-$II_{inner\ dorsal}$ (Yvone *et al*., 2017). Then, we additionally counted the number of Lmx1b-labeled neurons within laminae I-$II_{inner\ dorsal}$ from the same 3 μm-thick confocal slices of 6 hemisections per animal in 4 pairs of $Reln^{+/+}$ and $Reln^{-/-}$ mice (Yvone *et al*., 2017). Now we also report the percentage of Lmx1b neurons that co-express Dab1 within laminae I-$II_{inner\ dorsal}$. The mean numbers of Lmx1b-labeled neurons were compared with the Dab1 and Dab1-Lmx1b neurons by genotype and area stratified by each cell type using ANOVA as above. As with the analyses for Reelin-Lmx1b cells, the percentages of Dab1-Lmx1b neurons out of total Dab1 or Lmx1b neurons were obtained and compared between genotypes using ANOVA.

To estimate the number of cells in the lateral lamina V and LSN, we examined multiple 9-15 μm Z-stack (3-5 slices). Lateral lamina V counts were sampled in a 17,000 $\mu m^2$ boxed region adjacent and medial to the LSN (Yvone *et al*., 2017), whereas the LSN counts were done in an outlined region as reported in Wang *et al*. (2012). The numbers of Reelin, Reelin-Lmx1b and Lmx1b neurons were counted from 3-10 hemisections per mouse in 4 pairs of $dab1^{+/+}$ and $dab1^{-/-}$ mice. For all analyses, counts were restricted to cells with a diameter of at least 7 μm to

ensure neuronal identity according to analyses done with NeuN experiments (data not shown). For each area, the means of Reelin, Lmx1b, and Reelin-Lmx1b neurons were compared by genotype and cell type with 2x3 repeated measures ANOVA and post-hoc t-tests. The mean numbers of total Reelin and total Lmx1b neurons were compared using similar analysis as above.

## Results

### About 90% of Reelin-expressing superficial dorsal horn neurons also express Lmx1b

Because the majority of laminae I-II interneurons are excitatory, we first asked whether Reelin cells co-express the transcription factor Lmx1b. Reelin (green cytoplasm) and Lmx1b (red nuclei) were, in fact, co-localized in many laminae I-II neurons in *dab1*$^{+/+}$ (Fig. 10A-A3; yellow arrowheads) and *dab1*$^{-/-}$ (Fig. 10B-B3; yellow arrowheads). Some single-labeled Reelin neurons also were detected (Fig. 10A1-2; yellow arrows). Occasionally, large Reelin-positive neurons were observed in laminae I-II, most of which co-expressed Lmx1b, in both genotypes (Fig. 10B1-3; large yellow arrowheads). The total number of Reelin-expressing neurons in laminae I-II, with or without Lmx1b, did not differ between genotypes (*dab1*$^{+/+}$ 34±0.6 neurons; *dab1*$^{-/-}$ 31±1.4 neurons). Analyses revealed that 88-92% of Reelin-expressing superficial dorsal horn neurons co-express Lmx1b (*dab1*$^{+/+}$ 88±5.1%; *dab1*$^{-/-}$ 92±1.5%). These results imply that most Reelin-expressing superficial dorsal horn neurons are excitatory.

### Reelin-Lmx1b neurons are mispositioned in *dab1* mutant superficial dorsal horn

To assess whether the loss of Dab1 function results in similar neuroanatomical defects to those of *Reln*$^{-/-}$ mice (Yvone *et al*., 2017), we looked for evidence of positioning errors within the laminae I-II of the dorsal horn. Initially we examined the distribution of Reelin and Lmx1b neurons within the IB4 layer, which receives nonpeptidergic nociceptive afferents and terminates in the dorsal part of lamina II$_{\text{inner}}$ (i.e., lamina II$_{\text{inner dorsal}}$; Basbaum et al., 2009). When we evaluated the area of lamina II$_{\text{inner dorsal}}$, there was no difference between genotypes (Fig. 11A, B). There were, however, more Reelin-Lmx1b neurons within *dab1*$^{-/-}$ than in the *dab1*$^{+/+}$ lamina II$_{\text{inner dorsal}}$ (Fig. 11C; *dab1*$^{+/+}$ 10±1.6 neurons; *dab1*$^{-/-}$ 16±1.5 neurons; $p$=0.022). On the other hand, the numbers of single-labeled Reelin (Fig. 11C; *dab1*$^{+/+}$ 2±0.6 neurons; *dab1*$^{-/-}$ 2±0.4

neurons) and Lmx1b neurons (Fig. 11C; *dab1*$^{+/+}$ 58±6.6 neurons; *dab1*$^{-/-}$ 59±3.5 neurons) in this area showed no differences.

Next, we analyzed the area above the IB4 layer, which receives peptidergic afferent innervation and is termed laminae I-II$_{outer}$. We found that the size of the region was reduced in *dab1*$^{-/-}$ compared to *dab1*$^{+/+}$ dorsal horn (Fig. 11A, B; *dab1*$^{+/+}$ 21,226±755 μm$^2$; *dab1*$^{-/-}$ 16,598±1,223 μm$^2$; $p$=0.006). Neither the number of Reelin cells nor the number of Lmx1b neurons in laminae I-II$_{outer}$, however, differed between genotypes. Thus, the Reelin-Lmx1b neurons were specifically mispositioned within the lamina II$_{inner\ dorsal}$ of *dab1* mutant mice. Additionally, relatively few Reelin-expressing cells were present within lamina II$_{inner\ ventral}$, an area characterized by Protein Kinase C gamma (PKCγ)-positive interneurons (data not shown).

**Reelin- and Dab1-labeled superficial dorsal horn neurons are different subsets of the Lmx1b population**

Because both Dab1 (Yvone *et al*., 2017) and Reelin neurons in laminae I-II co-express Lmx1b, we asked whether they represent the same or different populations of these excitatory neurons. To best address this question, we used *Apoer2;Vldlr* mice as both Reelin and Dab1 are expressed at higher levels in double-receptor mutants than in wild-type mice (Trommsdorff *et al*., 1999). With triple immunolabeling, we showed that Reelin-Lmx1b neurons (Fig. 12A-A3 and 12B-B3; yellow arrowheads) and Dab1-Lmx1b neurons (Fig. 12A-A3 and 12B-B3; white arrowheads) were generally small and distributed throughout laminae I-II. More importantly, however, the Reelin- and Dab1-Lmx1b neurons represented different subsets of Lmx1b-expressing neurons. The large Reelin cells in laminae I-II were mostly Lmx1b-positive, but large Dab1 cells were either single or double-labeled and sometimes found in the deep dorsal horn in both genotypes (Yvone *et al*., 2017).

Then, we evaluated the percentage of Lmx1b-labeled neurons that co-express Reelin or Dab1 by quantifying the Lmx1b-expressing neurons within laminae I-II$_{\text{inner dorsal}}$ in 3 µm thick confocal images of *dab1* and *Reln* mouse pairs, respectively. The Reelin-Lmx1b neurons in laminae I-II$_{\text{inner dorsal}}$ made up 83-88% of total Reelin-labeled neurons (*dab1*$^{+/+}$ 83±3.5%; *dab1*$^{-/-}$ 88±1.9%) and 17-24% of total Lmx1b neurons (*dab1*$^{+/+}$ 17±1.7%; *dab1*$^{-/-}$ 24±2.2%; $p$=0.049; see Table 2 for the total numbers of Reelin and Lmx1b neurons). Additionally, we determined that Dab1-Lmx1b neurons comprised 71-74% of total Dab1 neurons (*Reln*$^{+/+}$ 74±2.1%; *Reln*$^{-/-}$ 71±2.2%) and 20-22% of total Lmx1b neurons in laminae I-II$_{\text{inner dorsal}}$ (*Reln*$^{+/+}$ 20±2.9%; *Reln*$^{-/-}$ 22±0.6%; see Table 3 for the total numbers of Dab1 and Lmx1b neurons).

In total, Reelin-Lmx1b and Dab1-Lmx1b neurons made up about 37% of the total Lmx1b-positive neurons within the laminae I-II$_{\text{inner dorsal}}$ in adult wild-type mice, whereas in mutants they comprised 46% of the total Lmx1b neurons in this area. Surprisingly, in spite of the fact that the area of laminae I-II$_{\text{outer}}$ was reduced in both *Reln*$^{-/-}$ and *dab1*$^{-/-}$ mice, there was no significant reduction in the number of Lmx1b, Reelin-Lmx1b, or Dab1-Lmx1b neurons (Yvone *et al*., 2017).

**Most Reelin neurons in the superficial dorsal horn are not inhibitory**

Given that most Reelin neurons in the superficial dorsal horn are excitatory, we asked if the remaining Reelin-labeled cells were inhibitory. We first assessed *Reln*$^{rl\text{-}Orl}$ mice interbred with a *GAD67*$^{GFP}$ line that expresses GFP under the GAD67 promoter (Tamamaki *et al*., 2003; Abadesco *et al*., 2014). Generally, Reelin cells in laminae I-II did not express GAD67 (Fig. 13A-A2). In addition, we co-labeled Reelin and Pax2, a transcription factor expressed by most inhibitory dorsal horn neurons (Lai *et al*., 2016). Almost none of the Reelin-expressing laminae

I-II dorsal horn neurons expressed Pax2 (Fig. 13B-B3), a finding that suggests that the remaining Reelin cells are excitatory.

**Lateral reticulated area and LSN: Reelin-Lmx1b neurons are mispositioned in *dab1*$^{-/-}$ mice**

The lateral reticulated area (Fig. 14A) contains wide-dynamic range projection neurons that respond to noxious thermal and mechanical stimuli (Menétrey *et al*., 1980, 1982). Here we determined that the number of Reelin-only neurons in lateral lamina V did not differ by genotype, but we found a reduced number of Lmx1b-only neurons in *dab1*$^{-/-}$ compared to *dab1*$^{+/+}$ lateral reticulated area (Fig. 14G; *dab1*$^{+/+}$ 4±0.5 neurons; *dab1*$^{-/-}$ 2±0.3; $p$=0.002). Additionally, there were more Reelin-Lmx1b neurons in *dab1*$^{+/+}$ than in *dab1*$^{-/-}$ lateral lamina V (Fig. 14C-C2, D-D2; yellow arrowheads; Fig. 14G; *dab1*$^{+/+}$ 2±0.2; *dab1*$^{-/-}$ 0.4±0.1; $p$=0.005). Overall, the Lmx1b and Reelin-Lmx1b neurons are greatly reduced in *dab1*$^{-/-}$ lateral reticulated area and therefore are likely to be incorrectly located in another dorsal horn area.

The LSN is composed of a small number of neurons within the dorsolateral funiculus and includes several projection neurons that relay pain information to the brainstem and thalamus (Fig. 14B; Menétrey *et al*., 1982; Burstein *et al*., 1990). Here we found a difference in the number of Reelin-only neurons (Fig. 14H; *dab1*$^{+/+}$ 1±0.5; *dab1*$^{-/-}$ 0.2±0.1; $p$=0.005). We also detected more Lmx1b-only neurons in *dab1*$^{+/+}$ compared to *dab1*$^{-/-}$ LSN (Fig. 14H; *dab1*$^{+/+}$ 2±0.1 neurons; *dab1*$^{-/-}$ 1±0.3 neurons; $p$=0.003), and more Reelin-Lmx1b neurons in *dab1*$^{+/+}$ than *dab1*$^{-/-}$ LSN (Fig. 14E-E2, F-F2; yellow arrowheads; Fig. 14H; *dab1*$^{+/+}$ 2±0.2; *dab1*$^{-/-}$ 0.7±0.3; $p$=0.015). These results show consistent losses of Reelin-, Lmx1b-, and Reelin-Lmx1b neurons in the LSN in the absence of functional Dab1.

**Embryonic Reelin-expressing neurons migrate together with Lmx1b dorsal horn neurons**

As most Reelin dorsal horn neurons co-express Lmx1b, we characterized their migration relative to the Lmx1b neurons. At E11.5, Reelin expression (green) was concentrated ventrally as axons of Reelin-expressing commissural neurons crossed in the ventral commissure (Fig. 15A, B), and Lmx1b nuclei (red) were present in the floor plate (Fig. 15A1, B1). In addition, Reelin was expressed along the dorsolateral part of the spinal cord in both genotypes (Fig. 15A, B). In E11.5 embryos, Lmx1b-labeled cells marked a distinct group of postmitotic neurons, the early-born dI5 group (Fig. 15A1, B1; Gross *et al*., 2002; Müller *et al*., 2002). The Lmx1b cluster appeared more dispersed in *dab1*$^{-/-}$ than in *dab1*$^{+/+}$ mice (Fig. 15A1, B1), and dorsolaterally-located Reelin cells that were single-labeled or double-labeled with Lmx1b also were detected (Fig. 15A, A2, B, B2; white arrows and arrowheads, respectively).

By E12.5, Reelin expression has expanded dorsally and medially (Fig. 15C, D; Kubasak *et al*., 2004) and many more Lmx1b neurons were found in the dorsal spinal cord. Previous studies classified this second Lmx1b-expressing group as the late-born glutamatergic population ($dIL_B$) that was derived from a broad progenitor domain (Fig. 15C1, D1; Gross *et al*., 2002; Müller *et al*., 2002). At E12.5, Reelin expression co-localized primarily with the dI5 subset of Lmx1b-positive neurons (Fig. 15C2, D2; white arrowheads), but single-labeled Reelin cells were also found (Fig. 15C, C2, D, D2; white arrows). The patterns of Reelin and Lmx1b expression appeared largely similar between the genotypes, although the lateral dI5 group was more tightly clustered in *dab1*$^{+/+}$ than *dab1*$^{-/-}$ mice (Fig. 15C1, D1).

Reelin-expressing cells at E13.5 were highly concentrated in the dorsolateral region with dI5 neurons and were either single-labeled (Fig. 16A, B; white arrows) or double-labeled with Lmx1b (Fig. 16A, B; white arrowheads). Notably, Reelin expression was widely detected within

the dorsal horn at this stage (Fig. 16A1, B1), compared to both earlier and later ages. In addition, there was an enormous expansion of the Lmx1b-positive $dIL_B$ population that filled the dorsal horn at E13.5 (Fig. 16A, B; Gross *et al*., 2002; Müller *et al*., 2002). A few Reelin-Lmx1b neurons were also observed medially and thus were derived from the $dIL_B$ population (Fig. 16A, B). Although Reelin cells were primarily located dorsolaterally in *dab1*$^{+/+}$ embryos, occasional Reelin-Lmx1b neurons did migrate circumferentially around the rim of the dorsal horn in *dab1* mutants (Fig. 16B, B1; white arrowheads), including one that appeared mispositioned (Fig. 16B, B1; yellow arrowhead).

By E14.5-15.5, the highest concentration of Reelin remained dorsolaterally, in a region just lateral to the nascent dorsal horn which represented the presumptive LSN and lateral lamina V (Fig. 16C-F). In contrast, the central dorsal horn area occupied by the majority of Lmx1b-positive nuclei contained relatively few Reelin-labeled neurons (Fig. 16C, C1, D, D1). Additionally, at E14.5-15.5, Reelin- (white arrows) and Reelin-Lmx1b-expressing cells (white arrowheads) formed a distinct band around the outer rim of the superficial dorsal horn, and the double-labeled cells in this region were derived from both dI5 and $dIL_B$ populations (Fig 16C-F). A few single-labeled Lmx1b and Reelin-Lmx1b-expressing neurons were detected around the midline at E14.5 and E15.5 (Fig. 16C-F, asterisks at midline). Previous studies identified this group as a late-born part of $dIL_B$ population (Escalante *et al*., 2013). By E15.5, the migration of most Reelin (white arrows) and Reelin-Lmx1b cells (white arrowheads) appeared complete, as the neurons along the rim contributed to the laminae I-II, and those neurons located dorsolaterally would settle in the LSN and the lateral reticulated area of lamina V (Fig. 16E-F).

**Embryonic Dab1 neurons also migrate together with Lmx1b neurons**

Because 70% of Dab1-labeled laminae I-II neurons express Lmx1b and the Dab1 and Dab1-Lmx1b neurons exhibit positioning errors (Yvone *et al*., 2017), we also examined the common migratory pathway of Dab1 and Lmx1b neurons in *Reln* mice. At E11.5, Dab1 was expressed ventrally by somatic motor neurons (Palmesino *et al*., 2010) and by axons that crossed in the ventral commissure (Fig. 17A, A2, B, B2). At both E11.5 and E12.5, the dI5 group of Lmx1b neurons was more tightly clustered in wild-type than in mutant mice (Fig. 17A1, B1). Both Dab1 and Dab1-Lmx1b neurons were detected in the dorsolateral region (Fig. 17A2, B2; white arrows and arrowheads, respectively). By E12.5, Dab1 expression expanded within the dorsolateral intermediate zone in both $Reln^{+/+}$ and $Reln^{-/-}$ embryos (Fig. 17C, C2, D, D2). Additionally, the Lmx1b-expressing $dIL_B$ population appeared (Fig. 17C1, D1; Gross *et al*., 2002; Müller *et al*., 2002), but there was little evidence of co-localization between Dab1 and this late-born Lmx1b cell group (Fig. 17C2, D2).

By E13.5, Dab1 was expressed along the lateral rim of the superficial dorsal horn and in the deep dorsal horn in both genotypes (Fig. 18A, A1, B, B1). Distinct clusters of Dab1 cells co-localized with the lateral Lmx1b-positive dI5 neurons (Fig. 18A, A1, B, B1; white arrowheads), and a few of the medial Lmx1b-expressing $dIL_B$ cells (Fig. 18A, B; white asterisks). We also detected Dab1-only cells (white arrows) interspersed with the Dab1-Lmx1b cells (white arrowheads) throughout the mediolateral extent of the dorsal horn (Fig. 18A, A1, B, B1). In E13.5, Dab1 immunoreactivity was higher and Dab1 cells appeared disorganized in $Reln^{-/-}$ compared to $Reln^{+/+}$ embryos (Fig. 18A1, B1).

The developmental differences in Dab1 expression when Reelin was absent were quite distinct at E14.5. First, the dorsolaterally-located Dab1-Lmx1b neurons derived from the dI5

group were apparent in both genotypes. The Dab1-Lmx1b neurons in *Reln*$^{-/-}$, however, had migrated further dorsally along the outer rim of the dorsal horn (presumptive laminae I-II; Fig. 18D, D1; white arrowheads) compared to the *Reln*$^{+/+}$ embryos (Fig. 18C, C1; white arrowheads). Second, it appeared that a limited number of Dab1-Lmx1b neurons arose from the dIL$_B$ population as much of the *Reln*$^{+/+}$ dorsal horn was completely devoid of Dab1 expression (Fig. 18C, C1). In *Reln*$^{-/-}$ E14.5, however, we consistently detected large single-labeled Dab1 (white arrows) and Dab1-Lmx1b neurons (white arrowheads) migrating across the deep dorsal horn (Fig. 18D, D1; large yellow arrow). Finally, there were distinct, large Dab1 neurons that mostly co-expressed Lmx1b in the dorsal midline of both genotypes derived from a late-born dIL$_B$ population (Fig. 18C, D; white asterisks; Escalante *et al*., 2013). In E14.5 *Reln*$^{-/-}$ mice (Fig. 18D, D1), we found that a greater number of these dorsal midline Dab1 and Dab1-Lmx1b neurons appeared to have migrated laterally into the deep dorsal horn compared to *Reln*$^{+/+}$embryos (Fig. 18C, C1).

The differences between Dab1 expression in wild-type versus mutant embryos seen at E14.5 remained obvious at E15.5. We found that many Dab1 (white arrows) and Dab1-Lmx1b neurons (white arrowheads), derived from both dI5 and dIL$_B$ populations, contributed to the rim of the superficial dorsal horn in *Reln*$^{-/-}$ (Fig. 18F, F1) but they were not as easily detected in *Reln*$^{+/+}$ mice (Fig. 18E, E1). Additionally, the central core of the dorsal horn in *Reln*$^{+/+}$ E15.5 (Fig. 18E, E1) was relatively devoid of Dab1-expressing neurons while several Dab1 and Dab1-Lmx1b neurons were obvious in the deep dorsal horn of the *Reln*$^{-/-}$ mice (Fig. 18F, F1). Finally, we found the dorsal midline dIL$_B$ group of Dab1-Lmx1b neurons (Fig. 18E, F; white asterisks) that appeared in an organized stream toward lamina V in *Reln*$^{+/+}$ mice (Fig. 18E, E1; white

arrowheads). In *Reln*$^{-/-}$, however, the Dab1 and Dab1-Lmx1b neurons were dispersed within the deep dorsal horn (Fig. 18F, F1).

## Discussion

In this study, we first identified the Reelin-expressing neurons in nociceptive areas of the dorsal horn. In adult wild-type mice, we found: 1) 88% of Reelin neurons in the superficial dorsal horn co-express Lmx1b, 2) 35% of Reelin-labeled cells in the lateral reticulated area of lamina V also express Lmx1b, and 3) 59% of Reelin cells in the LSN are double-labeled. Together with previous studies, these data suggest that the Reelin-Lmx1b neurons are glutamatergic (Cheng *et al*., 2004; Dai *et al*., 2008). Importantly, we also showed that Reelin and Dab1 make up separate subsets of Lmx1b neurons and together comprise around 40% of the adult population of Lmx1b-positive glutamatergic neurons in laminae I-$II_{inner\ dorsal}$. Compared to wild-type controls, *dab1* mutants had positioning errors of Reelin-expressing neurons in laminae $II_{inner\ dorsal}$, the lateral reticulated area of lamina V, and the LSN. Additionally, we showed that embryonic Reelin and Dab1-expressing dorsal horn neurons share a common migratory pathway with subsets of Lmx1b-positive dI5 and $dIL_B$ neurons. During development, the absence of Dab1 does not greatly affect the migration of Reelin-expressing embryonic dorsal horn neurons, however, the loss of Reelin causes substantial positioning errors of Dab1 dorsal horn neurons.

### *Reln* and *dab1* mutant dorsal horns show common neuroanatomical abnormalities

When the Reelin-signaling pathway is disrupted by the loss of Reelin (Yvone *et al*., 2017) or Dab1 (present study), strikingly similar positioning errors are detected in the dorsal horn. In both studies we found a reduction of the size of laminae I-$II_{outer}$ (see summary diagram in Fig. 19). We also detected increased numbers of Dab1-Lmx1b (Yvone *et al*., 2017) or Reelin-Lmx1b neurons (present study) within the lamina $II_{inner\ dorsal}$ compared to their respective wild-type controls (Fig. 19). Both *Reln* and *dab1* mutants also exhibited reduced numbers of Dab1-Lmx1b (Yvone *et al*., 2017) or Reelin-Lmx1b (current study), respectively, in the lateral reticulated area and LSN

versus wild-type mice (Fig. 19). Additionally, the superficial dorsal horn abnormalities were difficult to detect whereas neuronal losses in the lateral reticulated area and LSN were obvious. The fact that neuronal positioning errors are similar within the dorsal horn nociceptive areas in both mutant lines implies that these alterations are attributed to the loss of the canonical Reelin-signaling pathway.

Because Reelin-signaling pathway mutant mice exhibit heat hypersensitivity and mechanical insensitivity, it suggests that the Reelin-Dab1 signaling pathway differentially affects circuits that process noxious thermal and mechanical pain. We provide results that support this labeled-line theory of nociceptive circuits (Basbaum *et al*., 2009) in a separate report (Wang *et al*., in preparation). Here, we found that the ablation of Neurokinin-1-receptor (NK1R)-expressing laminae I-II neurons with a Substance P analog conjugated to Saporin, specifically rescued the heat hypersensitivity displayed by *dab1* mutant mice without altering their mechanical insensitivity (Wang *et al*., in preparation). Furthermore, we detected NK1R-expressing neurons that co-expressed Dab1 and Dab1-Lmx1b and were mispositioned in $Reln^{-/-}$ mice. Based on these findings, we proposed that mispositioned NK1R-expressing neurons, many of which expressed Dab1, contributed to the heat hypersensitivity seen in our mutant mice.

Two conditional knockout mouse models generated by Szabo *et al*. (2015) and Wang *et al*. (2013) exhibited losses of excitatory neuronal populations from laminae I-II and insensitivity to noxious mechanical stimuli. Szabo *et al*. (2015) found that when *Lmx1b* was deleted from cervical spinal cord level C5 and below, there were decreased numbers of Calbindin- and NK1R-expressing laminae I-II neurons. Both studies also detected a reduction of the size of laminae I-II and a loss of Reelin-labeled cells in the superficial dorsal horn in the mutants (Wang *et al*., 2013; Szabo *et al*., 2015). In contrast, $Reln^{-/-}$ and $dab1^{-/-}$ mice had increased numbers of Dab1-Lmx1b

and Reelin-Lmx1b neurons, respectively, within the lamina $II_{inner\ dorsal}$. Interestingly, the *Reln*$^{-/-}$ and *dab1*$^{-/-}$ mice, however, had similar numbers of Lmx1b-expressing neurons in this area compared to wild-type controls. This suggests that there may be specific Lmx1b neurons absent from lamina $II_{inner\ dorsal}$ in our mutants. Several studies have correlated the loss of mechanical sensitivity to certain populations of excitatory neurons such as the Calbindin- (Wang *et al*., 2013; Szabo *et al*., 2015), Somatostatin- (Duan *et al*., 2014), and Calretinin-expressing neurons (Peirs *et al*., 2015). Thus, we suspect that some of these neurons may also be mispositioned in the Reelin-signaling pathway mutant dorsal horn, leading to the profound mechanical insensitivity displayed by the adult mutant mice.

**Reelin- and Dab1-expressing neurons migrate together with dI5 and $dIL_B$ Lmx1b neurons**

Here we showed that many Reelin- and Dab1-Lmx1b neurons are derived from both the early-born dI5 (E10.5-12.5) and late-born $dIL_B$ (E11.5-13.5) dorsal interneuron populations (Gross *et al*., 2002; Müller *et al*., 2002; Helms and Johnson, 2003). Initially the dI5 group was proposed to contain larger-sized neurons that settled laterally and ventrally (Gross *et al*., 2002; Lai *et al*., 2016), and we found Reelin- and Dab1-Lmx1b cells in those locations. On the other hand, the $dIL_B$ group represented ipsilaterally projecting relay neurons that integrated sensory information within the dorsal horn (Gross *et al*., 2002; Müller *et al*., 2002). While there were many Reelin-Lmx1b neurons derived from the $dIL_B$ group, only a few Dab1 neurons were clearly members of this population. It is notable that a few Reelin-Lmx1b and a larger number of Dab1-Lmx1b neurons were present in the dorsal midline and represented a late-born $dIL_B$ population. Postmitotic late-born $dIL_B$ glutamatergic spinal neurons in the dorsal midline were identified by Escalante *et al*. (2013) at E14. These authors additionally determined that these midline neurons co-expressed Lmx1b and Zic2 and suggested that Zic2 functioned to prevent their axons from

crossing the dorsal midline, resulting in ipsilateral axon projections. Together, our findings suggest that Reelin and Dab1-expressing cells comprise interneurons and projection neurons derived from the Lmx1b-positive dI5 and $dIL_B$ populations.

**Reelin signaling modulates different types of neuronal migration which contribute to the superficial dorsal horn formation**

Based on birthdating studies, Altman and Bayer (1984) proposed that early-generated projection neurons migrated laterally first and then most of these neurons continued to migrate circumferentially to form the outer rim of the dorsal horn. They also described that numerous later-born interneurons migrated from the dorsal ventricular zone laterally to form the core of the dorsal horn (Altman and Bayer, 1984). We identified a cohort of dI5-derived Reelin- and Dab1-Lmx1b neurons that settled dorsolaterally, in the area that will become the LSN and lateral lamina V. A subset of Reelin and Dab1 neurons also migrated circumferentially to contribute to the outer rim formation, with the Dab1 neurons in *Reln* mutants being especially prominent. The $dIL_B$ population would be a component of Altman and Bayer's later-born interneurons and would include several Reelin-Lmx1b neurons. Additionally, the Dab1-Lmx1b neurons found in the dorsal midline would likely migrate into the deep dorsal horn, to a location characterized by large projections neurons.

The highest levels of Reelin and Dab1 expression in the embryonic dorsal spinal cord were just lateral to the curvature of the nascent superficial dorsal horn, at the site of the lateral-most dI5 neurons. Spinal neurons that migrated laterally from the ventricular zone are generally guided along the radial glia (Phelps *et al*., 1993). Chai *et al*. (2009) and Krüger *et al*. (2010) reported that when migrating Dab1 neurons encountered Reelin in wild-type mice, Cofilin was phosphorylated. This event acted to inhibit neuronal process extension, which in turn, arrested

neuronal migration and thus regulated neuronal positioning. In the absence of *Reln* and *Apoer2* receptors, however, Dab1-labeled neurons failed to stop at their correct locations (Krüger *et al*., 2010). In this study, numerous Dab1 and Dab1-Lmx1b neurons failed to stop and instead migrated circumferentially into the rim of the *Reln*$^{-/-}$ superficial dorsal horn. Other Dab1-labeled cells in *Reln*$^{-/-}$ mice, however, appeared to dissociate from the radial glia prematurely and migrate tangentially across the deep dorsal horn to end up mispositioned in deep laminae II-III (Villeda *et al*., 2006; Akopians *et al*., 2008). These distinctly different errors suggest that there are additional cues required for correct positioning of Dab1 neurons (Krüger *et al*., 2010; Phelps, 2010) or that the factors that guide Dab1-Lmx1b neurons may differ from those neurons that only express Dab1.

Although there are more migratory errors during the development of Dab1 neurons in *Reln*$^{-/-}$ mice than of Reelin neurons in *dab1*$^{-/-}$ mice, we did detect mispositioned Reelin-Lmx1b neurons and the loss of Lmx1b-only neurons from the LSN and lateral reticulated area in the adult *dab1* mutant dorsal horn. It is currently unclear why some Reelin and Lmx1b neurons are influenced by the aberrant migration of neighboring neurons so that they too end up in the wrong locations. In combination, these results suggest that the dorsal horn migratory errors caused by the loss of the Reelin-signaling pathway lead to characteristic positioning errors which contribute to the profound nociceptive abnormalities in the adult mutant mice.

**References**

Abadesco AD, Cilluffo M, Yvone GM, Carpenter EM, Howell BW, Phelps PE. 2014. Novel Disabled-1-expressing neurons identified in adult brain and spinal cord. Eur J Neurosci. 39:579-92.

Akopians AL, Babayan AH, Beffert U, Herz J, Basbaum AI, Phelps PE. 2008. Contribution of the Reelin signaling pathways to nociceptive processing. Eur J Neurosci. 27:523-37.

Altman J, Bayer SA. 1984. The development of the rat spinal cord. Adv Anat Embryol Cell Biol. 85:1-164.

Arnaud L, Ballif BA, Cooper JA. 2003. Regulation of protein tyrosine kinase signaling by substrate degradation during brain development. Mol Cell Biol. 23:9293-302.

Basbaum AI, Bautista DM, Scherrer G, Julius D. 2009. Cellular and molecular mechanisms of pain. Cell.139:267-84.

Bock HH, Herz J. 2003. Reelin activates SRC family tyrosine kinases in neurons. Curr Biol. 13:18-26.

Burstein R, Dado RJ, Giesler GJ Jr. 1990. The cells of origin of the spinothalamic tract of the rat: a quantitative reexamination. Brain Res. 511:329-37.

Chai X, Förster E, Zhao S, Bock HH, Frotscher M. 2009. Reelin stabilizes the actin cytoskeleton of neuronal processes by inducing n-cofilin phosphorylation at serine3. J Neurosci. 29:288-99.

Cheng L, Arata A, Mizuguchi R, Qian Y, Karunaratne A, Gray PA, Arata S, Shirasawa S, Bouchard M, Luo P, Chen CL, Busslinger M, Goulding M, Onimaru H, Ma Q. 2004. Tlx3 and Tlx1 are post-mitotic selector genes determining glutamatergic over GABAergic cell fates. Nat Neurosci. 7:510-17.

D'Arcangelo G, Miao GG, Curran T. 1996. Detection of the reelin breakpoint in reeler mice. Brain Res Mol Brain Res. 39:234-36.

Dai JX, Hu ZL, Shi M, Guo C, Ding YQ. 2008. Postnatal ontogeny of the transcription factor Lmx1b in the mouse central nervous system. J Comp Neurol. 509:341-55.

de Bergeyck V, Nakajima K, Lambert de Rouvroit C, Naerhuyzen B, Goffinet AM, Miyata T, Ogawa M, Mikoshiba K. 1997. A truncated Reelin protein is produced but not secreted in the 'Orleans' reeler mutation (Reln[rl-Orl]). Brain Res Mol Brain Res. 50:85-90.

Duan B, Cheng L, Bourane S, Britz O, Padilla C, Garcia-Campmany L, Krashes M, Knowlton W, Velasquez T, Ren X, Ross S, Lowell BB, Wang Y, Goulding M, Ma Q. 2014. Identification of spinal circuits transmitting and gating mechanical pain. Cell. 159:1417-32.

Escalante A, Murillo B, Morenilla-Palao C, Klar A, Herrera E. 2013. Zic2-dependent axon midline avoidance controls the formation of major ipsilateral tracts in the CNS. Neuron. 80:1392-406.

Frykman PK, Brown MS, Yamamoto T, Goldstein JL, Herz J. 1995. Normal plasma lipoproteins and fertility in gene-targeted mice homozygous for a disruption in the gene encoding very low density lipoprotein receptor. Proc Natl Acad Sci U S A. 92:8453-7.

Gross MK, Dottori M, Goulding M. 2002. Lbx1 specifies somatosensory association interneurons in the dorsal spinal cord. Neuron. 34:535-49.

Hammond V, So E, Gunnersen J, Valcanis H, Kalloniatis M, Tan SS. 2006. Layer positioning of late-born cortical interneurons is dependent on Reelin but not p35 signaling. J Neurosci. 26: 1646-55.

Helms AW, Johnson JE. 2003. Specification of dorsal spinal cord interneurons. Curr Opin Neurobiol. 13:42-9.

Howell BW, Hawkes R, Soriano P, Cooper JA. 1997. Neuronal position in the developing brain is regulated by mouse disabled-1. Nature. 389:733-7.

Krüger MT, Zhao S, Chai X, Brunne B, Bouché E, Bock HH, Frotscher M. 2010. Role for Reelin-induced cofilin phosphorylation in the assembly of sympathetic preganglionic neurons in the murine intermediolateral column. Eur J Neurosci. 32:1611-7.

Kubasak MD, Brooks R, Chen S, Villeda SA, Phelps PE. 2004. Developmental distribution of reelin-positive cells and their secreted product in the rodent spinal cord. J Comp Neurol. 468:165-78.

Lai HC, Seal RP, Johnson JE. 2016. Making sense out of spinal cord somatosensory development. Development. 143:3434-48.

Matsuki T, Pramatarova A, Howell BW. 2008. Reduction of Crk and CrkL expression blocks reelin-induced dendritogenesis. J Cell Sci. 121:1869-75.

Menétrey D, Chaouch A, Besson JM. 1980. Location and properties of dorsal horn neurons at origin of spinoreticular tract in lumbar enlargement of the rat. J Neurophysiol. 44:862-77.

Menétrey D, Chaouch A, Binder D, Besson JM. 1982. The origin of the spinomesencephalic tract in the rat: an anatomical study using the retrograde transport of horseradish peroxidase. J Comp Neurol. 206:193-207.

Müller T, Brohmann H, Pierani A, Heppenstall PA, Lewin GR, Jessell TM, Birchmeier C. 2002. The homeodomain factor Lbx1 distinguishes two major programs of neuronal differentiation in the dorsal spinal cord. Neuron. 34:551-62.

Niu S, Renfro A, Quattrocchi CC, Sheldon M, D'Arcangelo G. 2004. Reelin promotes hippocampal dendrite development through the VLDLR/ApoER2-Dab1 pathway. Neuron. 41:71-84.

Palmesino E, Rousso DL, Kao TJ, Klar A, Laufer E, Uemura O, Okamoto H, Novitch BG, Kania A. 2010. Foxp1 and lhx1 coordinate motor neuron migration with axon trajectory choice by gating Reelin signalling. PLoS Biol. 8:e1000446.

Peirs C, Williams SP, Zhao X, Walsh CE, Gedeon JY, Cagle NE, Goldring AC, Hioki H, Liu Z, Marell PS, Seal RP. 2015. Dorsal Horn Circuits for Persistent Mechanical Pain. Neuron. 87:797-812.

Phelps PE, Barber RP, Vaughn JE. 1993. Embryonic development of rat sympathetic preganglionic neurons: possible migratory substrates. J Comp Neurol. 330:1-14.

Phelps PE. 2010. Reelin induces a common signal for spinal cord and cerebral cortical migration (commentary on Krüger *et al*.). Eur J Neurosci. 32:1609-10.

Pramatarova A, Chen K, Howell BW. 2008. A genetic interaction between the APP and Dab1 genes influences brain development. Mol Cell Neurosci. 37:178-186.

Rice DS, Curran T. 1999. Mutant mice with scrambled brains: understanding the signaling pathways that control cell positioning in the CNS. Genes Dev. 13:2758-73.

Szabo NE, da Silva RV, Sotocinal SG, Zeilhofer HU, Mogil JS, Kania A. 2015. Hoxb8 intersection defines a role for Lmx1b in excitatory dorsal horn neuron development, spinofugal connectivity, and nociception. J Neurosci. 35:5233-46.

Tamamaki N, Yanagawa Y, Tomioka R, Miyazaki J, Obata K, Kaneko T. 2003. Green fluorescent protein expression and colocalization with calretinin, parvalbumin, and somatostatin in the GAD67-GFP knock-in mouse. J Comp Neurol. 467:60-79.

Todd AJ. 2010. Neuronal circuitry for pain processing in the dorsal horn. Nat Rev Neurosci. 11:823-36.

Trommsdorff M, Gotthardt M, Hiesberger T, Shelton J, Stockinger W, Nimpf J, Hammer RE, Richardson JA, Herz J.1999. Reeler/Disabled-like disruption of neuronal migration in knockout mice lacking the VLDL receptor and ApoE receptor 2. Cell. 97:689-701.

Ventruti A, Kazdoba TM, Niu S, D'Arcangelo G. 2011. Reelin deficiency causes specific defects in the molecular composition of the synapses in the adult brain. Neuroscience.189:32-42.

Villeda SA, Akopians AL, Babayan AH, Basbaum AI, Phelps PE. 2006. Absence of Reelin results in altered nociception and aberrant neuronal positioning in the dorsal spinal cord. Neuroscience 139:1385-96.

Wang X, Babayan AH, Basbaum AI, Phelps PE. 2012. Loss of the Reelin-signaling pathway differentially disrupts heat, mechanical and chemical nociceptive processing. Neuroscience. 226:441-50.

Wang X, Zhang J, Eberhart D, Urban R, Meda K, Solorzano C, Yamanaka H, Rice D, Basbaum AI. 2013. Excitatory superficial dorsal horn interneurons are functionally heterogeneous and required for the full behavioral expression of pain and itch. Neuron. 78:312-24.

Weeber EJ, Beffert U, Jones C, Christian JM, Forster E, Sweatt JD, Herz J. 2002. Reelin and ApoE receptors cooperate to enhance hippocampal synaptic plasticity and learning. J Biol Chem. 277:39944-52.

Yvone GM, Zhao-Fleming HH, Udeochu JC, Chavez-Martinez CL, Wang A, Hirose-Ikeda M, Phelps PE. 2017. Disabled-1 dorsal horn spinal cord neurons co-express Lmx1b and function in nociceptive circuits. Eur J Neurosci. 45:733-47.

**Table 1: List of primary antibodies used in this study.**

| Primary antisera | Source; Catalog # | Host species | Working dilutions |
|---|---|---|---|
| Reelin (G10) | EMD Millipore (Billerica, MA); MAB5364 | Mouse | 1:1,000 (TSA) |
| Reelin | R&D Systems (Minneapolis, MN); AF3820 | Goat | 1:1,000 (TSA) |
| Disabled-1 (Dab1) | Gift from Dr. Brian Howell (Howell *et al*., 1997); B3 | Rabbit | 1:5,000 (TSA) |
| LIM homeobox transcription factor 1 beta (Lmx1b) | Gift from Drs. Müller and Birchmeier (Müller *et al*., 2002) | Guinea pig | 1:20,000 (TSA) |
| Paired box 2 (Pax2) | Zymed Laboratories (Thermo Fisher Scientific, Rockford, IL); 71-6000 | Rabbit | 1:10,000 (TSA) |
| Biotinylated Griffonia (Bandeiraea) Simplicifolia Lectin I Isolectin B4 | Vector (Burlingame, CA); B-1205 | IB4 conjugate | 1:200 (IF) |
| Green Fluorescent Protein (GFP) | Aves Labs (Tigard, OR); GFP-1020 | Chicken | 1:1,000 (IF) |

**Table 2: Reelin-Lmx1b neurons in laminae I-II$_{\text{inner dorsal}}$ are increased in *dab1* mutants versus wild-type mice.**

| Genotype/Cell type | *dab1*$^{+/+}$ | *dab1*$^{-/-}$ | p-value |
|---|---|---|---|
| **Reelin-only** | 5±1.7 | 4±0.8 | n.s |
| **Lmx1b-only** | 101±9 | 101±9.8 | n.s |
| **Reelin-Lmx1b** | 20±1.6 | 31±1.6 | 0.004 |
| **Total Reelin** | 25±3.3 | 35±1.9 | 0.04 |
| **Total Lmx1b** | 121±8.8 | 131±10.1 | n.s |

Means±SEM shown per hemisections, combining the numbers within and above the IB4 layer from 4 pairs of *dab1*$^{+/+}$ and *dab1*$^{-/-}$ mice, 3 hemisections per mouse.

**Table 3: Single-labeled Dab1 neurons are increased in *Reln*$^{-/-}$ compared to *Reln*$^{+/+}$ laminae I-II$_{\text{inner dorsal}}$**

| Genotype/Cell type | *Reln*$^{+/+}$ | *Reln*$^{-/-}$ | p-value |
|---|---|---|---|
| **Dab1-only** | 10±0.7 | 12±0.6 | 0.03 |
| **Lmx1b-only** | 112±10.3 | 106±6.4 | n.s |
| **Dab1-Lmx1b** | 28±2.8 | 30±2.5 | n.s |
| **Total Dab1** | 37±3 | 43±2.5 | n.s |
| **Total Lmx1b** | 140±8.6 | 137±8.9 | n.s |

Means±SEM expressed per hemisection, combining the numbers within and above the IB4 layer from 4 pairs of *Reln*$^{+/+}$ and *Reln*$^{-/-}$ mice, 6 hemisections per mouse.

**Figure 10. About 90% of Reelin-expressing laminae I-II neurons co-express Lmx1b.** Confocal images (3 µm thick) of *dab1*$^{+/+}$ (***A; A1-3***) and *dab1*$^{-/-}$ (***B; B1-3)*** dorsal horns show that many Reelin neurons (green cytoplasm) co-express Lmx1b (red nuclei). Boxes in ***A*** and ***B*** are enlarged in ***A1-3*** and ***B1-3***, with individual channels shown in ***A2-3*** and ***B2-3***. ***A-B,*** Most Reelin-Lmx1b cells in laminae I-II are small interneurons (***A1-3***; small yellow arrowheads), but a few large neurons are present in the *dab1* mutants (***B1-3***; large yellow arrowheads). Examples of single-labeled Reelin neurons are marked with yellow arrows. Coronal lumbar confocal images are oriented with medial to the right and dorsal toward the top in this and subsequent figures. Scale bars: ***A, B,*** 100 µm; ***A1-3; B1-3,*** 50 µm.

**Figure 10**

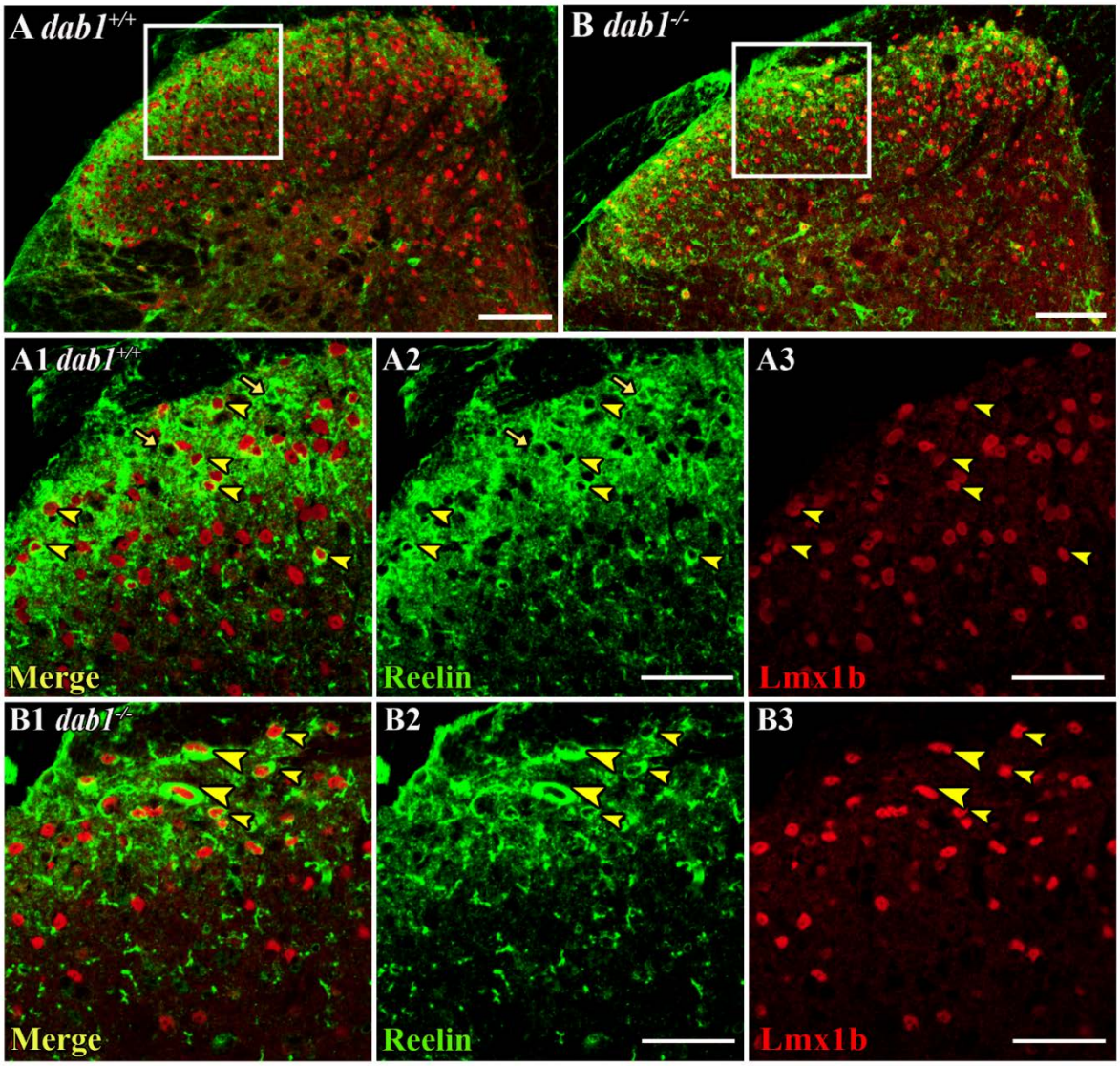
A dab1+/+
B dab1-/-
A1 dab1+/+
A2
A3
Merge
Reelin
Lmx1b
B1 dab1-/-
B2
B3
Merge
Reelin
Lmx1b

**Figure 11. Reelin-Lmx1b neurons are mispositioned within the lamina $II_{inner\ dorsal}$**

Reelin (red) and Lmx1b (blue) neurons are distributed within and above the IB4 (green) band, representing lamina $II_{inner\ dorsal}$ and laminae I-$II_{outer}$, respectively. Boxes in ***A*** and ***B*** are enlarged in ***A1-2*** and ***B1-2***. Reelin-Lmx1b cells are marked with yellow arrowheads, whereas single-labeled Reelin cells are marked with yellow arrows. ***A-B,*** The area overlaid by the IB4 terminal zone (lamina $II_{inner\ dorsal}$), outlined in ***A1-2*** and ***B1-2***, does not differ between *dab1*$^{+/+}$ (***A1-2***) and *dab1*$^{-/-}$ mice (***B1-2***). The area of laminae I-$II_{outer}$, i.e., above the IB4 terminal zone, is reduced in *dab1*$^{-/-}$ compared to *dab1*$^{+/+}$ mice. ***C,*** Within the IB4 terminal zone, the numbers of single-labeled Reelin and Lmx1b neurons do not differ between genotypes, but the Reelin-Lmx1b neurons are increased in *dab1*$^{-/-}$ versus *dab1*$^{+/+}$ mice. Scale bars: ***A, B,*** 100 μm; ***A1-2, B1-2,*** 50 μm.

**Figure 11**

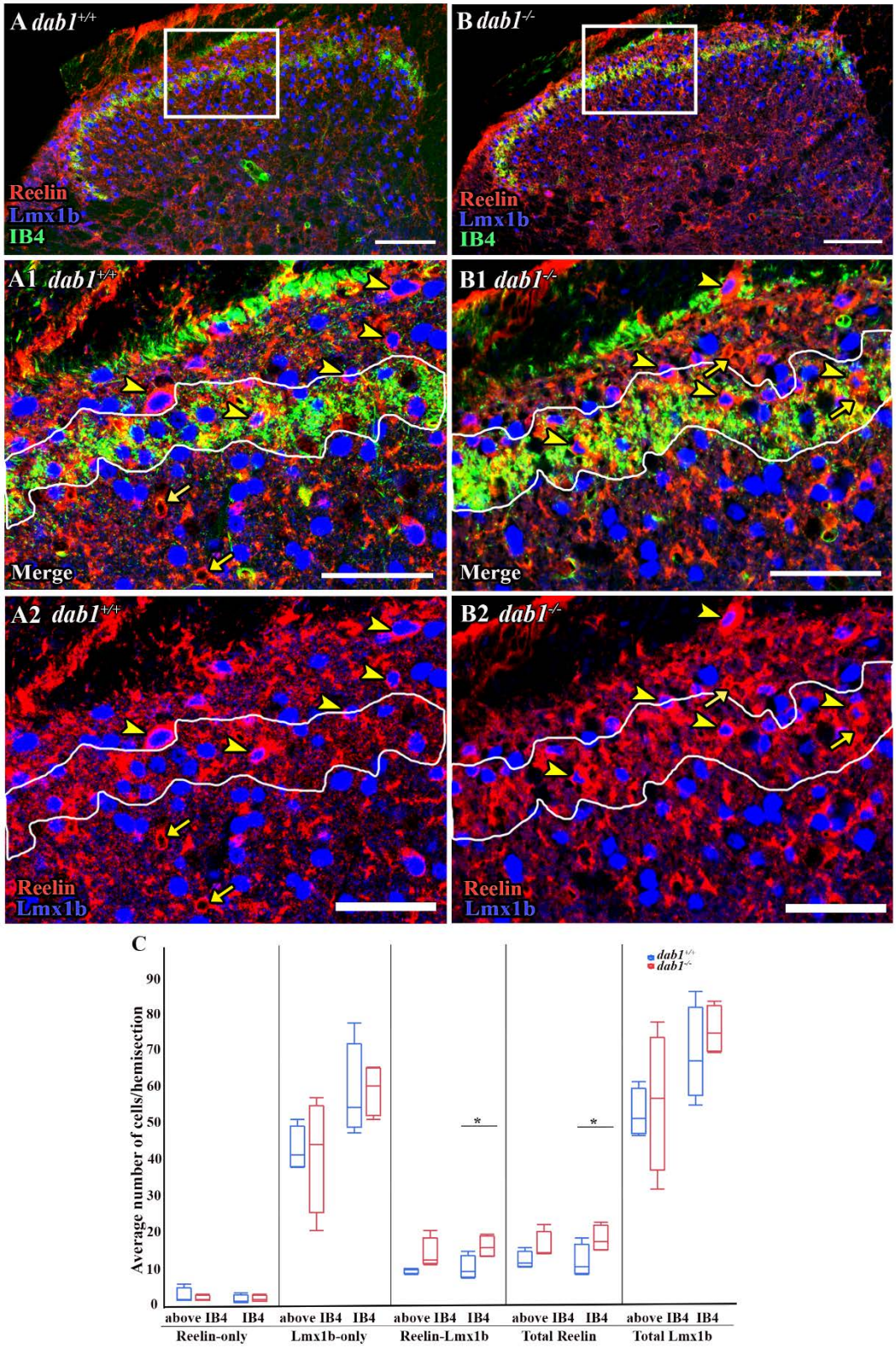
A dab1+/+
Reelin
Lmx1b
IB4
B dab1-/-
Reelin
Lmx1b
IB4
A1 dab1+/+
Merge
B1 dab1-/-
Merge
A2 dab1+/+
Reelin
Lmx1b
B2 dab1-/-
Reelin
Lmx1b
C
Average number of cells/hemisection
0
10
20
30
40
50
60
70
80
90
dab1+/+
dab1-/-
*
*
above IB4
IB4
Reelin-only
Lmx1b-only
Reelin-Lmx1b
Total Reelin
Total Lmx1b

**Figure 12. Reelin- and Dab1-Lmx1b neurons are different subsets of the Lmx1b population.**

Enlargements of 3 µm confocal superficial dorsal horn images show the distribution of Reelin-Lmx1b (green cytoplasm with blue nuclei, yellow arrowheads) and Dab1-Lmx1b (red cytoplasm with blue nuclei, white arrowheads) within laminae I-II of *Apoer2*$^{+/+}$*;Vldlr*$^{+/+}$ (***A-A3***) and *Apoer2*$^{-/-}$*;Vldlr*$^{-/-}$ (***B-B3)*** mice. ***A-B,*** In both wild-type and double-receptor knockout mice, Reelin-Lmx1b and Dab1-Lmx1b neurons are interspersed in laminae I-II and represent separate subsets of glutamatergic neurons. In the *Apoer2*$^{-/-}$*;Vldlr*$^{-/-}$ laminae I-II (***B-B3***), there is evidence of compaction of Reelin-Lmx1b neurons seen in the upper right corner (row of 4 yellow arrowheads). Scale bars: ***A-A3, B-B3,*** 50 µm.

**Figure 12**

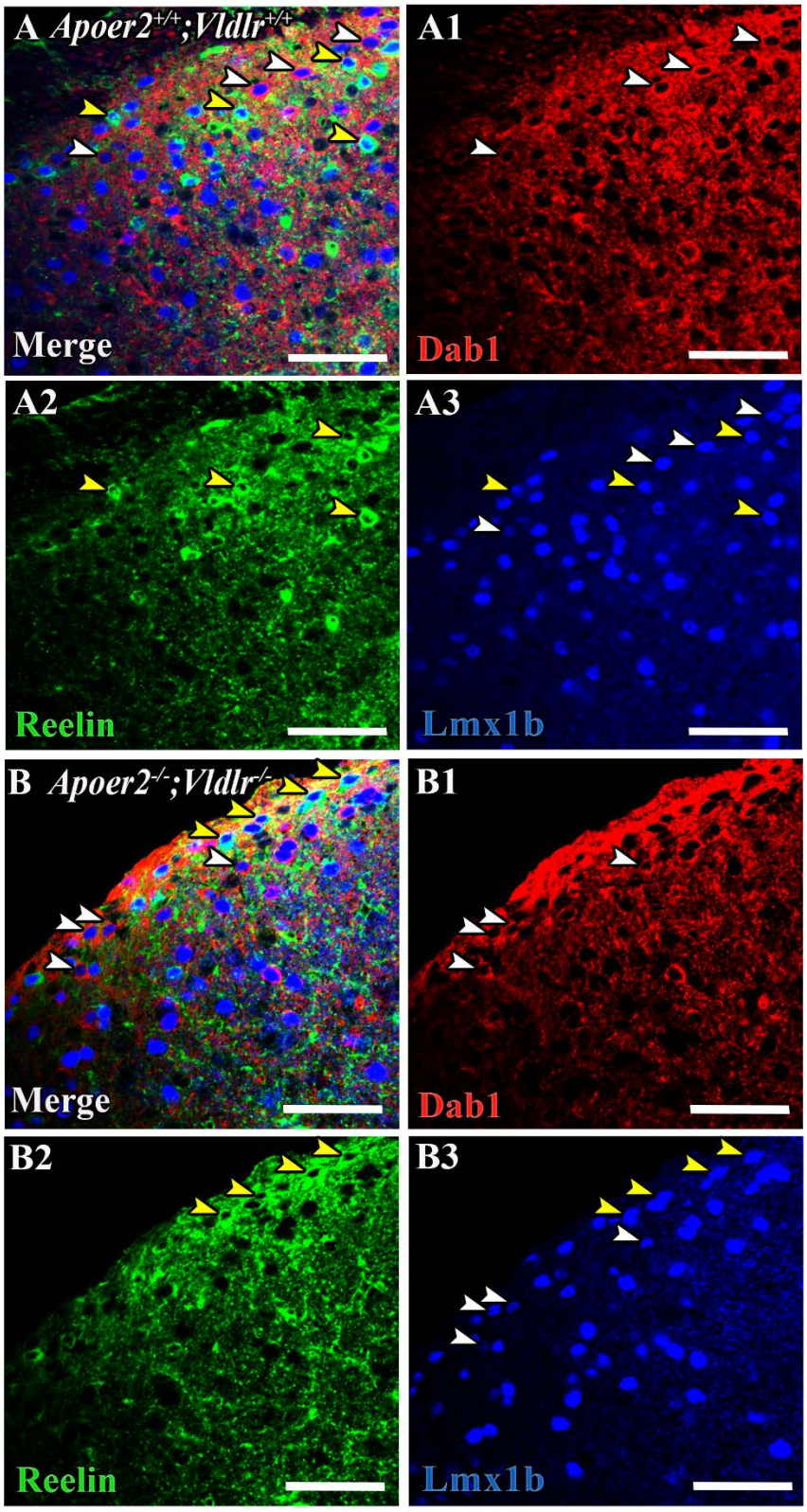
A Apoer2+/+;Vldlr+/+
Merge
A1
Dab1
A2
Reelin
A3
Lmx1b
B Apoer2-/-;Vldlr-/-
Merge
B1
Dab1
B2
Reelin
B3
Lmx1b

**Figure 13. Most Reelin-labeled superficial dorsal horn cells are not inhibitory.**

***A-A2***, Dorsal horns from *Reln[rl-Orl]*$^{+/+}$*; GAD67*$^{GFP/+}$ mice had little to no co-localization of Reelin (red) and GAD67$^{GFP}$ (green). ***B-B3***, Experiments with Reelin (red), Lmx1b (blue), and Pax2 (green) confirmed that most Reelin cells in laminae I-II are not inhibitory. Scale bars: ***A, B***; ***A1-2, B1-3,*** 50 µm.

**Figure 13**

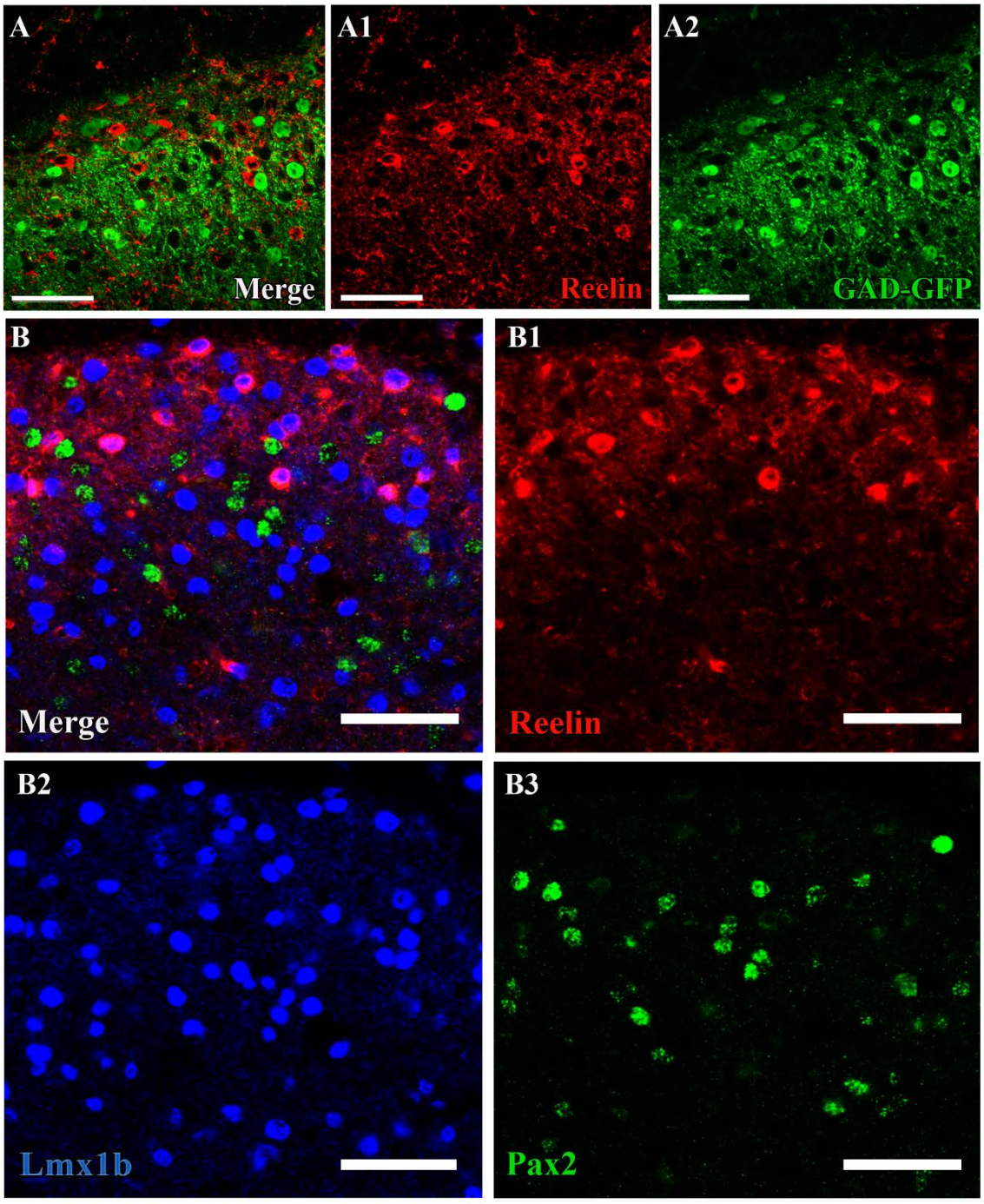

**Figure 14. Lateral reticulated area and LSN: Reelin-Lmx1b neurons are mispositioned in *dab1* mutant mice.**

Reelin (green) and Lmx1b (red) neurons are co-expressed in *dab1*$^{+/+}$ (***A, C, E***) and *dab1*$^{-/-}$ (***B, D, F***) lateral reticulated area (***C-D***) and LSN (***E-F***). Examples of double-labeled cells are marked with yellow arrowheads while single-labeled Reelin neurons are marked with yellow arrows. ***A-B,*** Box in ***A*** represents the location of lateral reticulated area and is enlarged in ***C***, whereas box in ***B*** outlines the LSN and is enlarged in ***F***. ***C-D***, In *dab1*$^{+/+}$ lateral reticulated area (***C***), there are more Reelin-Lmx1b neurons than in *dab1*$^{-/-}$ mice (***D***). Reelin-positive neurons in the lateral reticulated area are large and likely to be projection neurons. ***E-F***, Single-labeled Reelin neurons are rarely detected and only few Reelin-Lmx1b neurons are observed in *dab1*$^{+/+}$ (***E***) and *dab1*$^{-/-}$ LSN (***F***). ***G,*** *dab1*$^{+/+}$ mice contain more Lmx1b, Reelin-Lmx1b, total Reelin, and total Lmx1b neurons in the lateral reticulated area than the *dab1*$^{-/-}$ mice. ***H,*** The *dab1*$^{-/-}$ LSN exhibits a reduced number of Reelin, Lmx1b, double-labeled, total Reelin, and total Lmx1b neurons compared to the *dab1*$^{+/+}$ LSN. Scale bars: ***A, B,*** 100 µm; ***C-F***; ***C1-2, D1-2, E1-2, F1-2***, 50 µm.

**Figure 14**

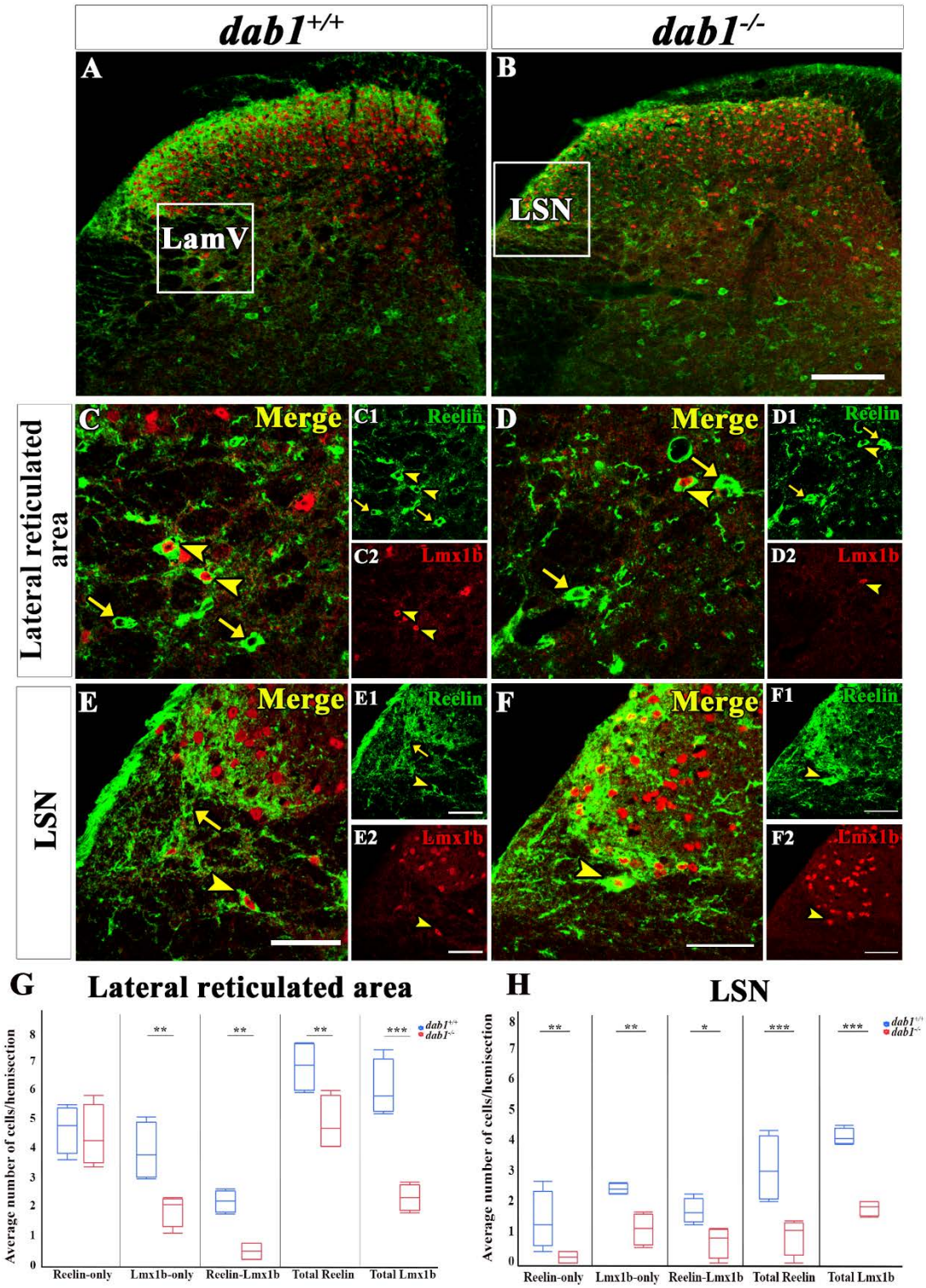
dab1+/+
dab1-/-
A
B
LamV
LSN
Lateral reticulated area
LSN
C
Merge
C1
Reelin
C2
Lmx1b
D
Merge
D1
Reelin
D2
Lmx1b
E
Merge
E1
Reelin
E2
Lmx1b
F
Merge
F1
Reelin
F2
Lmx1b
G
Lateral reticulated area
Average number of cells/hemisection
Reelin-only
Lmx1b-only
Reelin-Lmx1b
Total Reelin
Total Lmx1b
H
LSN
Average number of cells/hemisection
Reelin-only
Lmx1b-only
Reelin-Lmx1b
Total Reelin
Total Lmx1b

**Figure 15. The lateral dI5 group of Lmx1b neurons co-express Reelin in E11.5-12.5 dorsal spinal cord.**

Confocal slices (1 µm) show Reelin (green) and Lmx1b (red) co-localization in E11.5 (***A-B***) and E12.5 (***C-D***) *dab1*$^{+/+}$ (***A-A2; C-C2***) and *dab1*$^{-/-}$ (***B-B2; D-D2***) spinal cord. Double-labeled cells are marked with white arrowheads, and single-labeled cells are marked with white arrows. ***A-B,*** At E11.5, Reelin immunoreactivity (***A, B***) extends along the dorsolateral edge of the spinal cord and in the ventral commissure (VC). Lmx1b expression (***A1, B1***) is localized dorsolaterally as the dI5 group and in the floor plate (FP). The majority of Reelin expression co-localizes with the lateral cluster of Lmx1b-positive dI5 neurons (***A2, B2***). The ventricular zone (VZ) is devoid of Reelin and Lmx1b. ***C-D***, Reelin expression (***C, D***) at E12.5 has expanded dorsally and medially. A tight cluster of dI5 neurons express Lmx1b in *dab1*$^{+/+}$ (***C1***) but they are more dispersed in *dab1*$^{-/-}$ mice (***D1***). The $dIL_B$ group of Lmx1b nuclei are broadly detected in the dorsal spinal cord (***C1, D1***). Most Reelin-Lmx1b neurons are found laterally, as part of the dI5 group (***C2, D2***). The expression patterns of Reelin and Lmx1b in *dab1*$^{+/+}$ and *dab1*$^{-/-}$ dorsal horns appear largely similar except for the distribution of Lmx1b nuclei in the dI5 group. Scale bars: ***A-D; A1-2, B1-2, C1-2, D1-2,*** 50 µm.

**Figure 15**

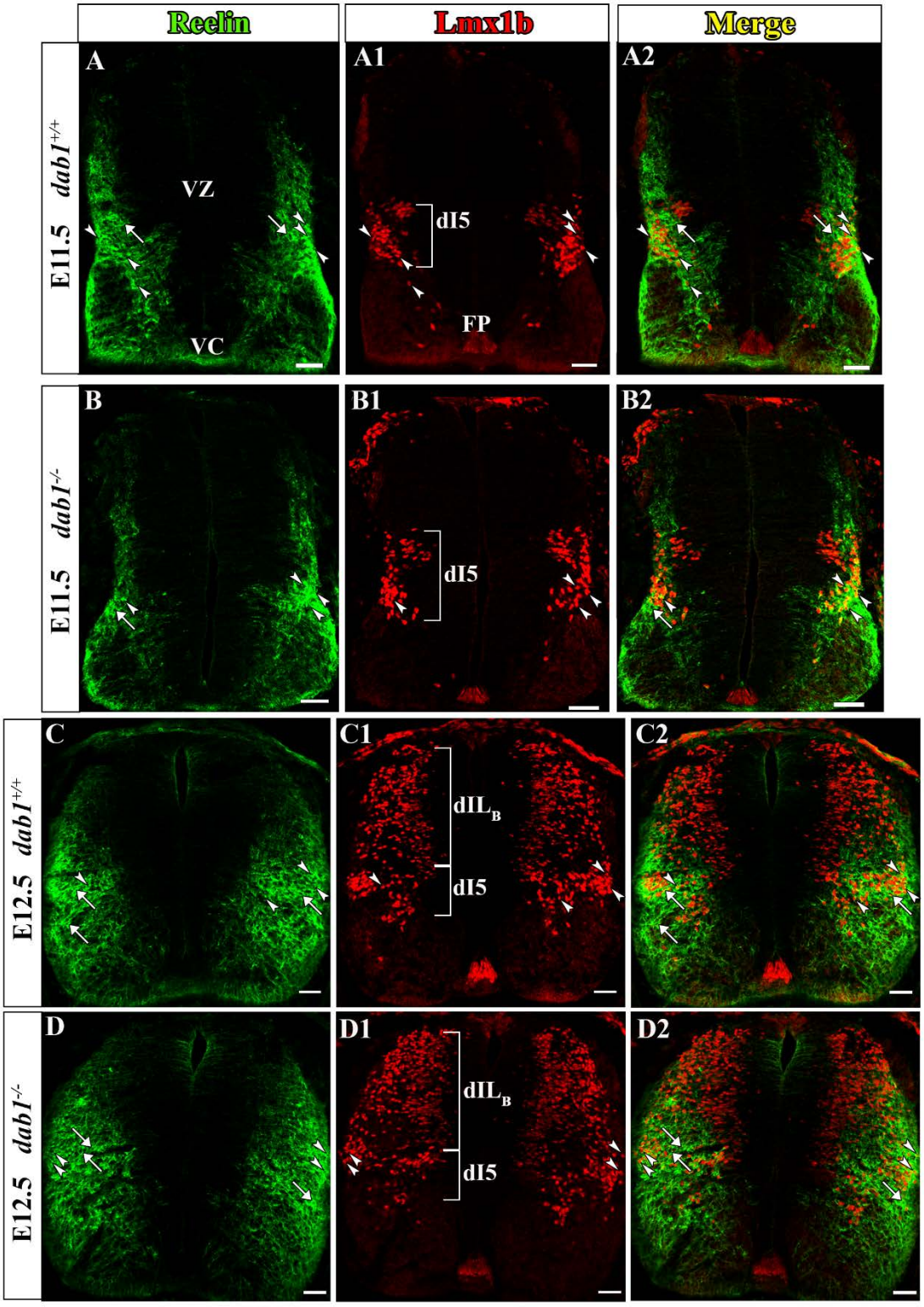
Reelin
Lmx1b
Merge
A
A1
A2
E11.5 dab1+/+
VZ
VC
dI5
FP
B
B1
B2
E11.5 dab1-/-
dI5
C
C1
C2
E12.5 dab1+/+
dIL_B
dI5
D
D1
D2
E12.5 dab1-/-
dIL_B
dI5

**Figure 16. Reelin neurons migrate together with both dI5 and dIL$_B$ groups of Lmx1b-positive neurons.**

Reelin (green) and Lmx1b (red) co-localization in 1 μm thick images of E13.5 (***A-B***), E14.5 (***C-D***) and E15.5 (***E-F***) dorsal horn hemisections of *dab1*$^{+/+}$ (***A-A1; C-C1; E-E1***) and *dab1*$^{-/-}$ mice (***B-B1; D-D1; F-F1***). ***A-B***, At E13.5, numerous Lmx1b neurons fill the dorsal horn, the majority of which are from the late-born dIL$_B$ cohort. Reelin-Lmx1b neurons (white arrowheads) are concentrated laterally in the dI5 group and medially with the dIL$_B$ group (***A, A1, B, B1***). Single-labeled Reelin neurons (white arrows) are also evident. In the *dab1* mutants, double-labeled cells are in the outermost rim of the lateral dorsal horn including one that is misoriented (***B, B1***; yellow arrow). ***C-D,*** Many Reelin-Lmx1b neurons derived from both dI5 and dIL$_B$ groups are positioned together in the outer rim of the dorsal horn by E14.5. Reelin expression is the highest in the area just lateral to the nascent superficial dorsal horn, and the Reelin band appears wider in *dab1*$^{-/-}$ (***D, D1***) than in *dab1*$^{+/+}$ embryos (***C, C1***). ***E-F***, In E15.5 *dab1*$^{+/+}$ mice (***E, E1***), Reelin-Lmx1b neurons are concentrated in the superficial dorsal horn. In *dab1*$^{-/-}$ mice (***F, F1***), Reelin-Lmx1b neurons are more compacted along the edge of the forming superficial dorsal horn than in wild-type mice. The medial late dIL$_B$ neurons (white asterisks in ***C***, ***D, E, F***) express Lmx1b and/or Reelin and are seen in both genotypes at E14.5 and E15.5. Scale bars: ***A-F; A1, B1, C1, D1, E1, F1,*** 50 μm.

**Figure 16**

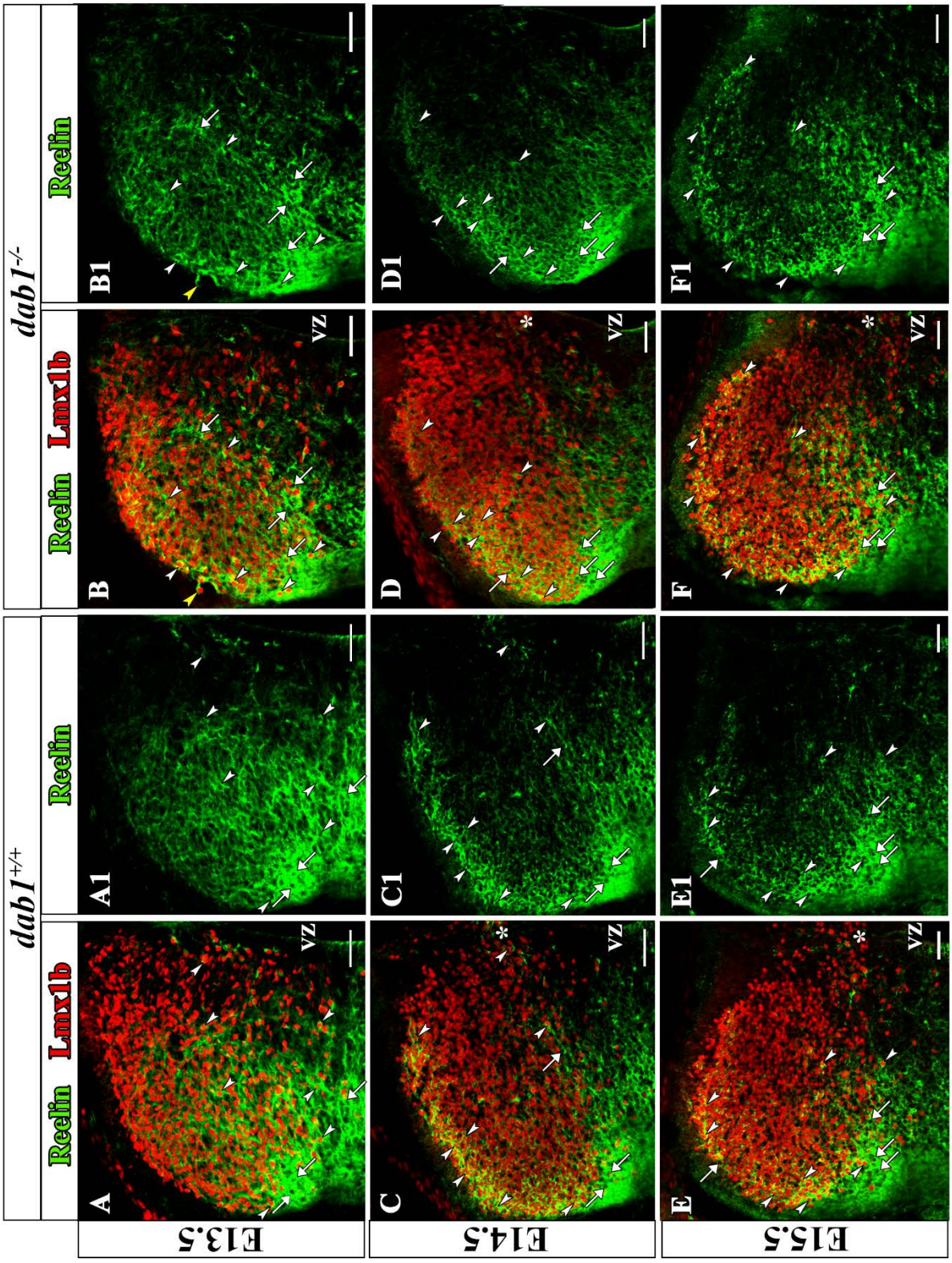
dab1+/+
dab1-/-
Reelin
Lmx1b
A
A1
B
B1
C
C1
D
D1
E
E1
F
F1
E13.5
E14.5
E15.5
VZ
*

**Figure 17. Some Dab1 neurons arise from the Lmx1b-positive dI5 population.**

Dab1 (green) and Lmx1b (red) co-expression at E11.5 (***A, B***) and E12.5 (***C, D***) in 1 µm slices of wild-type (***A-A2; C-C2***) and *Reln*$^{-/-}$ (***B-B2; D-D2***) mice. ***A-B,*** Dab1 immunoreactivity (***A, B***) is strongest ventrally as it marks somatic motor neurons and the ventral commissure. Lmx1b staining (***A1, B1***) is concentrated in the dorsolateral region, marking the dI5 group, and in the floor plate. Several single-labeled Dab1 neurons (white arrows) and double-labeled Dab1-Lmx1b (white arrowheads) are detected laterally in dI5 group (***A2, B2***). ***C-D***, By E12.5, more Dab1 cells are detected laterally (***C, D***), and 2 groups of Lmx1b neurons are evident in both genotypes, i.e., the lateral dI5 and dorsal $dIL_B$ groups (***C1, D1***). Both Dab1 and Dab1-Lmx1b cells are localized laterally in *Reln*$^{+/+}$ and *Reln*$^{-/-}$ mice (***C2, D2***). The Dab1 and Lmx1b expression patterns appear similar in both genotypes except that the dI5 group is less tightly clustered in *Reln*$^{-/-}$ than *Reln*$^{+/+}$ mice. Scale bars: ***A-D; A1-2, B1-2, C1-2, D1-2,*** 50 µm.

**Figure 17**

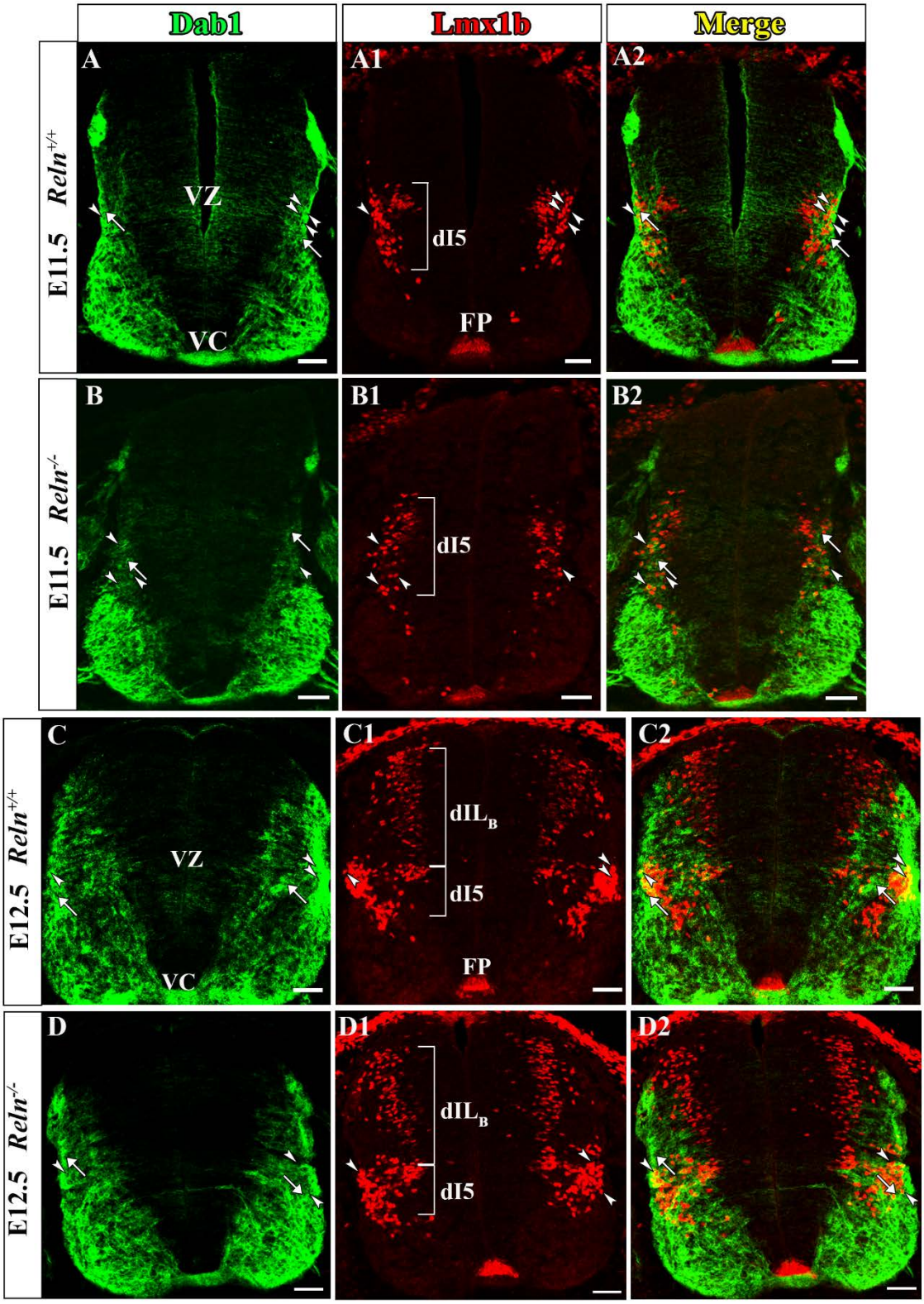
Dab1
Lmx1b
Merge
A
A1
A2
E11.5 Reln+/+
VZ
VC
dI5
FP
B
B1
B2
E11.5 Reln-/-
dI5
C
C1
C2
E12.5 Reln+/+
VZ
VC
dIL_B
dI5
FP
D
D1
D2
E12.5 Reln-/-
dIL_B
dI5

**Figure 18. Dab1 neurons display migratory errors in the absence of Reelin.**

Dab1 (green) and Lmx1b (red) expression patterns in *Reln*$^{+/+}$ (***A-A1; C-C1; E-E1***) and *Reln*$^{-/-}$ (***B-B1; D-D1; F-F1***) dorsal horn hemisections at E13.5 (***A-B***), E14.5 (***C-D***) and E15.5 (***E-F***). ***A-B***, At E13.5, Dab1 expression is concentrated laterally, and many Dab1 neurons co-localize with Lmx1b within the dI5 cohort (white arrowheads). Other Dab1-Lmx1b neurons are located medially (white asterisks) and are members of the $dIL_B$ group. The migration of Dab1 neurons at this age appears more disorganized in *Reln*$^{-/-}$ (***B, B1***) than in *Reln*$^{+/+}$ mice (***A, A1***). ***C-D,*** At E14.5, Dab1 (white arrows) and Dab1-Lmx1b neurons are found laterally (white arrowheads) and in the dorsal midline (white asterisks) in both *Reln*$^{+/+}$ (***C, C1***) and *Reln*$^{-/-}$ mice (***D, D1***). In *Reln*$^{-/-}$, many Dab1 and Dab1-Lmx1b neurons are positioned along the outer rim of the dorsal horn (***D, D1;*** 3 white arrowheads). A second migratory error is shown with nonradially-oriented neurons coursing across the deep dorsal horn (***D, D1;*** large yellow arrow). ***E-F,*** By E15.5, Dab1 and Dab1-Lmx1b neurons in wild-type mice are detected around the rim of the superficial dorsal horn and throughout lamina V (***E, E1***). Dab1 and Dab1-Lmx1b neurons in *Reln*$^{-/-}$ mice form a complete circumferential band of neurons around the superficial dorsal horn (***F, F1***). Scattered Dab1 and Dab1-Lmx1b neurons are found within the *Reln*$^{-/-}$ core of the dorsal horn that are not detected in *Reln*$^{+/+}$ mice. Scale bars: ***A-F; A1, B1, C1, D1, E1, F1,*** 50 µm.

**Figure 18**

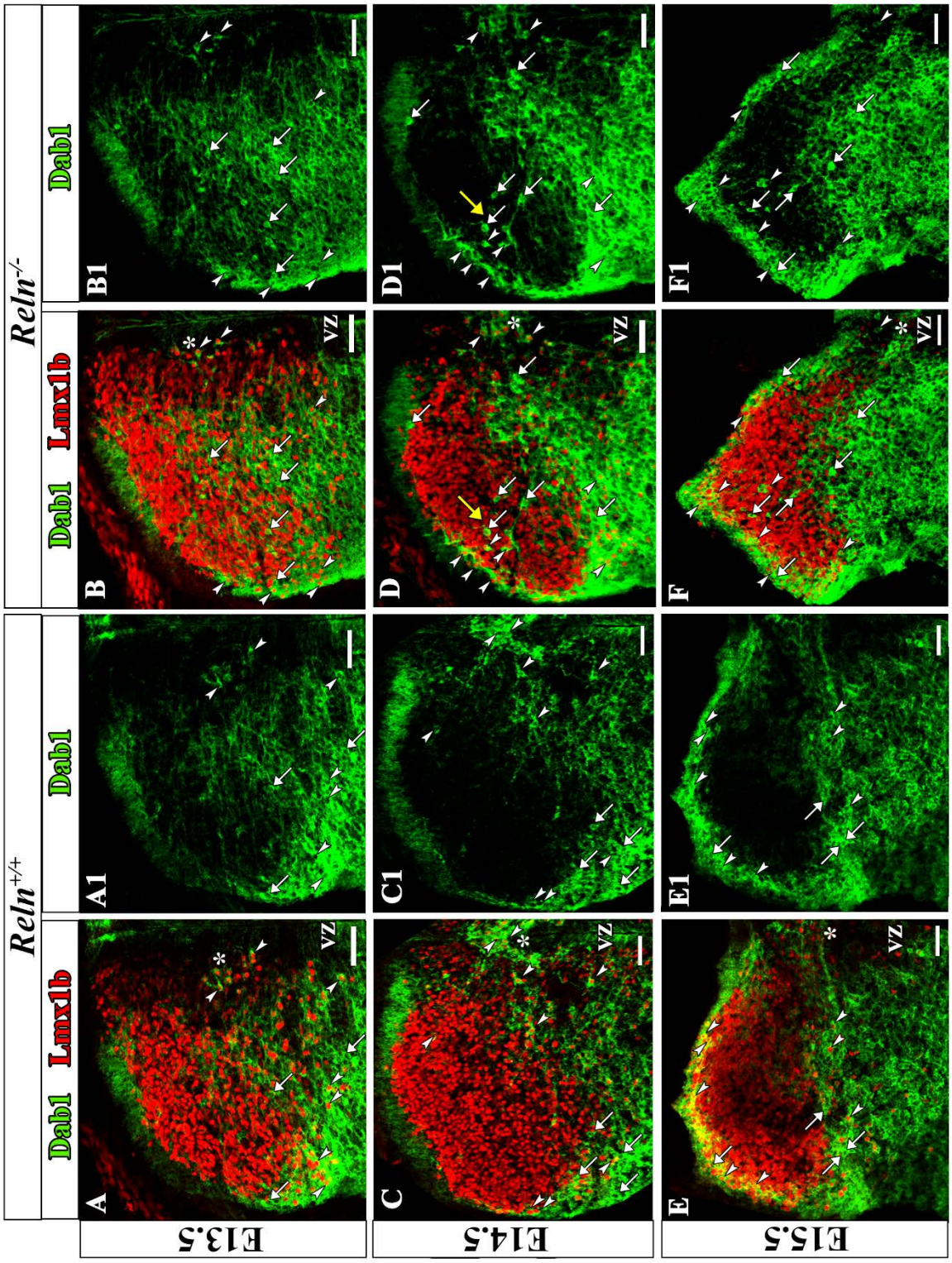
Reln+/+
Reln-/-
Dab1
Dab1 Lmx1b
A
A1
B
B1
C
C1
D
D1
E
E1
F
F1
E13.5
E14.5
E15.5
VZ

**Figure 19. Dorsal horn anatomical abnormalities are similar in *dab1*$^{-/-}$ and *Reln*$^{-/-}$ mice.**

***A,*** Schematic of the dorsal horn in wild-type mice. Both Reelin-Lmx1b and Dab1-Lmx1b-expressing neurons are seen in laminae I-II$_{outer}$ and lamina II$_{inner\ dorsal}$. Double-labeled cells are also present in the lateral reticulated area and LSN. ***B,*** The area of laminae I-II$_{outer}$ in *dab1*$^{-/-}$ mice was reduced compared to wild-type mice, but the number of Reelin-Lmx1b neurons did not differ. In contrast, the area of IB4 (lamina II$_{inner\ dorsal}$) did not differ between genotypes, but there were more Reelin-Lmx1b neurons in this area in *dab1*$^{-/-}$ than in *dab1*$^{+/+}$ mice. Decreased numbers of Reelin-Lmx1b neurons were found in the lateral reticulated area and LSN of *dab1*$^{-/-}$ versus *dab1*$^{+/+}$ mice. ***C,*** The area of laminae I-II$_{outer}$ in *Reln*$^{-/-}$ mice was also reduced compared to *Reln*$^{+/+}$ mice, but the number of Dab1-Lmx1b neurons was not different between genotypes. In contrast, the area of lamina II$_{inner\ dorsal}$ did not differ between genotypes, but there were more Dab1-Lmx1b neurons in this area in *Reln*$^{-/-}$ than in *Reln*$^{+/+}$ mice. Reduced numbers of Dab1-Lmx1b neurons were also found in the lateral reticulated area and LSN of *Reln*$^{-/-}$ versus *Reln*$^{+/+}$ mice.

**Figure 19**

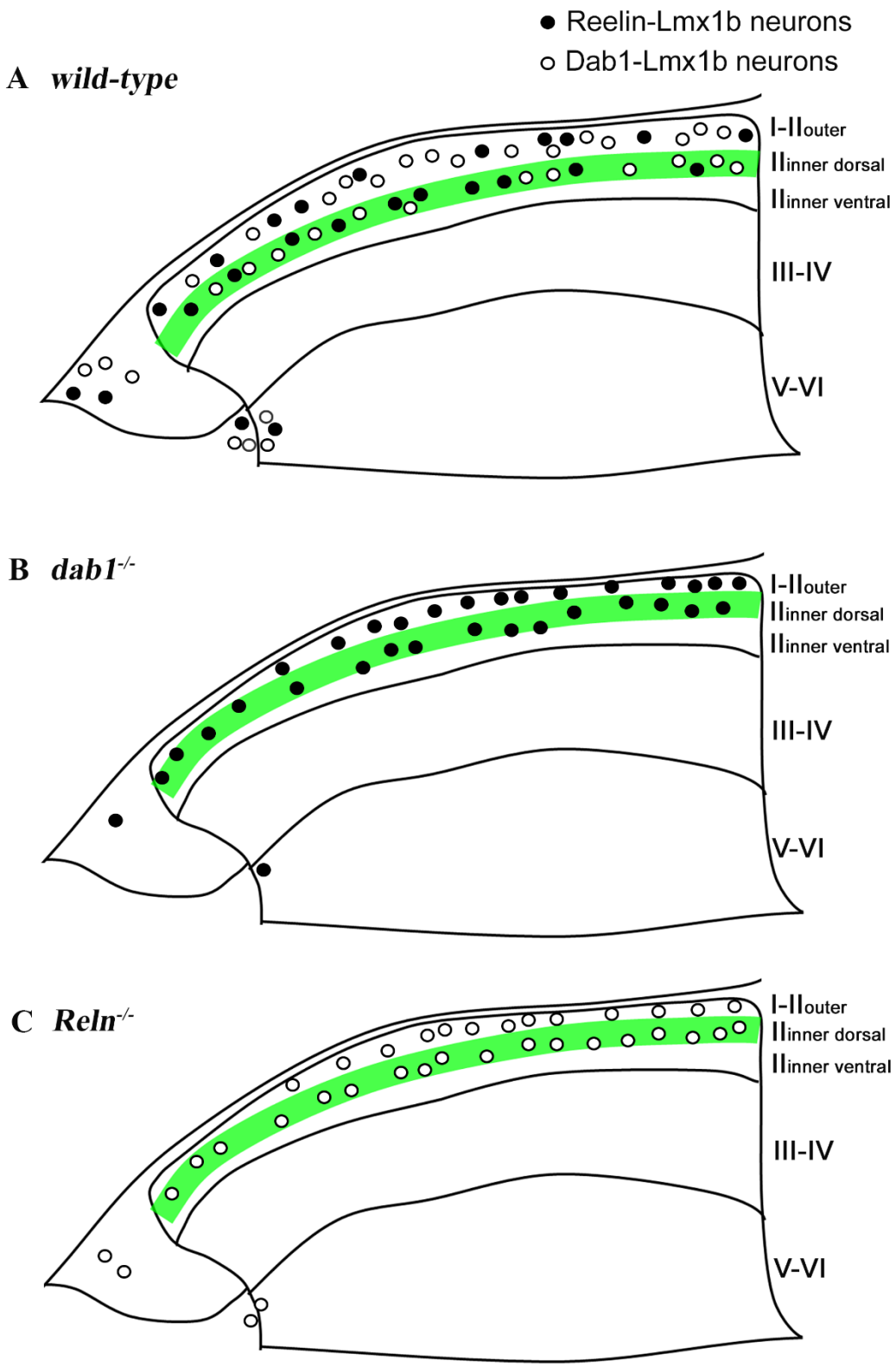
● Reelin-Lmx1b neurons
○ Dab1-Lmx1b neurons
A wild-type
I-IIouter
IIinner dorsal
IIinner ventral
III-IV
V-VI
B dab1-/-
I-IIouter
IIinner dorsal
IIinner ventral
III-IV
V-VI
C Reln-/-
I-IIouter
IIinner dorsal
IIinner ventral
III-IV
V-VI

*Chapter 4*

**Summary of findings**

**Specific Aim 1: Identify the Dab1-expressing dorsal horn neurons that respond to Reelin signaling and participate in nociceptive circuits. Characterize their neuronal positioning errors in *Reln*$^{-/-}$ mice.**

*Hypothesis 1a: Dab1 dorsal horn neurons are comprised of multiple neuronal populations that are both inhibitory and excitatory.*

Previous studies from our laboratory reported that Dab1 was expressed by neurons in nociceptive regions of the dorsal horn: laminae I-II, lateral lamina V, and the lateral spinal nucleus (LSN; Villeda *et al*., 2006; Akopians *et al*., 2008). Villeda *et al*. (2006) and Akopians *et al*. (2008) also showed several mispositioned Dab1 dorsal horn neurons that co-expressed the Neurokinin-1-receptor (NK1R) which binds substance P. We expanded these findings by identifying an average of 65-77 Dab1-positive neurons in a 3 µm confocal slice of wild-type or mutant laminae I-II, respectively (Yvone *et al.,* 2017). We also determined that about 70% of Dab1-expressing laminae I-II neurons co-expressed Lmx1b, a marker of glutamatergic neurons (Cheng *et al*., 2004). To identify the remaining Dab1 neurons, we examined co-expression with other dorsal horn markers (Todd, 2010; Gutierrez-Mecinas *et al*., 2016) and found that Dab1 laminae I-II neurons did not express Protein Kinase C gamma (PKCγ), but a few Dab1-Lmx1b neurons co-localized with Calbindin and Somatostatin. Additionally, a few Dab1 neurons in laminae I-II expressed GAD67, but markers of subsets of GABAergic dorsal horn neurons, such as neuronal nitric acid synthase and Parvalbumin did not co-localize with Dab1 (Yvone *et al*., 2017).

We determined that 67% of Dab1-expressing neurons in the lateral reticulated area of lamina V and the LSN co-expressed Lmx1b. In addition, a few cholinergic neurons in the lateral

reticulated area (Phelps *et al*., 1984) also co-expressed Dab1. These results suggest that Dab1 neurons comprise multiple populations in different nociceptive regions: projection neurons located in lamina I, lateral reticulated area of lamina V and LSN, and interneurons located in laminae I-II. We concluded that most Dab1 dorsal horn neurons are excitatory and co-express Lmx1b (Yvone *et al*., 2017).

*Hypothesis 1b: Dab1-expressing neurons exhibit positioning errors in the nociceptive regions of the Reln$^{-/-}$ dorsal horn, i.e., laminae I-II, lateral lamina V and the LSN.*

To identify additional positioning errors, we divided the dorsal horn into equal-sized dorsoventral or mediolateral bins but did not find differences in the numbers of Dab1 neurons between genotypes. Then, we compared the numbers of Dab1 and Dab1-Lmx1b neurons located within and above the IB4 layer in *Reln* mice. These analyses detected increased numbers of Dab1 and Dab1-Lmx1b neurons only within the *Reln*$^{-/-}$ IB4-positive terminal zone compared to *Reln*$^{+/+}$ mice. The area of IB4 layer did not differ between genotypes, but the area of laminae I-II$_{outer}$, that is, above the IB4 layer, was reduced in *Reln*$^{-/-}$ versus *Reln*$^{+/+}$ dorsal horn. Thus, in *Reln*$^{-/-}$ mice, the Dab1 and Dab1-Lmx1b neurons were mispositioned in the IB4 area of lamina II, and the IB4 band was shifted dorsally (Yvone *et al*., 2017).

When we examined the positioning of Dab1 neurons in the lateral reticulated area of lamina V, we found fewer Dab1-Lmx1b neurons and more Dab1-only neurons in *Reln*$^{-/-}$ compared to *Reln*$^{+/+}$ lateral reticulated area. In the LSN, there was an almost 50% reduction of Dab1-Lmx1b neurons in *Reln*$^{-/-}$ versus *Reln*$^{+/+}$ mice. We concluded that Dab1 neurons were mispositioned in the laminae I-II, the lateral reticulated area and LSN of *Reln*$^{-/-}$ mice (Yvone *et al*., 2017).

*Hypothesis 1c: Dab1-positive dorsal horn neurons participate in thermal and mechanical nociceptive circuits.*

After characterizing the identity and positioning errors of Dab1 dorsal horn neurons, we asked whether Dab1 neurons were activated following noxious thermal or mechanical stimulation. In wild-type dorsal horns, we found that Dab1-Lmx1b neurons in laminae I-II and the lateral reticulated area co-expressed Fos in response to either thermal or mechanical stimulation. We concluded that Dab1, Lmx1b, and Dab1-Lmx1b neurons all participated in both noxious heat and mechanical nociceptive circuits. Thus, their positioning errors might contribute to the nociceptive abnormalities exhibited by the mutant mice (Yvone *et al*., 2017).

**Specific Aim 2: Determine the identity of Reelin-positive dorsal horn neurons and ask whether these cells sustain positioning errors. Examine the migration patterns of Reelin- and Dab1-expressing dorsal horn neurons relative to those of Lmx1b-labeled neurons.**

*Hypothesis 2a: Reelin-labeled dorsal horn neurons are mostly glutamatergic neurons and co-express the transcription factor Lmx1b.*

In Chapter 3, we found that about 90% of the Reelin-expressing laminae I-II neurons were glutamatergic based on their co-expression of Lmx1b. On average we identified 34 and 31 Reelin-labeled neurons in a 3 µm thick hemisection of *dab1*$^{+/+}$ and *dab1*$^{-/-}$ superficial dorsal horn, respectively. Importantly, we then determined that Reelin-Lmx1b and Dab1-Lmx1b neurons represented different subsets of glutamatergic neurons in laminae I-II. Next, we estimated the percentage of Lmx1b neurons in laminae I-II$_{\text{inner dorsal}}$ (i.e., neurons within and above the IB4 layer) that were Reelin-positive in *dab1* mouse pairs and Dab1-positive in *Reln* mice. We found that Reelin-Lmx1b neurons comprised 83-88% of total Reelin neurons and 17-24% of total Lmx1b neurons in *dab1*$^{+/+}$ and *dab1*$^{-/-}$ mice, respectively. Using a similar analysis, we learned

that Dab1-Lmx1b neurons made up 74 and 71% of total Dab1 neurons and 20-22% of total Lmx1b neurons in *Reln*$^{+/+}$ and *Reln*$^{-/-}$ laminae I-II$_{\text{inner dorsal}}$, respectively. In combination, therefore, Reelin-Lmx1b and Dab1-Lmx1b neurons comprised 37% of the total Lmx1b neurons in wild-type laminae I-II$_{\text{inner dorsal}}$ and 46% of the total Lmx1b neurons in mutant mice. In addition, we confirmed that Reelin laminae I-II cells rarely expressed GAD67 or Pax2, markers of inhibitory dorsal horn neurons. Finally, in wild-type mice, we found that about 35% of Reelin cells co-expressed Lmx1b in the lateral reticulated area, whereas 59% of Reelin cells co-expressed Lmx1b in the LSN. Together, these results showed that the majority of Reelin-expressing dorsal horn neurons are excitatory (Chapter 3).

*Hypothesis 2b: Reelin-expressing neurons exhibit positioning errors in multiple dorsal horn areas, and these errors should match those found in the Dab1-labeled cells (Chapter 2).*
To assess whether the loss of Dab1 leads to neuroanatomical abnormalities in the dorsal horn, we compared the numbers of Reelin, Lmx1b, and Reelin-Lmx1b neurons within the IB4 terminal zone between *dab1*$^{+/+}$ and *dab1*$^{-/-}$ mice. Initially we found that the area of the IB4 layer itself did not differ between genotypes, but the area above the IB4 layer (laminae I-II$_{\text{outer}}$) was reduced in *dab1*$^{-/-}$ versus *dab1*$^{+/+}$ dorsal horn. Additionally, we detected an increase of Reelin-Lmx1b neurons within the *dab1*$^{-/-}$ compared to *dab1*$^{+/+}$ IB4 layer. The numbers of Reelin-only and Lmx1b-only neurons, however, did not differ between genotypes.

Next, we asked whether there were differences in the numbers of Reelin, Lmx1b, and Reelin-Lmx1b neurons in the lateral reticulated area and LSN between wild-type and mutant mice. Numbers of Lmx1b-only neurons and Reelin-Lmx1b neurons were reduced in *dab1*$^{-/-}$ compared to *dab1*$^{+/+}$ lateral reticulated area, but no differences were found in the number of single-labeled Reelin neurons between genotypes. Within the LSN, we found fewer numbers of

Reelin-only, Lmx1b-only, and Reelin-Lmx1b neurons in *dab1*$^{-/-}$ compared to *dab1*$^{+/+}$ mice. This finding is consistent with previous studies that also showed losses of LSN neurons in various Reelin-signaling pathway mutant mice (Villeda *et al*., 2006; Akopians *et al*, 2008; Yvone *et al.*, 2017). In conclusion, the neuroanatomical abnormalities in the nociceptive areas of the dorsal horn of *dab1* mutants (Chapter 3) are similar to those of *Reln* mutants (Chapter 2).

*Hypothesis 2c: Reelin and Dab1 dorsal horn neurons share a common migratory pathway with one or more subsets of Lmx1b dorsal horn neuronal populations.*

We characterized the migratory patterns of Reelin and Lmx1b dorsal horn neurons in *dab1*$^{+/+}$ and *dab1*$^{-/-}$ embryos. At E11.5, we detected Reelin expression dorsolaterally, as well as the lateral-most part of the early-born Lmx1b-expressing dI5 group (Gross *et al*., 2002; Müller *et al*., 2002). By E12.5, Reelin expression expanded dorsally and medially as a second population of Lmx1b-positive neurons, the dIL$_B$ group, was detected (Gross *et al*., 2002; Müller *et al*., 2002). At this age, Reelin expression primarily co-localized with the dorsolaterally-located Lmx1b-positive dI5 neurons. The lateral-most cohort of dI5 neurons was less tightly clustered in mutants than in wild-type embryos.

At E13.5, the highest concentration of Reelin remained in the dorsolateral region, together with the dI5 group. At this stage, the dIL$_B$-derived neurons have expanded enormously, and many Reelin-Lmx1b neurons were detected across the mediolateral extent of the dorsal horn. There were a few Reelin-Lmx1b neurons that appeared mispositioned along the rim of the dorsal horn in *dab1* mutant mice. Several single-labeled Lmx1b and Reelin-Lmx1b neurons were detected around the dorsal midline, representing a late-born part of the dIL$_B$ group. Between E14.5-E15.5, some Reelin-Lmx1b neurons from the dI5 group migrated into the outer rim of the dorsal horn, i.e., the presumptive laminae I-II, along with Reelin-Lmx1b-positive dIL$_B$ neurons.

The dorsal midline group that expressed Reelin-Lmx1b or Lmx1b-only was still detected at this age. By E15.5, most Reelin-Lmx1b neurons were located in the presumptive laminae I-II and dorsolaterally in the region that would become the LSN and the lateral reticulated area. Thus, Reelin-Lmx1b neurons were derived from both the dI5 and the $dIL_B$ groups during embryonic development, and their positioning was relatively similar between *dab1*$^{+/+}$ and *dab1*$^{-/-}$ embryos (Chapter 3).

Finally, we characterized the migratory patterns of Dab1 and Dab1-Lmx1b neurons during embryonic development. At E11.5 and E12.5, we found that most Dab1 neurons co-localized with the dorsolaterally-located dI5 group of Lmx1b-expressing neurons (Gross *et al*., 2002; Müller *et al*., 2002). The major difference between genotypes was that the tightly clustered lateral-most dI5 group in wild-type was somewhat more dispersed in *Reln*$^{-/-}$ embryos. By E13.5, distinct clusters of Dab1-Lmx1b neurons derived from the dI5 group were detected laterally. Dab1 neurons that were single- or double-labeled with Lmx1b also were observed medially, representing the late $dIL_B$ group. Differences in Dab1 localization were obvious at E13.5 with a higher Dab1 expression and disorganization of Dab1 neurons detected in *Reln*$^{-/-}$ versus *Reln*$^{+/+}$ mice.

In E14.5 wild-type embryos, Dab1-Lmx1b cells which originated from the dI5 group were still concentrated dorsolaterally. The core of the dorsal horn was relatively devoid of Dab1 expression; an observation that suggests most Dab1-Lmx1b cells were derived from the dI5 population. The dorsal midline group expressing Dab1-Lmx1b, however, likely came from the late-born $dIL_B$ group that was previously characterized (Escalante *et al*., 2013). Characteristic differences between genotypes were detected at E14.5. Many more Dab1 and Dab1-Lmx1b neurons migrated into the outer rim of the *Reln*$^{-/-}$ dorsal horn compared to those in the wild-type

mice. We also detected large single-labeled Dab1 and Dab1-Lmx1b neurons migrating across the deep dorsal horn in *Reln*$^{-/-}$ which were absent in *Reln*$^{+/+}$ mice. Additionally, in *Reln*$^{-/-}$ E14.5, more of the Dab1 and Dab1-Lmx1b neurons found in the dorsal midline were located laterally in the deep dorsal horn compared to those in the *Reln*$^{+/+}$embryos.

At E15.5, the differences of localization of Dab1 and Dab1-Lmx1b neurons between genotypes were still obvious. Many Dab1 and Dab1-Lmx1b neurons were clearly observed in the presumptive laminae I-II in *Reln*$^{-/-}$, but they were not as easily detected in *Reln*$^{+/+}$ embryos. Additionally, in *Reln*$^{+/+}$ mice, the core of the dorsal horn was relatively devoid of Dab1-expressing neurons. In *Reln*$^{-/-}$ mice, however, there were several large Dab1 and Dab1-Lmx1b neurons in the deep dorsal horn. Finally, we found that the dorsal midline Dab1-Lmx1b-positive $dIL_B$ group appeared as an organized stream of neurons between the dorsal ventricular zone and lamina V in wild-type embryos, whereas these Dab1-Lmx1b neurons in *Reln*$^{-/-}$ dorsal horn were more dispersed. In conclusion, Reelin and Dab1 neurons are different subsets of Lmx1b-expressing dI5 and $dIL_B$ populations. We also show that in the absence of Dab1, the migration of Reelin cells is relatively normal. The loss of Reelin, however, results in distinct migratory aberrations that contribute to positioning errors in adult mutant dorsal horn (Chapter 3).

**References**

Akopians AL, Babayan AH, Beffert U, Herz J, Basbaum AI, Phelps PE. 2008. Contribution of the Reelin signaling pathways to nociceptive processing. Eur J Neurosci. 27:523-37.

Cheng L, Arata A, Mizuguchi R, Qian Y, Karunaratne A, Gray PA, Arata S, Shirasawa S, Bouchard M, Luo P, Chen CL, Busslinger M, Goulding M, Onimaru H, Ma Q. 2004. Tlx3 and Tlx1 are post-mitotic selector genes determining glutamatergic over GABAergic cell fates. Nat Neurosci. 7:510-7.

Escalante A, Murillo B, Morenilla-Palao C, Klar A, Herrera E. 2013. Zic2-dependent axon midline avoidance controls the formation of major ipsilateral tracts in the CNS. Neuron. 80:1392-406.

Gross MK, Dottori M, Goulding M. 2002. Lbx1 specifies somatosensory association interneurons in the dorsal spinal cord. Neuron. 34:535-49.

Gutierrez-Mecinas M, Furuta T, Watanabe M, Todd AJ. 2016. A quantitative study of neurochemically defined excitatory interneuron populations in laminae I-III of the mouse spinal cord. Mol Pain. 12. pii: 1744806916629065.

Müller T, Brohmann H, Pierani A, Heppenstall PA, Lewin GR, Jessell TM, Birchmeier C. 2002. The homeodomain factor Lbx1 distinguishes two major programs of neuronal differentiation in the dorsal spinal cord. Neuron. 34:551-62.

Phelps PE, Barber RP, Houser CR, Crawford GD, Salvaterra PM, Vaughn JE. 1984. Postnatal development of neurons containing choline acetyltransferase in rat spinal cord: an immunocytochemical study. J Comp Neurol. 229:347-61.

Todd AJ. 2010. Neuronal circuitry for pain processing in the dorsal horn. Nat Rev Neurosci. 11:823-36.

Villeda SA, Akopians AL, Babayan AH, Basbaum AI, Phelps PE. 2006. Absence of Reelin results in altered nociception and aberrant neuronal positioning in the dorsal spinal cord. Neuroscience. 139:1385-96.

Yvone GM, Zhao-Fleming HH, Udeochu JC, Chavez-Martinez CL, Wang A, Hirose-Ikeda M, Phelps PE. 2017. Disabled-1 dorsal horn spinal cord neurons co-express Lmx1b and function in nociceptive circuits. Eur J Neurosci. 45:733-747.